
Saccharide Recognition – Boronic Acids as Receptors in Polymeric Networks

Dissertation
zur Erlangung des akademischen Grades
„doctor rerum naturalium“
(Dr. rer. nat.)

in der Wissenschaftsdisziplin Physikalische Chemie
eingereicht an der
Mathematisch-Naturwissenschaftlichen Fakultät
der Universität Potsdam

von

Soeren Schumacher



Potsdam, Februar 2011

Published online at the
Institutional Repository of the University of Potsdam:
URL <http://opus.kobv.de/ubp/volltexte/2011/5286/>
URN <urn:nbn:de:kobv:517-opus-52869>
<http://nbn-resolving.de/urn:nbn:de:kobv:517-opus-52869>

To my parents

During more than three years of research many inspiring discussions, fruitful collaborations and important friendships developed. Since “science” is a discipline in which teamwork is essential, this is the place to express my gratitude to many people. They all contributed to this thesis in many different ways and just their support enabled me to write this thesis.

I would like to express my gratitude to my doctoral supervisor Prof. Dr. Hans-Gerd Löhmannsröben for his support and for giving me the opportunity to do my doctorate in chemistry.

My special thanks is directed to the mentor of the group “Biomimetic Materials and Systems” Prof. Dr. Frieder W. Scheller who acted as a scientific supervisor. I am thankful for many fruitful discussions, interesting new aspects and many corrections of my written thesis or manuscripts.

Substantial guidance has also been given by Prof. Dr. Dennis G. Hall, University of Alberta, Edmonton. He gave me the chance to learn the chemistry of “boronic acids” in his lab and supported my work also after my return to Germany. Furthermore, I appreciated to work in his lively and great working group. The atmosphere was brilliant to learn as much as possible by many fruitful discussion with all members of the group.

I am especially thankful to Dr. Martin Katterle for giving me the opportunity to work in his junior group “Biohybrid Functional Systems”. His immense support and guidance during all years of my thesis were a significant part to write this thesis.

I am grateful to Dr. Nenad Gajovic-Eichelmann, head of the junior group “Biomimetic Materials and Systems” for his effort to support my thesis with many fruitful discussions and ideas. I acknowledge his creative way of thinking and his knowledge not only project related.

My special and deep gratitude is expressed to Dr. Bernd-Reiner Paulke, Fraunhofer IAP, for his significant effort to support my thesis with many scientific ideas and explanations. Also, I am deeply grateful that it was possible to use his lab infrastructure.

I am also grateful to Dr. Cornelia Hettrich for her contributions to my thesis, especially for her supporting work about the characterisation of the boronic acid derivatives by means of isothermal titration calorimetry. Furthermore, I would like to thank Franziska Grüneberger for her work as a student assistant and later on as a diploma student working on one aspect of this thesis.

Very supportive was the collaboration with Prof. Dr. Uwe Schilde, University of Potsdam, who determined the crystal structures of the biomimetic saccharide analogues. Also regarding this project, I would like to thank Dr. Jürgen Rose, University of Potsdam, for the structural superimposition of the crystal structures and his ambitions he put into this project.

I like to acknowledge Prof. Frank F. Bier and Dr. Eva Ehrentreich-Förster for their support, especially for setting the framework for my research stay in Canada and for giving me the opportunity to look into other interesting and challenging research projects and topics.

My gratitude is expressed to the working group “Biomimetic Systems and Materials”. Especially, I would like to thank Irene Schmilinsky for the atmosphere in our office and for many discussions not only but also a lot on chemistry. Furthermore, I could always rely on the backup from Bianca Herbst, our lab technician. I thank for her very conscientious work. In particular, before my Japan trip to the conference on MIPs in 2008 the great support by Christiane Haupt and Marcel Frahnke was very helpful. I am grateful to the team of the first years, Dr. Kai

Strotmeyer, Dr. Oliver Pänke, Dr. Birgit Nagel, Dr. Umporn Athikomrattanakul and Dr. Rajagopal Rajkumar, for the nice atmosphere in this new group and many discussions to find into my project. I would like to thank deeply Dr. Edda Reiß, Dr. Thomas Nagel, Ines Zerbe and Dirk Michel for their support during these years not only in scientific questions and their help in many different aspects. Furthermore, I am thankful to many people which contributed not scientifically but setting the framework such as IT infrastructure and providing technical or secretarial assistance. In general, I really enjoyed the open-minded atmosphere at the Fraunhofer IBMT which opened-up many possibilities.

Of substantial importance was also the help of many people not directly involved in this project, but still, I could rely on their support. In this regard I would like to thank Olaf Niemeyer, MPI-KG, Prof. Dr. Clemens Mügge, HU Berlin, Dr. Lei Ye, University of Lund, Prof. Dr. Bernd Schmidt, University of Potsdam, and Prof. Dr. Sabine Beuermann, University of Potsdam. Prof. Dr. Sabine Beuermann also supervised Franziska Grüneberger during her diploma thesis. I would like to express my thanks to Prof. Dr. Günter Wulff (University of Düsseldorf), Prof. Dr. Klaus Mosbach (University of Lund) and Ecevit Yilmaz (MIP Technologies) for their fruitful and productive discussions about the field of molecular imprinting and, in particular, about its patent situation.

Furthermore, I would like to thank Prof. Dr. Leo Gros, Hochschule Fresenius, for his ambitions also after being a student there. My deep gratitude is directed to Prof. Dr. Michael Cooke, Hochschule Fresenius, for his great and fast corrections on my manuscript.

In the end, I would like to express my deepest and sincere gratitude to my parents, my grandmother, my family and my friends. Without their support, their encouragement and their care, this work would never have been written.

This work was gratefully supported by the BMBF (BioHySys 03111993).

Soeren Schumacher
Potsdam, February 2011

Acknowledgment	i-ii
Table of Contents	iii-iv
List of Figures	v-vii
List of Tables	vii
Abbreviations	viii
Thesis Structure	ix
Chapter 1 - Introduction	1
Chapter 2 - Fundamentals and State-of-the-Art	
2.1 Molecular recognition and its elements	5
2.2 Saccharide recognition - Relevance and background	7
2.3 Concepts for saccharide recognition	
2.3.1 Natural occurring saccharide binding	8
2.3.2 Structure of saccharides	9
2.3.3 Supramolecular chemistry - Forces	12
2.3.4 Molecular imprinting	15
2.3.5 Boronic acids	17
2.3.6 Polymeric systems for saccharide recognition	23
2.4 Assay formats	
2.4.1 Binding.	24
2.4.2 Calorimetry	26
2.4.3 Electrochemistry	28
Chapter 3 - Thesis Goal	31
Chapter 4 - Results and Discussion	
4.1 Boronic acids in solution	
4.1.1 Introduction	33
4.1.2 Binding analysis via ¹ H-NMR spectroscopy	33
4.1.3 Mass spectrometry of boroxole - saccharide interaction	35
4.1.4 Synthesis of different arylboronic acid and benzoboroxole derivatives .	37
4.1.5 Determination of Binding constants using ITC	39
4.1.6 Temperature-dependent ITC measurements	43

4.1.7 Electrochemical behaviour of ARS in saccharide-boronic acid interaction47
4.1.8 Conclusion.	54
 4.2 Applications of boronic acids in polymeric networks	
4.2.1 General considerations57
4.2.2 Label-free detection of saccharide binding at pH 7.4 to nanoparticulate benzoboroxole based receptor units59
4.2.3 Benzoboroxole-modified nanoparticles for the recognition of glucose at neutral pH69
4.2.4 Molecular imprinting of fructose using a polymerisable benzoboroxole: Recognition at pH 7.475
4.2.5 Biomimetic monosaccharide analogues – (Easy) Synthesis, characterisation and application as template in molecular imprinting . .	.87
4.2.6 Conclusion97
 Chapter 5 – Summary99
 Chapter 6 – Materials and Methods	101
 Chapter 7 – References	111
 Appendix	119

- Figure 1.** Key structures described in this thesis; Phenylboronic acid derivatives **1**, derivatives of benzoboroxole **2**, different saccharide or *cis*-diol containing saccharide and other compounds **3a-e** and different boronic acid esters **4** thereof.
- Figure 2.** S-curve analysis based on a patent dataset analysis for the molecularly imprinted polymer
- Figure 3.** Mutarotation of D-fructose **3a** and D-glucose **3b** and the relative distribution of their anomers in water at 25°C or 31°C, respectively
- Figure 4.** Derivatives of glucose possessing different heteroatoms such as nitrogen **5**, sulphur **6** or carbon **7** (saccharide derivatives) and saccharide-like structures such as inositol **8** and sorbitol **9**
- Figure 5.** Dependence of the total potential energy and the distance of two approaching molecules described as Lennard-Jones potential
- Figure 6.** Possible intermolecular forces and their physicochemical properties in terms of binding strength and characteristics
- Figure 7.** Synthesis scheme of molecular imprinting; creation of the functional monomer – template complex, the polymerisation and subsequent extraction and rebinding process
- Figure 8.** Binding equilibria of phenylboronic acid **1a** with *cis*-diols and their coordination with hydroxyl ion
- Figure 9.** Comparison of esterification and ring strain between phenylboronic acid **1a** or benzoboroxole **2a** and *cis*-diol containing compounds **3**
- Figure 10.** Different boronic acid derivatives with intramolecular donor functions
- Figure 11.** Different synthesis methods for benzoboroxole derivatives **2** starting either from benzyl alcohol **12**, arylboronic acids **13-15** and linear substrates **16-18** for cyclisation
- Figure 12.** Different reported boronic acid based saccharide sensors with different principle of detection ranging from fluorescence to electrochemistry
- Figure 13.** Different fructose boronic acid complexes revealed by NMR spectroscopy
- Figure 14.** Saccharide anomers with *syn*-periplanar arrangements, their percentage in D₂O and binding constants with ARS at pH 7.4 (Springsteen, Wang, 2002, 5291)
- Figure 15.** Intramolecular arrangement of glucose **3b** after binding to a diboronic receptor **23** which initially binds in a pyranose form **26** and changes its conformation to the furanose **27** form (Shinkai, Norrild and Eggert)
- Figure 16.** Schematic drawing of an isothermal titration calorimeter; the guest molecule is stepwise inserted via a syringe into the sample cell which contains the receptor
- Figure 17.** Scheme of different aspects, key substances and systems of the present thesis
- Figure 18.** ¹H-NMR spectroscopic data (600 MHz) for the interaction between benzoboroxole **2a** and fructose **3a** or glucose **3b** in D₂O at pH 7.4 in deuterated phosphate buffer; Displayed are here the aromatic region **A**, and the saccharide regions for fructose **B** and glucose **C**
- Figure 19.** Example mass spectrum (ESI-MS) for the interaction of glucose **3b** and benzoboroxole **2a** in a 1:1 mixture of acetonitrile and water
- Figure 20.** Different phenylboronic acid derivatives **1a-1f** and benzoboroxole derivatives **2a-2f** for coupling on or incorporation into polymeric networks; derivatives **2e** and **2f** are chiral derivatives
- Figure 21.** Synthesis route for 3-carboxybenzoboroxole **2b**
- Figure 22.** Synthesis route for nitrobenzoboroxole **2e** as chiral derivative starting from 2-formylphenylboronic acid **32**
- Figure 23.** Synthesis route for nitrilebenzoboroxole **2f** as second chiral derivative also starting from 2-formylphenylboronic acid **32**
- Figure 24.** Synthesis of 3-methacrylamidophenylboronic acid **1d** starting from 3-aminophenylboronic acid **1c** and reaction with an acid chloride **33**
- Figure 25.** Binding constants determined at different temperatures for fructose binding to **1a** or **2a** at pH 7.4
- Figure 26.** Evolution of ΔH , $-\Delta S$ and ΔG dependent on the temperature for the interaction between benzoboroxole **2a** (A) or phenylboronic acid **1a** (B) and fructose **3a**
- Figure 27.** Van't Hoff – plot for the determination of ΔH_{vH}° of the benzoboroxole **2a** or phenylboronic acid **1a** interaction with fructose **3a**
- Figure 28.** Electrochemistry of Alizarin Red S **3e**, its interaction with phenylboronic acid **1a** and displacement through fructose **3a** at pH 7.4

- Figure 29.** All measurements were performed at a scan rate of 0.1 V s⁻¹ under oxygen exclusion; Cyclic voltammograms of 0.144 M ARS solution in 0.1 M phosphate buffer with 50 mM KCl at pH 7.4 at glassy carbon electrode ($\varnothing=3$ mm) vs. Ag/AgCl (KCl = 3 M), solid line: positive scan direction; dashed line: negative scan direction
- Figure 30.** Reaction scheme of possible equilibria of ARS **3e** and corresponding reduction and oxidation processes
- Figure 31.** Cyclic voltammogram of ARS solution with increasing phenylboronic acid **1a** concentrations
- Figure 32.** Cyclic voltammogram of ARS-PBA solution with differing fructose **3a** concentrations between 10 and 150 mM
- Figure 33.** Current intensities ARS redox peaks vs. the added concentration of fructose **3a**; three repetitions, \blacktriangle : oxidation peak P3, \bullet : oxidation peak P1, \blacksquare : reduction peak P2.
- Figure 34.** Different boronic acid derivatives in corresponding chapters
- Figure 35.** Graphical abstract for differently modified polystyrene nanoparticles and their fructose **3a** binding characterisation using ITC at pH 7.4
- Figure 36.** Synthesis of boroxole **2** (BX-NP), phenylboronic acid **1** (BA-NP) and aniline **34** (Ref-NP) modified nanoparticles using the appropriate amino-derivatives **2c** and **1c** at pH 7.4 for nucleophilic substitution
- Figure 37.** **A.** Control experiments performed with aniline modified nanoparticles (Ref-NP) titrated against buffer (20 mM phosphate) (1) and 75 mM fructose **3a** (2), and **3a** against buffer alone (dilution experiment, 3). **B.** Isothermal titration calorimetry experiments with benzoboroxole (gray) and phenylboronic acid (black) modified nanoparticles (BX-NP and BA-NP) titrated against 75 mM at pH 7.4 in 20 mM phosphate buffer. The data were corrected against the dilution experiments
- Figure 38.** Enthalpic and entropic contributions to the Gibbs free energy of fructose **3a** binding to free 3-aminophenyl boronic acid **1c**, phenylboronic acid **1a**, 3-aminobenzoboroxole **2c**, benzoboroxole **2a** and to the nanoparticles decorated with phenylboronic acid (**BA-NP**) and benzoboroxole (**BX-NP**)
- Figure 39.** Preparation of benzoboroxole modified nanoparticles (**BX-NP**), their loading with ARS **3e** and subsequent binding of monosaccharide such as fructose **3a** at pH 7.4
- Figure 40.** **A-C.** Absorption spectra of the benzoboroxole modified nanoparticles and their binding to ARS **3e** (A) and fructose **3a** (B) or glucose **3b** (C) in phosphate buffer at pH 7.4. **A.** Increasing nanoparticle concentration, **B.** and **C.** Competition assay with fructose, in which the ARS – loaded nanoparticles are titrated against increasing fructose/glucose concentrations; **D.** Concentration dependence of the absorption at $\lambda=466$ nm for fructose (squares) or glucose (dots) after displacement of **3e**
- Figure 41.** Absorption of the benzoboroxole modified latex at pH 7.4 with ARS before (solid line) and after (dashed line) heat treatment
- Figure 42.** Schematic drawing of a molecularly imprinted polymer for fructose employing a polymerisable benzoboroxole **2d** for effective fructose recognition at pH 7.4
- Figure 43.** Synthesis of different 3-methacrylamidobenzoboroxole and vinylphenylboronic acid esters for incorporation into a molecularly imprinted polymer
- Figure 44.** ¹H-NMR spectrum of neat benzoboroxole **2a** and 3-methacrylamidobenzoboroxole **2d** and their formed fructose esters
- Figure 45.** Synthesis scheme of the four different molecularly imprinted polymers MIP-BX(Fru), MIP-BA(Fru), MIP-BX(Pin) and MIP-BA(Pin) starting from the corresponding esters **4a** – **4f**
- Figure 46.** Media optimisation for 2 mM fructose at pH 7.4 with 10 % MeOH; MIP-BX(Fru) (dark bars); MIP-BX(Pin) (light bars)
- Figure 47.** Batch binding experiments for different fructose binding MIPs at different pH-values. **A-C:** Concentration dependency for fructose binding to MIP-BX(Fru) (\blacktriangle), MIP-BA(Fru) (\blacksquare), MIP-BX(Pin) (\blacklozenge) and MIP-BA(Pin) (\bullet); **A:** carbonate solution, pH 11.4, 10 % MeOH; **B:** phosphate buffer, pH 8.7, 10 % MeOH; **C:** phosphate buffer, pH 7.4, 10 % MeOH
- Figure 48.** D-fructose binding to MIP-BX(Fru) at pH 7.4 in phosphate buffer in presence of competitors at equimolar concentration
- Figure 49.** Schematic drawing of the imprinting process of biomimetic monosaccharide analogues and binding with glucose to these polymers; Crystal structures are new or published data
- Figure 50.** Synthesis of the biomimetic analogue *rac*-**3c** starting from cyclic dienes **35** and **36**
- Figure 51.** Molecular structure of the diboronic acid ester *rac*-**4e** and *rac*-**4f**: A) top view and B) side view. Shown here: S-enantiomer

- Figure 52.** **A:** Defined core atom set highlighted in red using for example glucopyranose boronic acid ester and the compound **4e**; **B:** Structural superposition of the fructofuranose boronic acid ester with **S-4e** and **R-4e**.
- Figure 53.** Molecular imprinting scheme
- Figure 54.** Binding isotherms obtained by batch binding of fructose (A) or glucose (B) to either MIP-Biomim or MIP-Pin at pH 11.4
- Figure A1.** Raw ITC-data of phenylboronic acid or benzoboroxole interaction with fructose
- Figure A2.** Determination of binding constant between the benzoboroxole-NP and fructose by means of the ARS-assay (S/P vs. Q).
- Figure A3.** Determination of binding constant between the benzoboroxole-NP and glucose by means of the ARS-assay (S/P vs. Q).
- Figure A4.** Binding isotherms for competitive binding

List of Tables

- Table 1.** Binding constants for the interaction between different arylboronic acid derivatives and either glucose or fructose obtained by ITC at pH 7.4 in 0.1 M phosphate buffer.
- Table 2.** Obtained binding constants between **1a** or **2a** and fructose at pH 7.4 for different temperatures.
- Table 3.** Determined entropy ΔS , enthalpy ΔH and Gibbs free energy ΔG for the interaction between fructose **3a** and **1a** or **2a** at different temperatures
- Table 4.** Thermodynamic parameters for the interaction between fructose **3a**, the arylboronic acid derivatives and the arylboronic acid modified particles (BA-NP and BX-NP) in phosphate buffer at pH 7.4 (*n.d.*=not detectable)
- Table 5.** Summarised pore volumes obtained by nitrogen sorption measurements (BET)
- Table 6.** Selected geometric parameters of crystal structures **4e**, **4f**, glucose and fructose boronic acid ester
- Table 7.** Results of the rms-distance after structural overlap between the biomimetic saccharide analogs and glucose or fructose phenylboronic acid esters
- Table A1.** Literature survey on molecularly imprinted polymers for glucose, fructose and fructosyl valine as templates
- Table A2.** Survey of recent literature: Polymeric networks bearing arylboronic acids for different applications
- Table A3.** X-ray crystallographic and refinement data for *rac-4e* and *rac-4f*.

Abbreviations

ACES	N-(2-Acetamido)-2-aminoethanesulfonic acid
Ag/AgCl	Silver / Silverchloride
AIBN	Azo- <i>bis</i> -isobutyronitrile
ARS	Alizarin Red S
BA-NP	Phenylboronic acid modified polystyrene nanoparticles (Chapters 4.2.2 and 4.2.3)
BES	N,N- <i>Bis</i> (2-hydroxyethyl)-2-aminoethanesulfonic Acid
BET	Brunauer, Emmet, Teller (nitrogen sorption)
BJH	Barret-Joyner-Halenda (mesopore distribution from nitrogen sorption)
BuLi	Butyllithium (n-)
BX-NP	Benzoboroxole modified polystyrene nanoparticles (Chapters 4.2.2 and 4.2.3)
CGM	Continuous glucose monitoring
CTAB	Cetyltrimethyl ammonium bromide
D ₂ O	Deuterium oxide
DNA	Desoxyribonucleic acid
DVB	Divinylbenzene
EDG	Electron donating group
EGDMA	Ethylene glycol dimethacrylate
ESI-MS	Electrospray ionisation mass spectrometry
EWG	Electron withdrawing group
h	hour
HCl	Hydrochloric acid
HEPES	2-(4-(2-Hydroxyethyl)-1-piperazinyl)-ethanesulfonic acid
HK	Horvath-Kawazoe (micropore distribution of adsorption)
IF	Imprinting Factor
ISFET	Ion Sensitive Field Effect Transistor
ITC	Isothermal titration calorimetry
HEMA	Hydroxyethyl methacrylate
KOH	Potassium hydroxide
MeCN	Acetonitrile
MEMS	Micro-Electro-Mechanical Systems
MeOH	Methanol
MgSO ₄	Magnesium sulphate
MIP-BA(Fru)	Molecularly imprinted polymer with 3-vinylphenylboronic acid as functional monomer and fructose as template (Chapter 4.2.4)
MIP-BA(Pin)	Molecularly imprinted polymer with 3-vinylphenylboronic acid as functional monomer and pinacol as template (Chapter 4.2.4)
MIP-BX(Fru)	Molecularly imprinted polymer with 3-methacrylamidobenzoborxol as functional monomer and fructose as template (Chapter 4.2.4)
MIP-BX(Pin)	Molecularly imprinted polymer with 3-methacrylamidobenzoborxol as functional monomer and pinacol as template (Chapter 4.2.4)
MOPS	3-(N-morpholino)propanesulfonic acid
NBS	N-Bromosuccinimide
NIPAM	N-isopropylacrylamide
NMR	Nuclear magnetic resonance
NP	Nanoparticle
PBA	Phenylboronic acid 1a
PS	Polystyrene
QCM	Quartz crystal microbalance
rms	Root-mean-square
s	second
SPM	3-Sulfopropylmethacrylate potassium salt
SPR	Surface Plasmon resonance
TEMED	Tetramethylethylenediamine
THF	Tetrahydrofuran
V	Volt
vs.	versus / against

Chapter 1 - Preface

The motivation for the present thesis are described in the first chapter in a general manner (i) to define the scientific field, (ii) to integrate the presented work into the scientific scenery, (iii) to give the aim of the thesis and (iv) to provide different strategies for its solution.

Chapter 2 - Fundamentals and State-of-the-art

The second chapter shows the scientific background of the field starting from the concept of molecular recognition and goes into deeper detail about saccharide recognition, its relevance and possible natural and artificial concepts. This is finalised by a closer look to arylboronic acids for saccharide binding in general and as motifs in either random polymeric networks or molecularly imprinted polymers. The last part describes different assay formats to characterise the binding between the saccharide and boronic acids in solution or immobilised in polymeric networks whereas a special interest is given to isothermal titration calorimetry and electrochemistry.

Chapter 3 – Thesis goals

The third chapter specifies all key points of the thesis which are addressed in the following “Results and Discussion” part and can be understood as a guideline for the following chapter.

Chapter 4 – Results and Discussion

The “Results and Discussion” chapter is subdivided into two main and several sub-parts. In general, two different parts can be distinguished: a part in which free arylboronic acids are synthesised and characterised and a part in which different arylboronic acid derivatives are used for different applications. The free arylboronic acid part is further divided into a synthesis part and parts describing different methods for the saccharide binding characterisation. The application part is intersected into four different applications in which nanoparticles as well as bulk polymers (as molecularly imprinted polymers) are described. The part will be completed by a conclusion showing the holistic aspects of the applications. Furthermore, the application part is partitioned classically in an abstract, introduction, results and discussion and conclusion chapter.

Chapter 5 – Summary

The fifth chapter gives a summary.

Chapter 6 – Materials and Methods

The chapter “Materials and Methods” presents the detailed experimental and set-up and parameters of all experiments and is divided accordingly to the “Results and Discussion” chapter.

Chapter 7 – References

The last chapter cites all referred published paper and books.

The chapters 4.1.5 (together with 4.1.6), 4.1.7 and chapters 4.2.2 to 4.2.5 are submitted for publication to different journals. Chapter 4.2.4 was supported by a diploma thesis by Franziska Grüneberger and therefore *co*-authored as “contributed equally”.

Parts of these chapters are already published:

Chapter 4.1.7

Schumacher, S.; Nagel, T.; Scheller, F. W.; Gajovic-Eichelmann, N.; "Alizarin Red S as an electrochemical indicator for saccharide recognition"; in *Electrochim. Acta*, 2011, Article in press; doi:10.1016/j.electacta.2011.04.081

Chapter 4.2.2

Schumacher, S.; Katterle, M.; Hettrich, C.; Paulke, B.-R.; Hall, D.G.; Scheller, F. W.; Gajovic-Eichelmann, N.; "Label-free detection of enhanced saccharide binding at pH 7.4 to nanoparticulate benzoboroxole based receptor units"; *J. Mol. Rec.*, 2011, Article in press, Peer-pre review version

Chapter 4.2.3

Schumacher, S.; Katterle, M.; Hettrich, C.; Paulke, B.-R.; Pal, A.; Hall, D.G.; Scheller, F. W.; Gajovic-Eichelmann, N.; "Benzoboroxole-modified nanoparticles for the recognition of glucose at neutral pH"; *Chem. Sensors*, 2011, 1, 1-7

Chapter 4.2.4

Schumacher, S.; Grüneberger, F.; Katterle, M.; Hettrich, C.; Hall, D.G.; Scheller, F. W.; Gajovic-Eichelmann, N.; "Molecular Imprinting Of Fructose Using A Polymerizable Benzoboroxole: Effective Complexation at pH 7.4 "; *Polymer*, 2011, 52, 2485-2491, doi:10.1016/j.polymer.2011.04.002

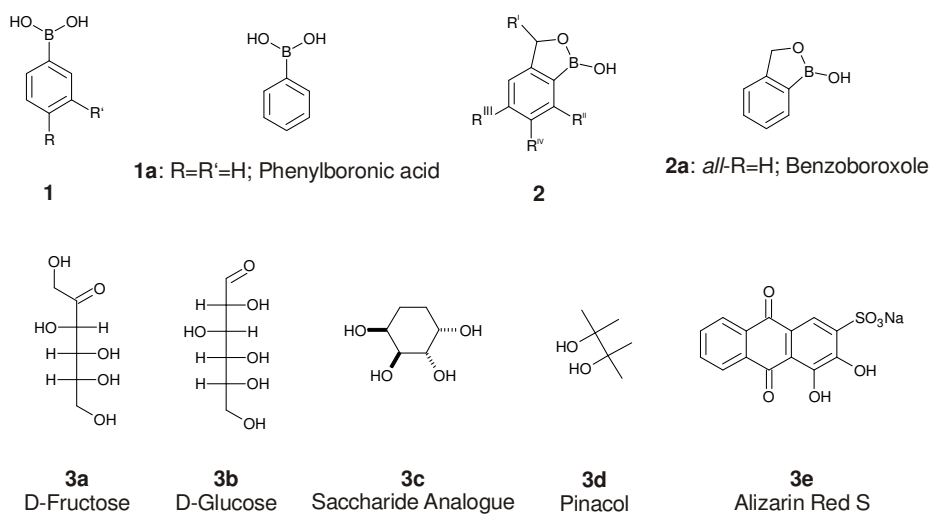
The aim of creating tailor-made artificial receptors for the recognition and sensing of target molecules has a long and noble history as underlined by giving the Nobel Prize in Chemistry in 1987 to Cram, Lehn and Peterson “for their development and use of molecules with structure-specific interaction of high selectivity”.^{1,2} New findings, especially through X-ray crystallography or computer-based modelling approaches, have paved the way for new insights in the relationship of host and guest interactions in naturally occurring systems.³⁻⁷ It is well known that many types of interactions exist and that a distinct interplay between chemical forces in a defined 3D-arrangement results in a high binding strength and selectivity.^{8,9} Consequently, many approaches and interesting ideas have been developed and the number of concepts has increased dramatically.^{10,11} Moreover, different possibilities and principles for the detection of the binding event have been developed.¹²⁻¹⁴ A variety of synthetic approaches have been used in order to create artificial receptor molecules since they are more attractive than biological recognition elements regarding their stability against temperature or harsh solvent conditions.^{15,16} Here, a span of different designs and efforts can be distinguished ranging from biomimetic, synthetic to more generic principles differing in type of interactions, complexity and expenditure of work.¹⁷⁻¹⁹

The combination of recognition and signalling opens the possibility for artificial receptor units to monitor different analytes of interest for industrial, environmental and biological applications. In medical diagnostics especially, easily available and selective receptor units are required.²⁰ After the great scientific achievements of genomics and proteomics the role of carbohydrates and their structures in life sciences has become more and more evident.^{21,22} Beside complicated glycan structures which are relevant for example in cell-cell communication also monosaccharides still have a great importance due to their role in basic metabolic processes and related diseases. Thus, tailored recognition of saccharide structures, and especially monosaccharides such as glucose, is one of the major targets for artificial molecular recognition elements.²³⁻²⁵ One of the main challenges is the recognition of unsubstituted monosaccharides in aqueous media at pH 7.4 due to the competition between hydroxyl groups attached to the carbohydrate backbone and hydroxyl groups from water.^{26,27} Many attempts have been undertaken to address this problem. Besides hydrogen bonds also coordinated or cleavable covalent bonds have been applied to enable a more precise differentiation between these different hydroxyl groups. The most prominent used chemistry for (cleavable) binding to saccharides in aqueous solutions is the use of arylboronic acids.^{28,29}

Arylboronic acids are known to bind to *cis*-diols present in saccharides at alkaline pH values. The cyclic boronic acid ester formed can be cleaved at low pH values.³⁰ Thus, boronic acids are one possible way to overcome the competition between hydroxyl groups of water and saccharide. Based on boronic acids, there exists a variety of different synthetically designed receptors but the considerable effort necessary for their synthesis makes these receptors unattractive. A more generic and hence easier approach is the use of polymeric systems with incorporated or attached boronic acid entities. The properties of the polymer enhance the binding capability beyond that of the thermodynamic binding character. Moreover, secondary effects induced by a high receptor concentration, involving the possibility of a subsequent rebinding of the targeted analyte or multivalent binding events, can lead to a higher apparent binding constant and thus preferred binding.³¹ Since these approaches target the overall binding affinity, the selectivity is rarely addressed. In this regard, a polymeric approach called “molecular imprinting” was established and is described in literature in which a polymerisation is carried out in the presence of a template molecule which is in most cases the analyte of later interest.^{22,32,33} Through the interaction between the analyte/template molecule and functional monomers within the polymerisation mixture a pre-orientation is taking place which is fixed into the polymeric network during polymerisation. The template can be extracted leading to an artificial binding site which is “imprinted” on a molecular scale. In the 1970s the first publications of this principle described the imprinting of glyceric acid with arylboronic acids as the functional monomer for racemic resolution.³⁴⁻³⁷ The binding of glyceric acid to the imprinted polymer was performed in organic solvents such as methanol. To use imprinted polymers with arylboronic acids as functional monomers in aqueous media, which can be intended for practical applications, the pH-value has to be chosen alkaline.^{38,39}

The aim of this work is the “Development of polymeric systems with boronic acid entities which are able to bind unprotected monosaccharides at neutral pH.” Thus, the key factors of enhancing the binding strength through multiple binding sites on the polymeric network, the development and employment of arylboronic acid derivatives for saccharide recognition at pH 7.4, their characterisation in terms of spectroscopic and calorimetric methods and the use of molecularly imprinted polymers for the selective binding of specific saccharides were targeted. In this regard, two different classes of arylboronic acid derivatives are employed (Figure 1). Arylboronic acid derivatives of phenylboronic acid **1** are used. For these derivatives the binding to saccharides is favoured in alkaline media. Therefore, also derivatives of an *ortho*-substituted phenylboronic acid known as benzoboroxole **2** are employed since through an intramolecular coordination a binding of saccharides at pH 7.4 is favoured.^{27,40} Moreover, by applying a biomimetic saccharide analogue *rac*-**3c** as template for the generation of molecularly imprinted polymers a strategy has been evaluated to overcome the problems of mutarotation and different

observed binding structures between boronic acids and saccharides such as fructose **3a** and glucose **3b**.



4 Different boronic acid esters

Figure 1. Key structures described in this thesis; Phenylboronic acid derivatives **1**, derivatives of benzoboroxole **2**, different saccharides and other *cis*-diol containing compounds **3a-e** and different boronic acid esters **4** thereof.

2.1 MOLECULAR RECOGNITION

The concept of molecular recognition can be defined as the specific interaction of a “host and guest”, “lock and key” or “ligand and receptor” pair.⁴¹ In these systems, different types of interaction are responsible for the fit of a target molecule. Hence, not only the binding is of importance. Moreover, the selectivity of the interaction is of considerable interest. The main challenge is therefore to design pairs which are able to complex each other in a highly selective way by matching their electronic, geometric, structural or polar features. In general, interplay of many different types of interactions is, in most cases, envisaged and has to be chosen very carefully. In nature, many examples of specific interactions can be found between an enzyme and its substrate, antigen and antibody and hormone and receptor which can be described by the “key-lock” principle. This principle shows in a very simple way that structural design and functional group complementarity are crucial to bind analytes of interest with high selectivity. Enzymes in particular may exhibit a high substrate-, reaction- and stereo- specificity. The rigid key-lock principle was improved by findings that a further activation takes place through changes in the tertiary and quaternary structure of the protein induced by the substrate (“induced-fit” model).⁴² Many attempts nowadays are undertaken to synthesise various different artificial receptors mimicking the natural binding pocket. Insight into the understanding of biological recognition offers new courses of action leading to a more sophisticated design of receptor units.

There are a variety of receptor units which act as specific binding agents for different applications. If the chemical recognition process is combined with a physical read-out artificial receptors can be used as recognition elements for various fields of interest. Depending on the receptor element a differentiation between synthetic sensors and biosensors can be made. Whereas biosensors employ biological elements such as enzymes or antibodies for recognition, synthetic sensors make use of designed and synthetically prepared elements.⁴³ The major advantage of biological receptor units is their overwhelming specificity for the target molecule.⁴⁴ With an appropriate transducer a biosensor is created for an analyte of interest.⁴⁵⁻⁴⁷ The major advantage of synthetic receptors in contrast is their stability in terms of temperature performance and their tolerance against harsh media such as extreme pH-values or organic solvents.⁴⁸ The disadvantage in most cases is the high synthetic effort to be made and their moderate specificity and selectivity.

Different biological recognition elements are described for classical biosensors.^{46,49} Microbial cells, receptors, tissue materials and organelles are employed, but to a minor extent.⁵⁰⁻⁵⁵ Especially for commercial use, enzymes, antibodies and nucleic acids are of great importance.

Enzymes are the most dominant species used in sensor applications due to their combination of specificity and catalytic properties leading to signal amplification.^{56,57} For example, for blood glucose monitoring, enzymes are applied.⁵⁷ Nowadays, most of the commercially available diabetes tests are based on glucose dehydrogenase or glucose oxidase combined with an electrochemical read-out.⁵⁸⁻⁶⁰

Antibodies are raised for many different analytes through infection of a host animal.⁶¹ The animal responds to the foreign material with an immune response leading to antibodies against the analyte. After fusion of antibody-creating B-cells of the infected animal with immortal myeloma cells and via a selection medium (for example, Hypoxanthine aminopterin thymidine medium (HAT)) monoclonal antibodies of high specificity and binding affinity can be obtained.^{62,63} Whereas enzymes and antibodies are against molecules of different chemical structures, nucleic acids are mainly for the diagnosis of genetic and infectious diseases. In this application, DNA probes complementary to the target DNA are mostly immobilised onto plain substrates (for example microarrays) and the sample containing the target DNA is incubated.^{64,65} After binding the target sequence, in most cases a fluorescent readout through reporter dyes, leads to an analytical answer.

DNA as a receptor molecule can be described as semi-synthetic recognition element since biological building blocks are used to synthesise artificial receptor units. DNA sequences have to be synthesised complementary to the targeted, from sequence analysis known DNA. Beside DNA sequences which are complementary to the target strand also DNA sequences for the recognition of non-DNA based molecules are described. These are, for example, aptamers which are screened via a process called Systematic Evolution of Ligands by EXponential Enrichment (SELEX) in which the best binding aptamers are enriched and amplified.^{66,67} The aptamers are raised for a variety of different targets and binding constants such as those of antibodies in the nano- to picomolar range are possible. Also artificial peptide based binders can be created via normal solid-phase synthesis. In this case, the extraction of binding peptides within the paratope of antibodies leads to a potential binding for linear epitopes.⁶⁸⁻⁷⁰ Furthermore, their screening is possible using combinatorial analysis with (evolution) techniques such as, for example, phage display and also here binding strengths down to the nano-molar range can be obtained.^{71,72}

Apart from biologically based receptor units also purely synthetic ones are possible. Although it is possible to create a design “from scratch” the main disadvantage is the tedious and time-consuming effort for their synthesis. Basic principles for the design are the interplay of size/shape and intermolecular forces such as hydrogen bonds and electronic or hydrophobic interactions.⁷³ Some synthetically described systems can form shapes which are defined in size and orientation of surface properties during synthesis. These are, for example, calixarenes or cyclodextrines which build ring-like structures with fixed diameters.^{18,74-76} Other chemical

receptors are tailor-made, for example, mechanically bonded catenanes and rotaxanes or differently bonded encapsulation complexes, creating a defined structure of size and electron density.⁷⁷⁻⁷⁹

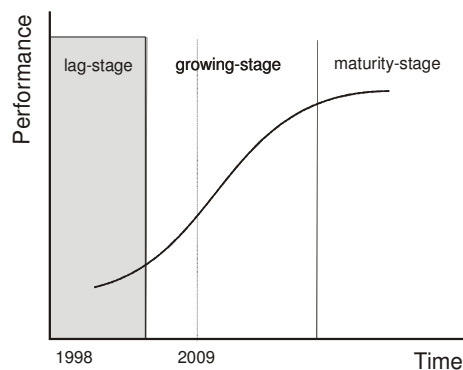


Figure 2. S-curve analysis based on a patent dataset analysis for the molecularly imprinted polymer market³³

Beside the synthesis of small artificial receptors by chemical synthesis also approaches in which the binding site is introduced into macromolecular, polymeric networks has been well-known for many years. One of the most useful, easily-adaptable principle is the molecular imprinting approach.²² Based on the concept of mimicking a natural binding site in a polymeric network, molecularly imprinted polymers have the potential to replace biological and semi-biological receptor units. This is displayed by the immense increase of publications and patent applications of different molecularly imprinted polymer systems since 2007.³³ In a market analysis based on the patent situation it was predicted that the market is in the growing stage of an S-curve analysis (Figure 2), which shows also the high commercial potential of this technique.

2.2 SACCHARIDE RECOGNITION

Relevance and background

As the product of photosynthesis carbohydrates and similar structures fulfil a significant role as building blocks in living systems. Primary saccharides are metabolised and different structures ranging from branched to linear oligomers, up to long polysaccharides, can be built up. Through their structural diversity their biological role can dramatically vary starting from energy storage (starch and glycogen), structure-giving elements (cellulose) and biological functionalities (glycoproteins) to compounds in metabolic processes.⁸⁰ During recent years, especially through the new emerging field of “glycomics”, carbohydrates have become of great importance for biomedicine and related areas.^{21,81-83} As it is known that mainly carbohydrate structures are

responsible for many physiological aspects that comprise cell-to-cell communication, fertilisation, cell-growth, immune response, cancer cell growth, metastasis and microbial/viral infections, the characterisation of saccharides and glycoprotein structures is of great interest.⁸⁴ From another viewpoint the understanding of the role of saccharide structures in living matter and the subsequent design of targeted oligosaccharide structures, gives rise to new pharmaceutical efforts in state-of-art drug discovery or the development of vaccines.^{85,86}

From a more “daily” medical perspective also monosaccharides, and in particular, D-glucose are of eminent relevance because pathways in sugar metabolism and recognition are described and understood.^{25,87} In many cases interference therein is related to defects such as cystic fibrosis, renal glycosuria, diabetes mellitus and even cancer.⁸⁸⁻⁹¹ In addition tracking of saccharides is important for diagnostic monitoring - for example, measuring the level of glycated haemoglobin for long-term diabetes control.⁹² The precise screening of carbohydrates in biological samples is therefore necessary. Not only has the medical point of view made saccharide recognition worth investigating but also biotechnological improvements. In fermentations, for example, carbohydrate sensing is used to screen the metabolic activity of the culture batch.

2.3 CONCEPTS FOR SACCHARIDE RECOGNITION

2.3.1 Natural occurring saccharide binding

Since carbohydrates are a class of very important building blocks in nature, the binding characteristics between saccharide structures and different receptors which are found in nature is an important and large field of investigation. There are four main different substance classes found in nature which are able to bind to saccharides. Due to the great importance of saccharides as nutrients many enzymes are known to bind saccharides for their metabolism and represent the first class. Here, it is possible to differentiate between enzymes for poly- and oligosaccharide such as lysozyme or amylases and enzymes for monosaccharides such as glucose oxidase and glucose dehydrogenase. The latter are moreover of particular commercial interest because of their use in commercially available glucose sensors.^{45,46,57}

Antibodies form the second substance class and are known to be recognition elements for saccharides. As described before, to raise an antibody a host animal has to be exposed to the substance (or later analyte) of interest. For oligosaccharides this is possible through stimulation using whole cells because structurally-complicated not easy metabolisable saccharide antenna are located on the surface of cells.⁹³ Antibodies can be formed against these entities. In contrast, it is not possible to produce antibodies against monosaccharides due to their rapid degradation. Consequently, polymeric saccharides such as dextrans are used to immunise host animals. Thus,

antibodies against glucose could be obtained but only a weak binding strength (binding to glucose $K_B = 53 \pm 6 \text{ M}^{-1}$) was detected.⁹⁴

The third substance class is the group of lectins which are the most prominent recognition element for mono- and oligosaccharides.⁹⁵ Lectins were originally isolated from plants but today it is known that they are ubiquitous in nature and consist of proteins or glycoproteins.^{96,97} Their role can vary and is not yet fully understood. They are, for example, able to bind to the glycopattern of different cells leading to agglutination and a subsequent response of the immune system. Also regulatory effects, for example in mitosis or cell adhesion, have been proven.^{98,99}

The fourth important class is the class of bacterial periplasm proteins which are responsible for carbohydrate transport and chemotaxis of gram-negative bacteria.¹⁰⁰ Due to their role in transportation their binding constant is with typically 10^6 to 10^7 M^{-1} (at least three orders of magnitude) higher when compared with other binding elements for monosaccharides found in nature.^{84,101-103}

In general, the protein-saccharide interaction in aqueous media is a complicated interplay between different types of interaction. The most common type of interaction is hydrogen bonding followed by hydrophobic interactions such as CH- π -interactions between aromatic amino acid residues and the carbohydrate scaffold. More specifically, in lectins and periplasm proteins mostly multivalent side chains are responsible for hydrogen bonding.¹⁰⁴ The most abundant amino acids are asparagine, aspartic acid, glutamic acid, arginine and histidine.¹⁰⁵ In antibodies, the most prominent type of interactions are hydrogen bonds between amides and hydroxyl groups of the saccharide.^{106,107} Furthermore, the presence of metal ions such as calcium ions can be necessary as a *co*-factor.

2.3.2 Structure of saccharides

The term “carbohydrates” which is used in a similar way to the term “saccharide” (or even sugar) is derived from its structure which can be described by the general molecular formula $C_n(H_2O)_n$. Carbohydrates exhibit a large number of different functionalities such as several hydroxyl groups and, usually, one carbonyl group. Depending on the position of the carbonyl group aldoses (polyhydroxylaldehydes) and ketoses (polyhydroxylketones) can be distinguished. Different saccharides can be categorised by their C-chain length. Aldoses are derived from glyceraldehyde and a formal HCOH insertion between the carbonyl group and the adjacent stereogenic centre leads to aldotetroses, aldopentoses and so on. The same is valid for ketoses derived from 1,3-dihydroxyacetone. Through formal HCOH insertion tetrols, pentuloses and so on can be described. Every saccharide is defined by a certain arrangement of the hydroxyl groups which shows that many stereoisomers are possible. In general, aldoses and ketoses exist as

two enantiomeric forms (D- and L-form) defined by the configuration of the highest-numbered stereo centre of the monosaccharide. After formal insertion of HCOH-groups to aldohexoses or hexuloses different diastereomers are created. Also in carbohydrate chemistry the term “epimer” is quite often used for diastereomers in which just the hydroxyl group attached to the adjacent carbon atom of the carbonyl group differs.

Due to the presence of a carbonyl group and different hydroxyl groups inter- or intramolecular acetalisation can occur. Entropically favoured is the intramolecular reaction since acyclic hemiacetals formed by the intermolecular reaction are known to be labile. The intramolecular cyclisation reaction can take place on different hydroxyl groups which leads to the formation of five- or six-membered rings known as the furanose or pyranose form of the saccharide. Depending on the site of nucleophilic attack of the hydroxyl group to the carbonyl function two different configurations at C1 (the anomeric centre) are possible. The two forms, α or β , can be distinguished by the relationship between the stereochemistries of the anomeric carbon and the carbon most distant from the anomeric centre. If they are in a *cis*-conformation it is indicated as α -anomer compared to the β -anomer in which these hydroxyl groups are *trans*-aligned.

After solubilisation of a saccharide intramolecular cyclisation starts to occur. This interconversion known as mutarotation leads to the formation of a mixture between the different anomers and ring forms (Figure 3).

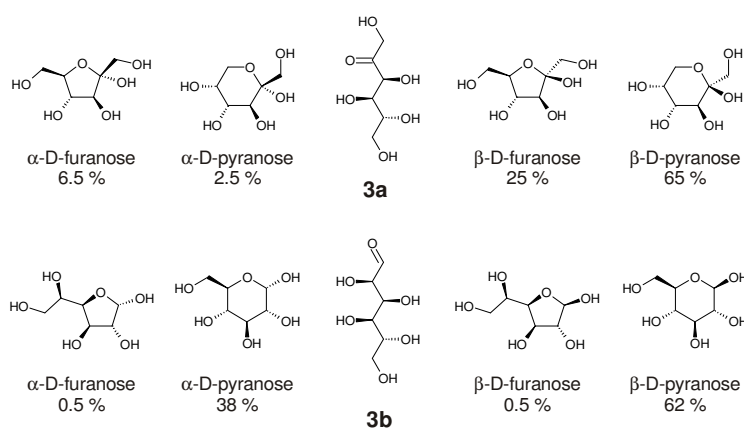


Figure 3. Mutarotation of D-fructose **3a** and D-glucose **3b** and the relative distribution of their anomers in water at 25°C or 31°C, respectively

The composition of different anomers and ring forms is strongly dependent on the saccharide itself and its environment. Thus, it is influenced by solvent, temperature or pH value. The degree of mutarotation can be monitored by the torsion angle of the solution since it is a time-dependent process until equilibrium is reached. In this respect, for example, the β -pyranose form in a mixture of **3b** in water at 31°C is the predominant species with 62% followed by the

α -D-pyranose with 38%.⁸⁰ Importantly, recognition of saccharides, for example by enzymes such as the glucose oxidase which is able to bind just the β -anomer, or synthetic receptors, only favours the binding of one anomer.^{57,108} After binding, the solution starts to interconvert again to the initial equilibrium. To obtain a faster equilibrium between the different saccharide anomers an enzyme called mutarotase is able to interconvert saccharides to a specific anomeric form.

Different derivatives of saccharides exist (Figure 4). Of particular interest are derivatives which possess other heteroatoms such as nitrogen **5**, sulphur **6** or carbon **7** instead of the endocyclic oxygen.¹⁰⁹⁻¹¹² These derivatives are used for different applications, *e.g.* as therapeutic agents due to their differences in geometry, conformation, ability to mutarotate, flexibility, polarisation and electronegativity. In addition saccharide-like structures are also described in the literature. One prominent example are cyclitols which are cyclic polyhydroxyalkanes possessing, in the case of inositols (here: *myo*-inositol **8**) six-membered rings with six hydroxyl functionalities in different stereochemical orientations. Another kind of polyhydroxyalkanes which have a linear conformation is the group of alditols, such as sorbitol **9**. They are synthesised by mild reduction of aldoses and ketoses.

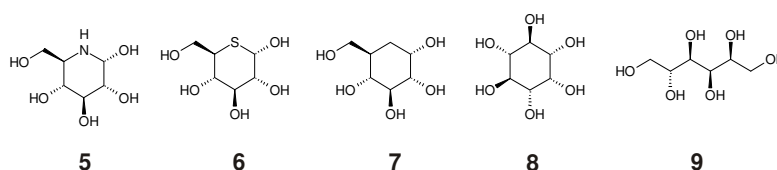


Figure 4. Derivatives of glucose possessing different heteroatoms such as nitrogen **5**, sulphur **6** or carbon **7** (saccharide derivatives) and saccharide-like structures such as *myo*-inositol **8** and sorbitol **9**

Since numerous hydroxyl groups are attached to the carbohydrate backbone hydrogen bonds are easily formed between different hydroxyl groups of saccharides and, in aqueous environment, with water molecules. In general, saccharide molecules solubilised in water are surrounded by a water shell. Moreover, the influence between water and saccharides is concentration dependent. At low concentrations saccharides are able to interpenetrate the water clusters acting as “structure-breakers” whereas at high concentrations it has been shown that saccharides are forming structures and are therefore referred as “structure-makers”.¹¹³ The high probability of the water-saccharide interaction and the chemical similarity between the hydroxyl groups are problems to be circumvented in saccharide recognition.¹¹⁴

2.3.3 Supramolecular chemistry – Forces

Beside biological recognition elements artificial units can be designed and synthesised with special functionalities for specific analytes. Here, in many cases principles which are found in biological systems, such as in enzymes or antibodies, are being transferred in so-called biomimetic receptors. Furthermore, principles not found in biological systems can also be used. Nevertheless, in both cases the intra- and intermolecular interactions between the guest and its synthetic host have to be considered.

In biological systems mainly intermolecular forces are found and can be distinguished. They can be described by electromagnetic forces which are repulsive or attractive between two molecules which are in proximity.

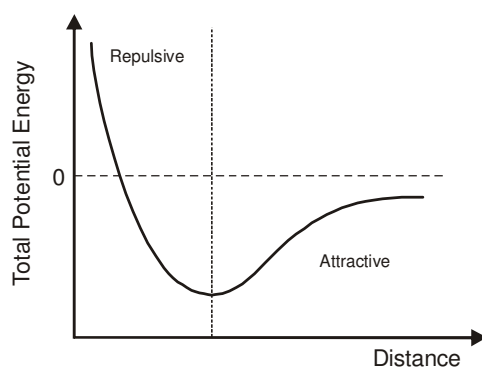


Figure 5. Dependence of the total potential energy and the distance of two approaching molecules described as Lennard-Jones potential

This principle can be described by the Lennard-Jones-potential and is based on the interactions of subatomic charged nuclei and electrons and their interaction with subatomic particles of another atom.⁷³ Depending on the distance of the atoms these forces can be attractive or at much shorter distances turn to be repulsive. If a molecule approaches another the forces between them are attractive and result in a lowering of the overall potential energy until at a certain distance an energy minimum is reached (Figure 5). Beyond this minimum the forces are repelling because the effect of charge-to-charge interactions between the electrons becomes evident. The force F between two molecules can be derived from the Lennard-Jones-potential by the first derivative of the energy E with respect to their distance s (1).

$$F = \frac{dE}{ds} \quad (1)$$

Depending on their chemical nature, the different intermolecular forces can be categorised. The most common type of interactions is hydrogen bonding. Hydrogen bonds are

formed with molecules in which a hydrogen atom is attached to a strong electronegative atom such as oxygen, nitrogen or fluorine. Due to the large difference in electronegativity a dipole is formed, the hydrogen atom becomes partially charged and can interact with a free lone pair of an atom in proximity. Hydrogen bonds are found in many cases for intermolecular interactions and their character is highly cooperative. Other types of interactions are dependent on the interplay between ions, dipoles and induced dipoles. Depending on the particular combination, the forces can be distinguished between ionic (ion-ion, Coulomb), ion-dipole, ion-induced dipole, dipole-dipole (Keesom), dipole-induced dipole (Debye) and induced dipole-induced dipole interactions.¹¹⁵⁻¹¹⁷ In some substances, a dipole can be induced because the electron distribution within the atom is not symmetric and fluctuations in the partial polarisation of the atom occur. A certain amount of distortion is created and can be influenced by external forces such as ions, dipoles or other neutral molecules with a different electron distortion. The degree to which neutral molecules can be influenced by others is called polarisability.

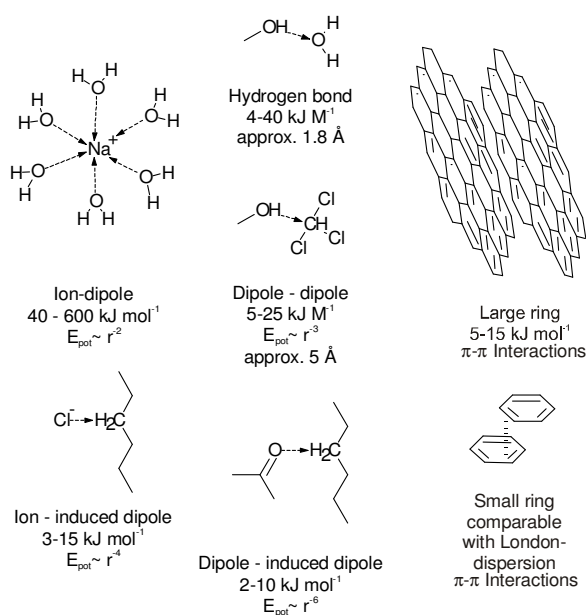


Figure 6. Possible intermolecular forces and their physicochemical properties in terms of binding strength and characteristics

Furthermore, hydrophobic interactions such as π - π stacking or π -CH interactions play a huge role in molecular recognition. If a small number of ring atoms are involved in the binding, the binding can be described by London dispersion forces. This is also true for π -CH interactions in which the CH acts as a donor and the π -system as an acceptor. For example, it is reported that the same energies for interactions can be found for saturated hydrocarbons of the same size compared with unsaturated ring systems.¹¹⁸ Therefore, the interaction between two small hydrophobic entities has a contribution by dispersion interaction whose strength is comparably

small. In addition, the proximity of these entities influences the overall surface energy because a smaller surface area is exposed to compounds which are more hydrophilic. This principle, also found in many systems which form inclusion sites for host molecules, leads to higher and favoured binding strength. For larger ring systems the overlap of the π -systems of proximal rings leads to a real interplay between electrons within their p-orbitals.

The properties of the different interactions vary significantly in terms of strength and distance dependency (Figure 6). For example ion-dipole interactions exhibit a strength between 40-600 kJ mol⁻¹ and a distance dependency of r^{-2} London dispersion forces have a strength up to 40 kJ mol⁻¹ and a distance dependency of r^{-6} .¹¹⁵ In addition intermolecular forces are strongly governed by environmental parameters such as pH, temperature and solvent.

Beside intermolecular forces intramolecular forces can also be found in nature. These are covalent, ionic and metal bonding. A covalent bond is formed when two non-metal atoms are able to form a molecule by sharing their electrons. The driving force for a covalent linkage is the fulfilment of eight electrons in the outer shell of the atoms leading to more stability. If the difference of electronegativity between the two atoms forming the bond is high, the electrons to fill the outer shell will stay at the atom of higher electronegativity. In this case an ionic bond is formed. For metal bonding the electron shell of each metal atom is overlapping in a way that the electrons are able to move freely between the atoms leading to an electron cloud. For molecular recognition in general intramolecular forces play a secondary role. Only covalent bonds are described for molecular recognition which are cleavable upon change in pH or temperature. For example, the formation of Schiff's bases or boronic acid esters as cleavable covalent bonds are used in artificial receptors for the recognition of targeted substances.¹¹⁹

For recognition of saccharides in synthetic receptors an elaborated interplay of different forces has to be developed because saccharides interact strongly with hydroxyl groups of the water by hydrogen bonding and are therefore wrapped in a water shell.^{26,114} Furthermore the recognition unit has to distinguish between these two types of hydroxyl groups and therefore many examples are described for organic, non-aqueous environments. Mostly organised macrocyclic structures act as host and deliver a binding pocket which is hydrophobic in character, similar to binding pockets found in nature for saccharide binding. On the outer shell of the molecule there are different functionalities for delivering the possibility for hydrogen bonding (mostly hydroxyl groups) or ionic interactions (phosphate groups or carboxyl acids).^{120,121} So far recognition elements based on porphyrins, calixarenes, cyclodextrines, cholophenes (steroid based), resorcinols and resocarenes have been used.²⁶ For all different synthetic approaches a considerable synthetic effort has to be undertaken. Therefore, a more generic approach for specific recognition elements is required which is easy-adaptable for the recognition of target molecule.

2.3.4 Molecular imprinting

Molecular imprinting is a technique used to insert artificial binding pockets into a polymeric network on a molecular level for the detection of different analytes (Figure 7).^{19,22,32} In the process of molecular imprinting, a polymerisation is carried out in the presence of the target analyte (here: called template). By adding a functional monomer to the polymerisation mixture which can interact with the template molecule in a covalent, non-covalent or metal coordinated way a template-functional monomer complex is formed. This mixture is then polymerised leading to a polymer with incorporated template molecules. Due to the chemical nature of the template-functional monomer complex the binding is cleavable and so the template molecule can be washed out leaving an artificial cavity in which the template molecule - in this case now the analyte - can bind again. By utilising crosslinking agents (forming the polymeric backbone) selectivity is obtained through the rigidity/morphology of the polymer.

Dependent upon the kind of interaction between functional monomers and template molecules different imprinting approaches can be categorised. The most common method for the preparation of molecularly imprinted polymers (MIPs) is the non-covalent approach which is based on different types of intermolecular interactions.^{122,123} Here, hydrogen bonds, electrostatic and hydrophobic forces are used as interactions between the functional monomer and the template complex. Alongside the non-covalent approach there is also the possibility of using complementary functional monomers.^{124,125} Here, the interaction between the functional monomer and the template is dependent on a variety of different forces *e.g.* hydrogen bonds in a distinct alignment. More general is that during the synthesis of the polymer a large amount of functional monomer is used to force the complexation to occur since there is thermal motion which interferes with the association. Consequently, the template-functional monomer complex is not too rigid during polymerisation leading to a heterogeneous recognition site distribution. The most well-known functional monomer for this purpose is methacrylic acid (MAA).^{126,127}

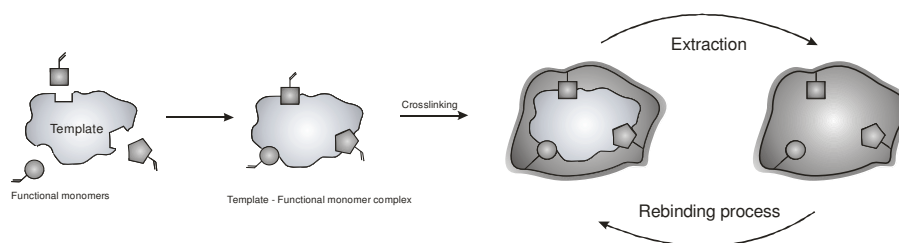


Figure 7. Synthesis scheme of molecular imprinting; creation of the functional monomer – template complex, the polymerisation and subsequent extraction and rebinding process

One possibility to circumvent a heterogeneous binding site distribution is described by the covalent imprinting approach.^{119,128} Here, the template-functional monomer complex is covalent and therefore a fixed stoichiometry is provided during the polymerisation. After polymerisation the covalent bond is cleaved dependent on the type of interaction, for example by changing the pH of the solution. Different bond types are described and among others Schiff bases, boronates, ketals, carboxylic amides and esters have been applied. The most interesting and historically most important functional monomers for the covalent imprinting approach are boronates.^{34,35,37} Boronic acid esters are formed between boronic acids as functional monomers and different saccharides as template molecules. A major drawback of this system is rebinding since the creation of a covalent bond is, in kinetic terms, slow compared to the easily formed hydrogen bonding or electrostatic interactions. Therefore, more recently the semi-covalent approach has been developed in which the initial functional monomer-template complex is covalent and, by the introduction of a sacrificial spacer, the rebinding is non-covalent.^{129,130} Another important type of interaction is (metal-) coordination since many reactions can take place on a coordination basis.^{131,132} In all cases, the polymeric backbone forming the binding pocket itself has an important influence on recognition because of its properties in terms of possible interactions or rigidity.

In more detail, imprinting of saccharides is performed by many groups and covalent, non-covalent and metal-coordinated approaches have been described. For example, Mosbach *et al.* described a non-covalent molecularly imprinted polymer with p-nitrophenyl- α -D-galactoside in ethylene glycol dimethacrylate (EGDMA) crosslinked polymers.¹³³ More recently, sucrose has been imprinted with MAA and EGDMA for aqueous rebinding.¹³⁴ Metal coordination is also a well-known method used to bind saccharides by incorporating copper-ligands as functional monomer into a molecularly imprinted polymer.^{135,136} As described already above, more prominent are arylboronic acids which are incorporated into polymeric networks since they are able to form a cleavable, but still covalent bond with *cis*-diol containing compounds. The work on boronic acids in molecular imprinting was initiated by Wulff in the 1970s. Whereas Wulff described imprinting in 3D-structures, recent examples have been described and principles ranging from 0D in fullerenes, over 1D in linear cationic and anionic polymers to 2D structures in poly-L-lysine have been reported.¹³⁷⁻¹⁴⁰

The imprinting of glucose **3b** and fructose **3a**, in special, has been described by many groups. Some trends can be derived (detailed list of different systems for glucose, fructose or fructosyl-valine imprinting; see Appendix Table A1^{39,141-158}). Mostly, polymers such as N-isopropylacrylamide and EGDMA have been employed. Many attempts were undertaken by Peppers *et al.* to imprint glucose-6-barium phosphate as a model compound into PAA-HCl polymers with epichlorohydrin as a crosslinking agent.¹⁴⁸ They proved that rebinding with a fluorescently labelled glucose was possible. Surprisingly, a reinvestigation by Fazal and Hansen

revealed that no imprinting on a molecular scale was possible within this polymer.¹⁵⁹ The rebinding was rather explained by differences in template solubility within the polymer which is not the case for acrylamide and methacrylic polymers.

Described systems for D-glucose **3b** imprinting are mainly based on non-covalent or metal-coordinated interactions. In the case of D-fructose **3a** more boronic acid based functional monomers have been reported. Beside bulk polymers some examples of elaborated polymeric structures such as core-shell nanoparticles, dendrimers or star-shaped polymers have been described. The rebinding is mostly conducted in deionised water with the pH not specified. In some examples, especially for imprinting with arylboronic acids, pH-values above 10 are used but there are also examples given for rebinding of fructose at pH 7.4 in PBS (phosphate buffered saline). Noteworthy is a polymer prepared on N, N'-bisacrylamide as monomer with a polymerisable Cu²⁺-ligand which binds glucose from porcine serum at pH 10.¹⁵²

2.3.5 Boronic acids

Boronic acids, in general, are trivalent boron containing compounds with one alkyl or aryl substituent and two hydroxyl groups.¹⁶⁰ Hence, the sp²-hybridised boron atom lacks two electrons and therefore possesses a vacant p-orbital. With its mild organic Lewis-acid character, boronic acids are attractive building blocks in organic synthesis. There exist a variety of different organic reactions which can be conducted with boronic acids or their esters as starting materials.^{160,161} The best known synthesis is the Suzuki cross-coupling using boronic acids and Pt or Pd catalyst for C-C bond formation.¹⁶²⁻¹⁶⁴ Other applications for boronic acids as a starting material can be found in metallation, oxygenation, amination and halogenation.¹⁶⁵⁻¹⁶⁹ Furthermore, boronic acids have also been used as catalysts for amidation reaction or click-chemistry, to name two recent examples.^{170,171} Boronic acids are also used in organic synthesis, for example as antimicrobial agents, enzyme inhibitors (due to their analogy to sp³-hybridised carbon), and protecting groups.¹⁷²⁻¹⁷⁴ It can be divided between alkyl- and arylboronic acids. Nevertheless, due to the higher stability of alkylboronic acids they are more frequently used, for example, in saccharide sensing.²⁸

In contrast to synthetic receptors for saccharides which form non-covalent interactions to the saccharide, boronic acids are widely used for the covalent binding to 1,2- or 1,3- *cis*-diols which are present in saccharides (Figure 8).^{29,175} In general, boronic acids form esters analogous to carboxylic acids by replacement of their hydroxyl groups. Possibly alkoxy and aryloxy groups can undergo esterification leading to a more apolar product since the hydrogen donor capability of the boronic acid is lost.^{176,177}

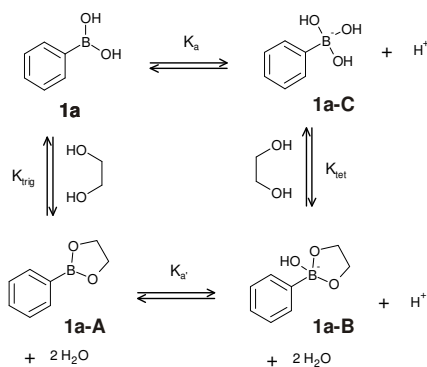


Figure 8. Binding equilibria of phenylboronic acid **1a** with *cis*-diols and the coordination of hydroxyl ions to the boron centre

In literature, the formation of esters with monoalcohols such as methanol has been described but the formation of a cyclic ester with 1,2- or 1,3- *cis*-diols is more favoured.¹⁷⁸⁻¹⁸⁰ This esterification is moreover of importance for organic synthesis and mainly steric demanding ligands are used to have access to stereo delegating catalysts or reactants such as a cyclopropyl boronic acid ester.^{181,182} In most cases, the esterification can be conducted by normal stirring if the boronic acid ester formed is insoluble in the solvent which acts as the driving force.¹⁸³ Also, either azeotropic distillation or the addition of a dehydrating agent is used to eliminate the water produced during the reaction to drive the equilibrium to the product side. Beside these methods the *trans*-esterification of a boronic acid ester with a volatile ester group such as methanol can be performed by distillation of the volatile compound.

In case of the formation of a saccharide-boronic acid ester the esterification is especially challenging in an aqueous environment. Böseken has described the synthesis procedures of different saccharide boric acid - esters which were used later on in analogy for boronic acids.^{184,185} Later works by Kuivila and Lorand and Edwards revealed that the esterification is favoured at alkaline pH values which underline the Lewis-acid character of the boron and the possible coordination of hydroxyl ions to the boron.^{183,186,187} The experimental finding was that, after a pH equilibration of a phenylboronic acid **1a** solution and subsequent addition of a saccharide, the pH of the solution decreased. This led to the conclusion that not only the trigonal boronic acid **1a-A** but also a tetrahedral form **1a-B** exists which releases one proton after coordination with a water molecule (Figure 8).³⁰

The saccharide – boronic acid interaction is known to be a delicate equilibrium between the acidity constant K_a for the acidity of the boronic acid, K_a' – the acidity constant for the ester and K_{tet} and K_{trig} which are the equilibrium constants for the esterification of the boronate **1a-C** and the boronic acid **1a**, respectively. Furthermore, the predominant esterification of the boronate **1a-C** species can be described thermodynamically by taking the ring strain of the cyclic ester into account. When a hydroxyl group coordinates to the boron of a cyclic boronic ester a change in

hybridisation from sp^2 to sp^3 occurs accompanied by a decrease in angle strain from 113° to 109.5° (Figure 9).^{188,189}

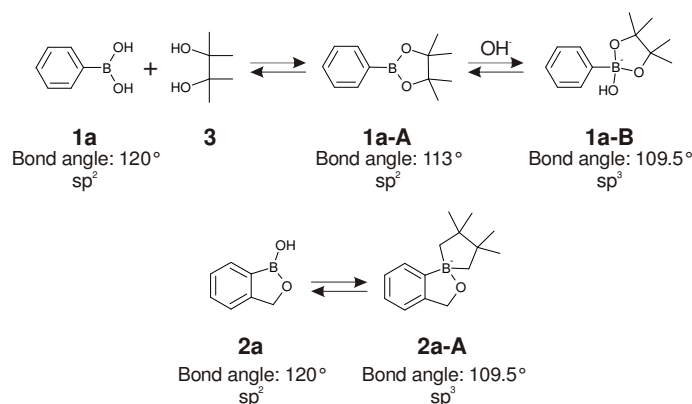


Figure 9. Comparison of esterification and ring strain between phenylboronic acid **1a** or benzoboroxole **2a** and *cis*-diol containing compounds **3**

Therefore, the esterification of unsubstituted phenylboronic acids **1a** is favoured in alkaline environment. Experimentally, the binding constant increases with increasing pH. For example, the binding constant for fructose increases about two orders of magnitude from 4.8 M^{-1} at pH 5.8 to 560 M^{-1} at pH 8.5.³⁰ It has been stated that the optimal binding pH value between a boronic acid derivative and a diol is dependent on their pK_a values and can be estimated by the following equation:

$$pH_{\text{optimal}} = \frac{pK_a(\text{Diol}) + pK_a(\text{BA})}{2} \quad (2)$$

The pK_a of the boronic acid can be approximated by taking the Hammett-plot into account.³⁸ It was found that, for recognition of saccharides in physiological media, the boronic acid has to exhibit a low pK_a value. This can be accomplished by the insertion of electron-withdrawing groups such as fluoro- and nitro-. Furthermore, another possible way to reduce the binding pH is the use of intramolecular donor functions in the *ortho*-position to the boron (Figure 10). Wulff *et al.* synthesised different boronic acid derivatives with proximal intramolecular donor functionalities (hemilabile ligands) such as amines **10** for saccharide recognition, undergoing a dative bond formation.^{190,191} These derivatised boronic acids were embedded into a polymeric matrix and used within molecularly imprinted polymers.¹⁹² Lowe *et al.* showed the coordination of boron with the lone pair of a carbonyl-group within an amide bond **11** in a crystal structure.¹⁹³ More recently, Hall and *co-workers* studied a boronic acid derivative with a hydroxyl group in the *ortho*-position to the boron called benzoboroxole **2a**.^{27,40} Due to the strong interaction

between boron and oxygen a covalent intramolecular B-O bond is formed, which is also stable at pH 7.4 and reduces therefore the ring strain to 109.5° (Figure 9). This intramolecular bond formation favours the hybridisation change from sp^2 (**2a**) to sp^3 (**2a-A**) leading to a release of ring strain of a formed boronic acid ester (Figure 9).

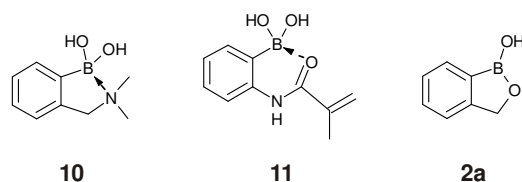


Figure 10. Different boronic acid derivatives with intramolecular donor functions^{40,192,193}

Growing interest in **2a** as the binding unit for the binding of carbohydrates at pH 7.4 has been shown recently. Hall and *co-workers* reported a derivative of **2a** as the saccharide recognition unit attached to a peptidic backbone for the targeted recognition of the Thomson-Friedenreich antigen.¹⁹⁴ Furthermore, Jay *et al.* described a polymeric network with attached entities of **2a** for the recognition of the glycoprotein 120 on HI viruses.¹⁹⁵

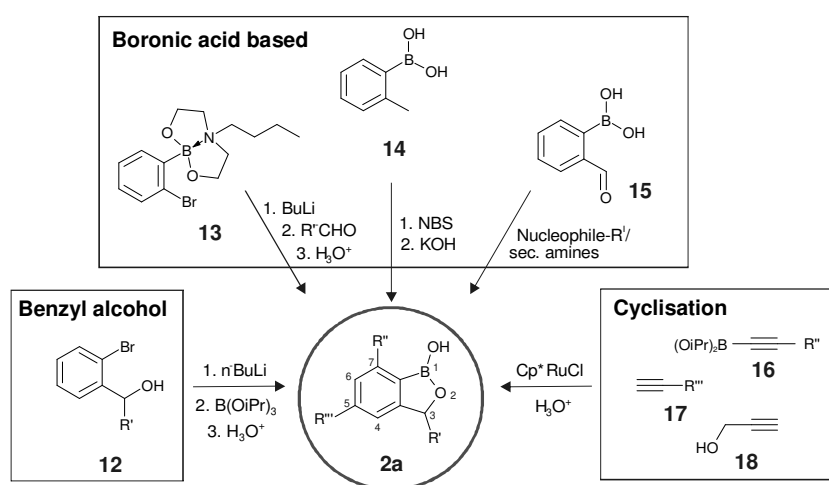


Figure 11. Different synthesis methods for benzoboroxole derivatives **2** starting either from benzyl alcohol **12**, arylboronic acids **13-15** and linear substrates **16-18** for cyclisation

Differentially substituted benzoboroxoles **2** can be synthesised by a variety of different methods (Figure 11).^{196,197} In general, three different starting materials can be chosen. Firstly, direct reaction of *ortho*-substituted arylboronic acids **13-15** can lead to different benzoboroxole derivatives **2**.^{198,199} Protection as MIDA **13** or other boronic acid esters is sometimes helpful to obtain higher yields.²⁰⁰ Employing this method, a substitution at the phenyl ring and in the

3-position (R' , methylene group) is possible. Also, via synthesis starting from benzyl alcohols **12** in the *ortho*-position to the bromine can lead to derivatised benzoboroxoles **2**.²⁰¹ Substituted benzoboroxoles **2** in positions 5 and 7 are able to be synthesised by cyclotrimerisation starting from three linear alkine derivatives **16-18**.²⁰²

A variety of different arylboronic acid derivatives for saccharide recognition have been described (Figure 12).²⁸ Many different principles for the detection are also reported and ranges from receptors with fluorescence shift, energy transfer systems, colourimetric changes and electrochemical properties. One of the first fluorescent sensors for saccharides was 2-anthryl boronic acid **19** which changes its fluorescence intensity upon binding and formation of a boronate ion.²⁰³ A shift in fluorescence can also take place through intramolecular coordination of the nitrogen's electron lone pair. In a phenylboronic acid derivative **20** which is attached to an anthracene unit *via* a tertiary amine linker the amine function can coordinate to the boron leading to a fluorescence shift and hence to an analytical signal.^{204,205} The anthracene unit enhances the binding due to a possible hydrophobic interaction with the C6-ring of the saccharide. These approaches tend to bind non-selectively. Consequently, efforts were also undertaken to bind selectively to saccharides such as glucose. For example, a computer based-calculation was conducted to design a diboronic acid **21** towards glycopyranoside which changes its fluorescence upon binding of glucose.²⁰⁶ Another approach was described by Heagy and *co-workers*.^{207,208} They synthesised a naphthalimide derivative **22** whose fluorescence is quenched after binding to a saccharide. Interestingly, the recognition behaviour and sensitivity was influenced by the synthesis of different derivatives. In particular, the nitro-derivative **22** exhibits a selective sensitivity to glucose.²⁰¹

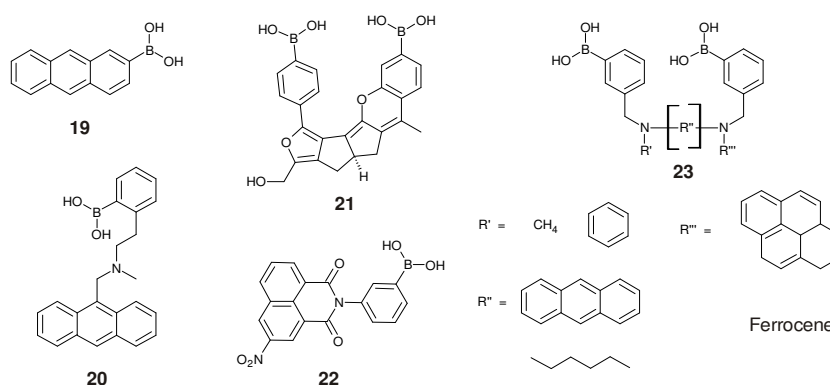


Figure 12. Different reported boronic acid based saccharide sensors with different principle of detection ranging from fluorescence to electrochemistry¹⁹⁷⁻²⁰³

Furthermore, considerable efforts have been made to design empirically a diboronic acid sensor **23** selective for glucose **3b** with different principles of detection such as PET or

electrochemistry (Figure 12).^{205,209} To obtain the glucose selectivity, the linker unit was varied to find a glucose specific recognition unit. It was found that a C6-distance between the boronic acid entities enhances the glucose selectivity.

In general, the mechanism and structure of the fructose and glucose-arylboronic acid complexes are crucial for the design of recognition units. From an experimental point of view fructose **3a** exhibits the highest binding constant to boronic acids compared with other saccharides. ¹H- and ¹³C-NMR experiments have revealed different binding structures between p-tolylboronic acid and fructose **3a** (Figure 13).²¹⁰ In an alkaline environment, the dominant complex is a tridentate complex of a p-tolylboronic acid with fructose. Bidentate complexes were also reported but to a minor extent. By increasing the boronic acid concentration diboronic complexes are formed and in a ratio of 4:1 almost 60% of the esters formed are diboronic. In this case, the tridentate form is still present with 40%.

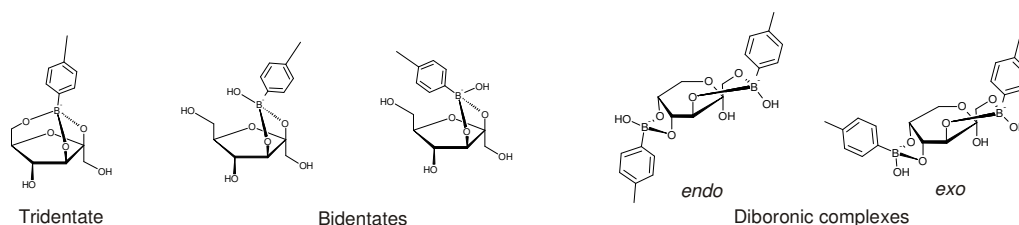


Figure 13. Different fructose boronic acid complexes revealed by ¹H- and ¹³C-NMR spectroscopy²¹⁰

By comparing the proposed binding complexes with the different anomers present during the mutarotation of fructose **3a**, it can be concluded that the binding form, in this case the β -D-fructofuranose form, exists in aqueous solution at around 25%. **3a** binds favourably to boronic acids because of the high presence of *syn*-periplanar hydroxyl groups in this anomer. This can explain the different binding constants to other saccharides such as galactose **24**, mannose **25** or glucose **3b** (Figure 14).^{211,212}

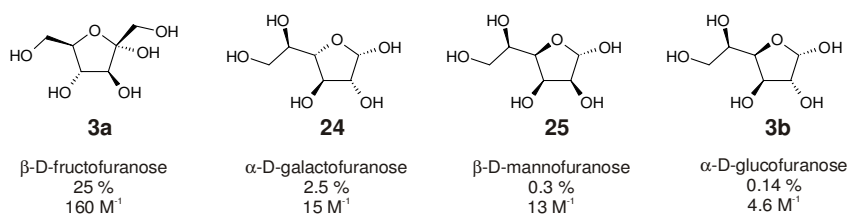


Figure 14. Saccharide anomers with *syn*-periplanar arrangements, their percentage in D₂O and binding constants with ARS at pH 7.4³⁰

In case of glucose **3b**, the complex formation is described to be more difficult.²¹³ For a diboronic sensor **23** (R^H =anthracene), prepared by Shinkai *et al.* it has been shown that glucose forms initially to complex **26** with the α -D-pyranose as the binding form (Figure 15). Then, the α -D-glucopyranose converts depending on the solvent to the α -D-glucofuranose leading to complex **27**.^{204,214}

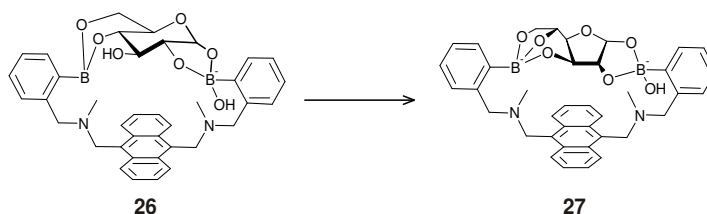


Figure 15. Intramolecular arrangement of glucose **3b** after binding to a diboronic receptor **23** which initially binds in a pyranose form **26** and changes its conformation to the furanose **27** form^{204,214}

2.3.6 Polymeric systems for saccharide recognition

The use of polymeric systems with incorporated boronic acid entities has been described by many authors because of the possibility of forming the functional polymer in a manner which suits the application of interest (See Appendix Table A2 for detailed list of recent reported boronic acid containing polymers).²¹⁵⁻²³¹ A variety of different systems has been described. In general, there is a difference between systems in which a polymerisable boronic acid derivative is employed or systems which are post-modified after the polymer synthesis. In many cases as polymerisable derivatives boronic acids with a vinyl- (**1e** or **1f**) or methacrylamido- (**1d** or **2d**) residue are used. For surface modifications mainly nucleophilic substituents for example amino- (**1c** or **2c**) or thio- substituted boronic acids have been applied. Furthermore, the incorporation of receptors which are already known for the recognition of saccharides in solution into polymeric networks has been investigated and changes in their performance have been described. Depending on the system used, the selectivity and especially the cross-reactivity was altered. For example, in a very recent example a derivative of the diboronic saccharide receptor **23** has been incorporated into a hydrogel for *in-vivo* continuous glucose monitoring.²³²

Although there are many applications for boronic acid containing polymers most applications are found in saccharide sensing or sensing of *cis*-diol containing compounds such as NADH or AMP. Saccharide sensing can be divided into different application categories. Nevertheless, in most cases acrylamidophenyl boronic acid **1d** is employed as a monomer during the synthesis of an acrylamide backbone. As a crosslinker N,N-bisacrylamide is often used. As described above, due to the good compatibility of polyacrylamides in systems for *in-vivo* use

efforts have been undertaken to use these systems as recognition elements for continuous glucose monitoring (CGM).²³² The required property of the hydrogel formed is that the saccharide can bind to the boronic acid entity which correlates with a volume change due to the change in hydrophilicity of the polymer. By inclusion of glucose **3b**, the boronic acid becomes negatively charged and water can easily diffuse into the gel leading to a change of the volume of the polymer. In addition, glucose can act as a crosslinking agent within the polymeric network and again the volume of the polymer changes. This change can, for some applications, be monitored by optical devices such as holographic sensors. Beside the sensor application, a really promising approach has been the use of these polymeric networks with enclosed substances such as insulin which is released after binding of glucose. Here, many different systems and polymeric formats have been described since these could be used as an efficient retarded, glucose-triggered insulin therapy.²³³⁻²³⁷

The format of the polymer has also been altered and systems for films, gels, bulk and particles have been described. In addition, by the use of aminophenyl, hydroxyphenyl or thiophene boronic acids polymer films can be created by means of electropolymerisation.

Boronic acids are also incorporated into polymeric networks for other applications than saccharide recognition. One application is the employment of boronic acids for affinity chromatography. Here, different systems have been described for capillary electrophoresis and analytes ranging from nucleotides to glycoproteins have been reported.²³⁸ Furthermore, the modification of surfaces can be conducted with boronic acid polymer films. For example, the hydrophilicity of a surface may be dramatically changed if boronic acid entities within the polymer can be triggered by the addition of different concentrations of carbohydrates.²²⁸ Thus, changeable polymer coatings can easily be prepared. A possible application for boronic acid containing polymeric films is found in the cultivation of different cells lines.²¹⁷ From the view of materials sciences boron containing films can act *via* addition of fluorides as doped materials in organic semiconductors.^{229,230}

2.4 ASSAY FORMATS

2.4.1 Binding

If a receptor for a certain analyte is created, a crucial step is its characterisation in terms of binding behaviour and the determination of binding constants. In general, different methods have been applied and, depending on the method, different factors have been analysed. In general, the methods can be divided into labelled and label-free methods.^{239,240} Beside their function as a tool for binding characterisation, these methods can also be applied as an analytical read-out in a

sensor assembly. To characterise receptors in solution titration experiments are usually conducted and, dependent on the experimental design, either the change in properties after equilibration (steady-state) or the time-resolved changes (kinetics) have been measured and analysed. In both cases binding constants have been determined since the dissociation constant can be derived either from the law of mass action or the kinetic rate constants (on/off rate). In this regard either the association or the reciprocal dissociation constant can be gained. In this thesis mostly the association constants in M^{-1} are given, whereas in the written context, especially to define ranges of binding constants it is referred to the dissociation constant, *e.g.* mmolar- or mM-range.

The most commonly used method for the characterisation of binding events is spectroscopy. Depending on the system different types such as absorption, fluorescence or NMR could be used.²⁴¹⁻²⁴⁵ In some cases, the internal change of properties, such as absorption maximum differences, are sufficient as an analytical signal. In other cases, a reporter substance has to be used in order to gain an analytical signal. In the wide context of spectroscopy also mass spectrometry can be used to obtain insights into a binding event. Beside spectroscopic methods triggering the optical change of the systems also other methods are applied for the characterisation of a binding event. Very common are methods which are mass-sensitive, *i.e.* the mass increase or decrease of a binding event to a receptor molecule is measured. These analyses are, for example, measured by an oscillating piezo-electric crystal in a quartz crystal microbalance (QCM) device.²⁴⁶⁻²⁴⁸ Depending on the Sauerbrey equation the shift in frequency of the crystal is proportional to the mass increase or decrease. Another very common method, especially used for the determination of binding constants is surface plasmon resonance (SPR).^{249,250} Here, the change in the local refractive index near a gold surface caused by a binding reaction is detected. Beside these methods also electrochemistry or calorimetry can be applied. Since both methods are relevant for this thesis they will be described in more detail in the following chapters. In special for applications in biosensors the most important determination method is electrochemistry since in a typical biosensor the reaction of a redoxactive enzyme with a certain substrate is monitored.^{45,46} Nevertheless, the importance of spectroscopy increases, for example due to the smaller fabrication of diodes as light emitting sources.

For the determination of binding constants of a saccharide - boronic acid interaction, a displacement assay with Alizarin Red S (ARS) **3e** is reported in literature.^{30,38,251} In this case the competition between the *cis*-diol containing dye **3e** and the saccharide is monitored. The determination of binding constants is more complicated since now, not only the binding equilibrium between host and guest has to be considered, but also the equilibrium between the reporter (dye) and the host has to be known and evaluated (for a mathematical description: see Appendix). Since the *cis*-diol groups of the dye are attached to an aromatic system, hence exhibiting a low pK_a , the esterification takes place with a high binding constant of about $1300 M^{-1}$

to phenylboronic acid **1a** in phosphate buffer at pH 7.4. The analytical signal is the change of the wavelength maximum of the free dye (which is red) and the bound dye (yellow).

The determination of binding constants in polymeric systems is different since it is often not possible to monitor directly the binding event. Therefore, batch binding studies have been performed in which the polymer particles have been incubated for a certain time until the equilibrium is reached. The particles were then centrifuged and the supernatant was analysed for unbound analyte. *Via* determination of the free and bound fraction, different mathematical isotherms such as a Langmuirian isotherm have been described and the binding constants were determined.²⁵²⁻²⁵⁴

2.4.2 Calorimetry

In recent years calorimetric methods have gradually become a more and more powerful technique for label-free indication and quantification of binding events.²⁵⁵ In contrast to label-based methods, ITC offers the major advantage of simple sample preparation combined with a fast calorimetric response and thermal equilibration.^{256,257} Furthermore, the major advantage of this technique is that the entire set of thermodynamic parameters, *i.e.* enthalpy ΔH , the free energy ΔG , entropy ΔS , the association constant K and the stoichiometry of the interaction n can be quantified by a single experiment.²⁵⁸

An isothermal titration calorimeter consists of a sample cell, in which the host is placed and a guest molecule is injected *via* a syringe (Figure 16). The temperature change, which depends on the interaction between the host and the guest, is compared with a reference cell which only contains the solvent.

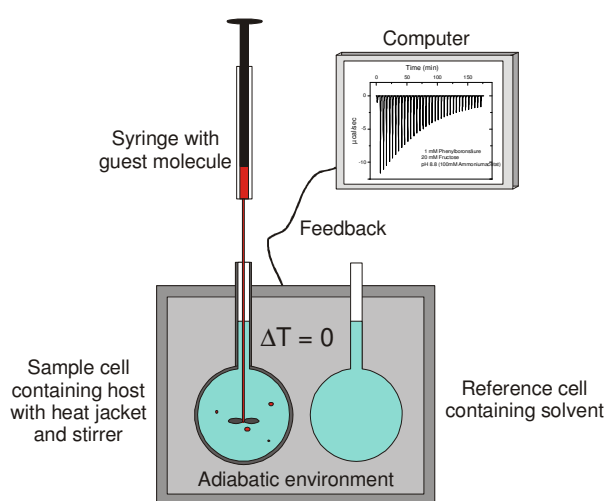


Figure 16. Schematic drawing of an isothermal titration calorimeter; the guest molecule is stepwise inserted via a syringe into the sample cell which contains the receptor

Using a feedback mode, the temperature of the sample cell is either increased or decreased to maintain a temperature difference of zero between the sample and the reference cell.²⁵⁹ The primary analytical signal is therefore the power q which is proportional to the concentration of the ligand ΔL in i^{th} each step combined with the volume of the sample cell v and the binding enthalpy ΔH for this reaction.

$$q_i = v \cdot \Delta H \cdot \Delta L_i \quad (3)$$

The heat for each injection can then be calculated by integration of the peaks obtained from a diagram of q versus time. Considering now the law of mass action, the increase in concentration of the ligand after the i^{th} injection is defined for a possible 1:1 binding in which K is the binding constant of the reaction and $[R]$ the concentration of the receptor within the sample cell.

$$\Delta L_i = [R] \cdot \left[\frac{K [L]_i}{1 + K [L]_i} - \frac{K [L]_{i-1}}{1 + K [L]_{i-1}} \right] \quad (4)$$

Through rearrangement of the equations (3) and (4), an equation with the variables ΔH and K can be created which can be fitted using a Levenberg-Marquardt algorithm. Since in this system the binding proceeds in an equilibrium the Gibbs' free energy is equal to zero. In this regard, the standard Gibbs' free energy ΔG° relates to the binding constant K (5).

$$\Delta G^\circ = -RT \ln K \quad (5)$$

Furhtermore, also the standard entropy ΔS° can be calculated via the Gibbs-Helmholtz equation (6).

$$\Delta S^\circ = \frac{\Delta H^\circ}{T} - \frac{\Delta G^\circ}{T} \quad (6)$$

These standard values describe the system under the chemical equilibrium. In recent literature on isothermal titration calorimetry the thermodynamic data are reported not as standard parameters. According to the van't Hoff'sche reaction isobare, the deviation from equilibrium in the reaction mixture in terms of activity has to be considered.²⁶⁰ Hence, the obtained values are given as ΔG , ΔH and ΔS .

The experimental conditions have to be chosen with respect to the binding constants of the interaction under investigation. For a proper curve fitting to the data obtained a sigmoidal shape of the curve is preferred.²⁶¹ This can be obtained if a dimensionless parameter c ranges from 5 to 500. The parameter c is defined as the product of the stoichiometric factor n , the affinity constant K and the concentration of the receptor in the cell $[R]$:

$$c = n \cdot [R] \cdot K \quad (7).$$

This allows the calculation of the best concentration of the ligand and the receptor.

From an ITC experiment an additive signal is obtained which is composed of many types of actions. Most obviously, a contribution comes from the interaction under investigation. Apart from that, heat signals from mixing two solutions and the dilution heat of both guest and host can be determined. Therefore, crucial for the experimental design are the reference measurements in order to determine the different contributions.

2.4.3 Electrochemistry

One prominent example for an easy and commercially used assay method is electrochemistry.^{45,46} Here, electron transfer processes can be followed *via* cyclic voltammetric measurements and shows the redox reaction at the electrode/solution interface. In a three-electrode assembly the current is measured after alteration of the voltage. In the three-electrode assembly the working and counter electrodes are used to measure the current, whereas the reference electrode is used to avoid overpotentials. By applying a voltage, anodic oxidations and cathodic reduction can be determined which can be differentiated by altering the algebraic sign of the voltage direction.

A redox reaction can be evaluated by measuring a cyclic voltammogram. The peak potentials for the cathodic and anodic peak E_{pc} and E_{pa} are determined which gives information about the chemical electron transfers taking place. In most cases, if no secondary effects are involved, the intensity represents the concentration of the species and can therefore be used as analytical signal. Different parameters can be derived to characterise the redox processes involved. Of great importance are the midpoint potential $E_{1/2}$ and the peak separation ΔE_p . The midpoint potential shows in case of equimolar concentration of both redox species the redoxpotential of the substance. The peak separation is a parameter for the electron transfer. If the value is about 0 mV the electron transfer is reversible whereas for values over 0 mV the redoxprocess is quasi-reversible or irreversible.

The recognition of saccharides for different applications is an important target since the role of carbohydrates in many scientific fields is evident. Many examples which need a considerable synthetic effort to create a receptor have been described for synthesis of saccharide receptors. The use of polymers can overcome this problem. Beside their easy synthesis the polymeric backbone can influence the binding property to a target molecule.

However, due to the chemical nature of saccharides one predominant problem which is challenging is the recognition of unprotected monosaccharides in aqueous media at pH 7.4 - the competition between hydroxyl groups attached to the carbohydrate scaffold and hydroxyl groups from water. To circumvent this problem, in this thesis boronic acids are employed as primary recognition elements and are attached in different ways onto polymeric networks.

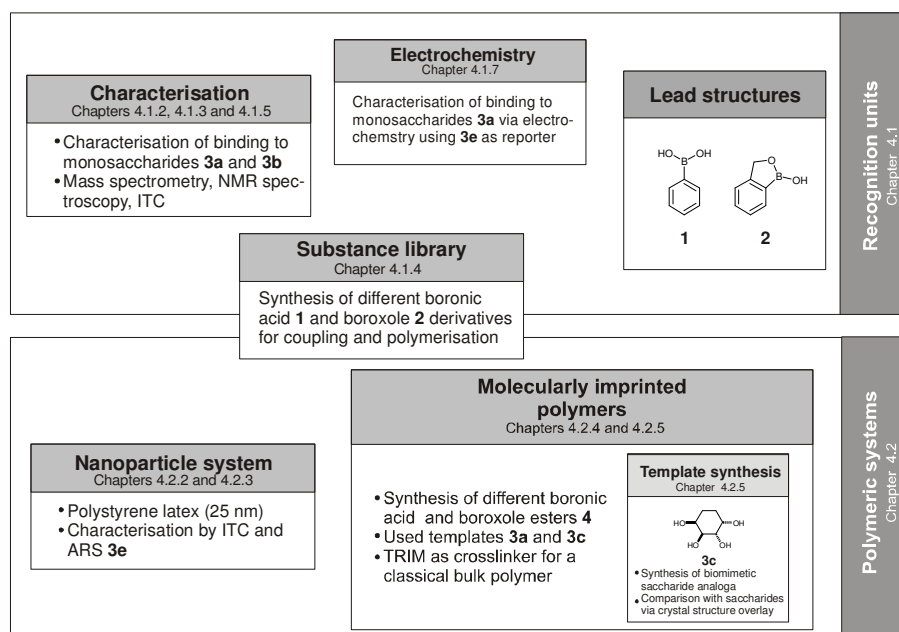


Figure. 17. Scheme of different aspects, key substances and systems of the present thesis

Within this work the following key points are addressed:

- **Synthesis and characterisation of different arylboronic derivatives:**

Since the binding of unsubstituted arylboronic acids to *cis*-diols is known to be favoured at alkaline pH-values, different arylboronic acids are synthesised and

characterised for their binding ability to fructose and glucose. Herein, special attention has been given to an arylboronic acid derivative bearing a methyl hydroxyl-group in *ortho*-position to the boron (called benzoboroxole) because, by intramolecular coordination of the oxygen to the boron, the favoured binding pH can be reduced to pH 7.4. Furthermore, different derivatives are synthesised and compared in order to obtain a variety of substances for different applications. Moreover, the use of Alizarin Red S as reporter dye in an electrochemical set-up for the determination of binding between phenylboronic acid **1a** and fructose **3a** was evaluated.

- **Attachment of selected derivatives to polymeric scaffolds.**

To show the behaviour of selected derivatives to act as recognition elements for saccharides on polymeric scaffolds, nanoparticles have been synthesised and their surface has been subsequently modified. Fructose and glucose were chosen as saccharides and the binding characteristics at pH 7.4 in aqueous media were determined. The characterisation was performed label-free by ITC and UV-Vis spectroscopy making use of Alizarin Red S as a reporter dye.

- **Development of selective artificial recognition units binding saccharides at pH 7.4**

Further selectivity of these boronic acid derivatives to special saccharides was intended. One possibility for the synthesis of artificial binding cavities within a polymeric backbone has been described by the molecular imprinting approach. So, covalently imprinted polymers were developed for fructose recognition at pH 7.4.

- **Development of biomimetic saccharide structures**

Due to mutarotation and the complexity of especially glucose - boronic acid ester interaction biomimetic saccharides were synthesised and used as template molecules within a molecularly imprinted polymer.

4.1 BORONIC ACIDS IN SOLUTION

4.1.1 Introduction

To provide a variety of arylboronic acid derivatives for the following applications (Chapter 4.2) different boronic acids were synthesised. A characterisation of these and commercially available derivatives was undertaken which leads to a deeper knowledge about influences such as electronic effects of side groups or geometrical effects such as intramolecular coordination to the boron. Since the benzoboroxole **2a** is described as boronic acid derivative for saccharide recognition at pH 7.4, the focus was also set on the elucidation of the binding between **2a** and glucose **3b** or fructose **3a**.

Therefore, this chapter is divided into different parts. The first part describes the interaction of **2a** with **3a** or **3b** by means of $^1\text{H-NMR}$ spectroscopy and mass spectrometry to show the characteristics of the formed complexes.

The second part describes the synthesis and the characterisation of phenylboronic acid **1** and benzoboroxole derivatives **2** by means of ITC-experiments. The values obtained were compared to reported data in literature. In these chapters mainly the binding constants are described and discussed whereas in chapter 4.2.2 a detailed discussion about the influences of all determined thermodynamic parameters is given. Furthermore, ITC experiments were conducted (Chapter 4.1.7) in respect to the temperature dependence of the binding constants. The influence of temperature on enthalpy and entropy for the interaction of **3a** and either **1a** or **2a** are discussed.

In the last part of this chapter the electrochemistry of ARS **3e** is characterised. In analogy to the well-established ARS assay using UV-Vis spectroscopy the dye was used as electrochemical reporter to monitor the interaction between **1a** and **3a**.

4.1.2 Binding analysis via $^1\text{H-NMR}$ spectroscopy

$^1\text{H-NMR}$ spectroscopic measurements were performed to analyse the binding of saccharides **3a** and **3b** to the benzoboroxole **2a**. Thus, a solution containing 15 mM of **2a** was prepared in deuterated phosphate buffer at pH 7.4 and either **3a** or **3b** with equimolar concentration were added.^{27,40}

In line with findings by M. Dowlut after addition of fructose or glucose the initial $^1\text{H-NMR}$ spectrum changed.²⁶² In the absence of monosaccharides the $^1\text{H-NMR}$ spectrum of **2a**

showed sharp distinguishable peaks in the aromatic region between 7.3-7.7 ppm (Figure 18, A). By addition of either fructose **3a** or glucose **3b** two different effects could be observed. On one hand additional peaks started to occur. These peaks are mainly found between 7.1 and 7.3 ppm which make them distinguishable from the initial peak set. On the other hand, a peak broadening (combined with a qualitative intensity decrease) of the initial peaks could be observed which can either be due to a slow time scale until the complexation equilibrium is reached or due to the presence of multiple bound conformations.²⁷ It is noteworthy, that the effect of peak broadening and intensity decrease can be found to a greater extent for the interaction between fructose **3a** and **2a**. In this regard it can be assumed due to the higher binding constant between **3a** and **2a** the amount of free **2a** decreases whereas the complex (between 7.1 and 7.3 ppm) starts to increase in intensity. Consequently for the interaction between glucose **3b** and benzoboroxole **2a** a smaller peak broadening could be observed. An estimation of the kinetics of this complexation can hardly be performed since transesterification experiments revealed that the kinetic is strongly dependent on the solvent, the pK_a of the boronic acid and the *cis*-diol, possible steric effects and possible catalysis via ligands which can coordinate to the boron.²⁶³⁻²⁶⁵

The saccharide region between 3.7 - 4.5 ppm (for **3a**) and 3.0-6.0 ppm (for **3b**) shows a similar behaviour. A peak broadening due to the addition of **2a** could be observed in both cases. Furthermore, different additional peaks could be detected which are shifted downfield. This again underlines the slow exchange of the formed ester. In case of fructose significant additional peaks were observed at 4.4 ppm and 4.2 ppm. For glucose different additional peaks could be seen between 4.0 and 5.0 ppm. It is hard to distinguish which of the peaks corresponds to the CH₂ - protons of the borolane ring since this peak shows also a shift due to the formation of the saccharide ester (for the pure **2a** this peak is around 5.0 ppm). In general, the results show that protons within the saccharide are more deshielded after binding to **2a**. Nevertheless, an easy interpretation of these spectra is not possible since the measurement of coupling constants, which are necessary for a further analysis, cannot be performed due to the high peak broadening. Also, a temperature change to sharpen the obtained NMR-peaks will influence the binding behaviour. Maybe, further studies, especially 2D-NMR experiments need to be performed to investigate the binding complexes in parallel to the NMR experiments by Norrild and Eggert.^{210,213}

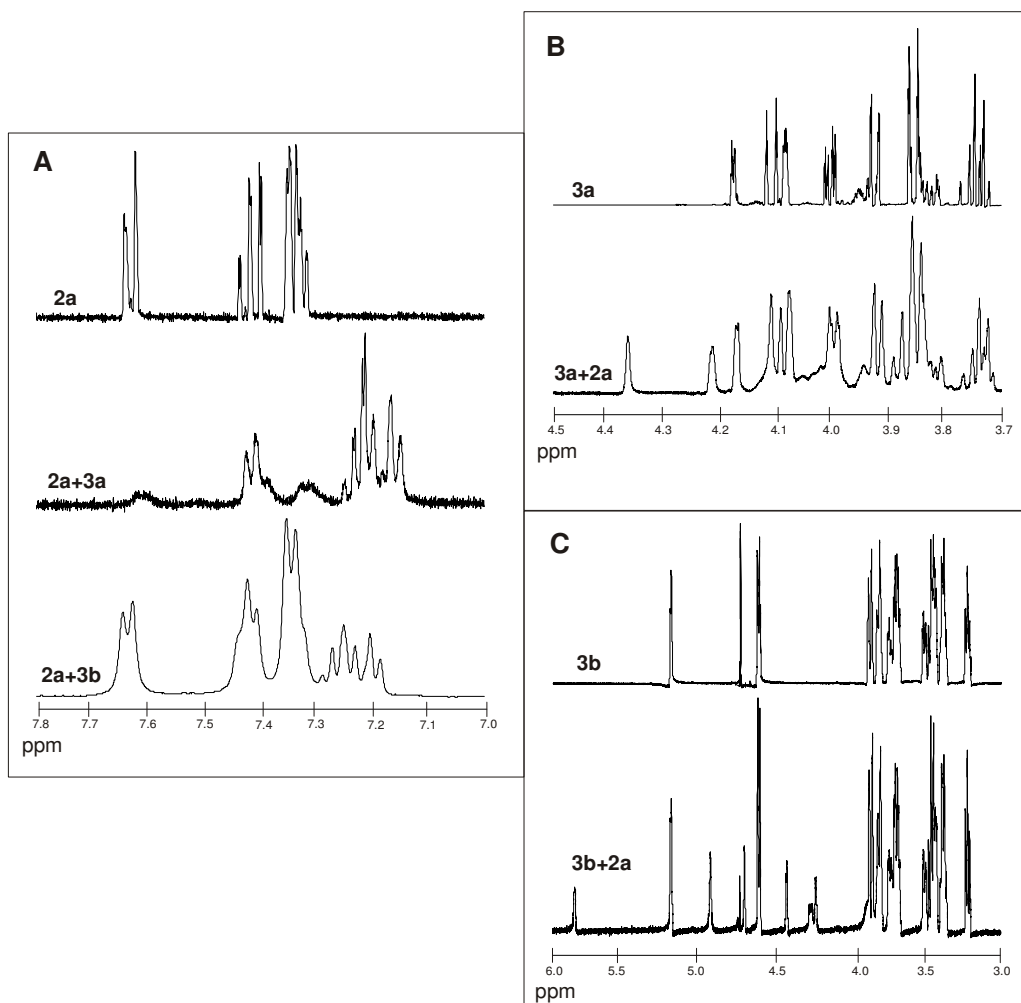


Figure 18. $^1\text{H-NMR}$ spectroscopic data (600 MHz) for the interaction between benzoboroxole **2a** and fructose **3a** or glucose **3b** in D_2O (peak at 4.8 ppm) at pH 7.4 in deuterated phosphate buffer; Displayed are here the aromatic region **A**, and the saccharide regions for fructose **B** and glucose **C**

4.1.3 Mass spectrometry of benzoboroxole-saccharide interaction

In literature different binding structures for fructose and glucose are assigned by different spectroscopic methods and semi-empirical calculations.^{27,210,213} Fructose characterised by a high affinity towards boronic acids forms 1:1 and 1:2 binding patterns, whereas in the case of the 1:1 binding tridentate or bidentate structures are favoured (s. Figure 13). Glucose is described to bind mainly arylboronic acids in a ratio of 1:2 (s. Figure 14). In case of benzoboroxole **2a** and fructose/glucose **3a/b** interactions very little is known about the binding stoichiometries. Therefore, it was necessary to investigate the binding between **2a** and **3a** or **3b**. As described by Hall and *co-workers* the binding stoichiometry can be determined by mass spectrometry employing negative electrospray ionisation.²⁷ Hence, a mixture of 10:1 benzoboroxole **2a** and **3a**

or **3b** was prepared in 1:1 acetonitrile and water mixture and different binding stoichiometries could be observed (Figure 19, Shown here for the interaction with **3a**; but similar results obtained with **3b**).

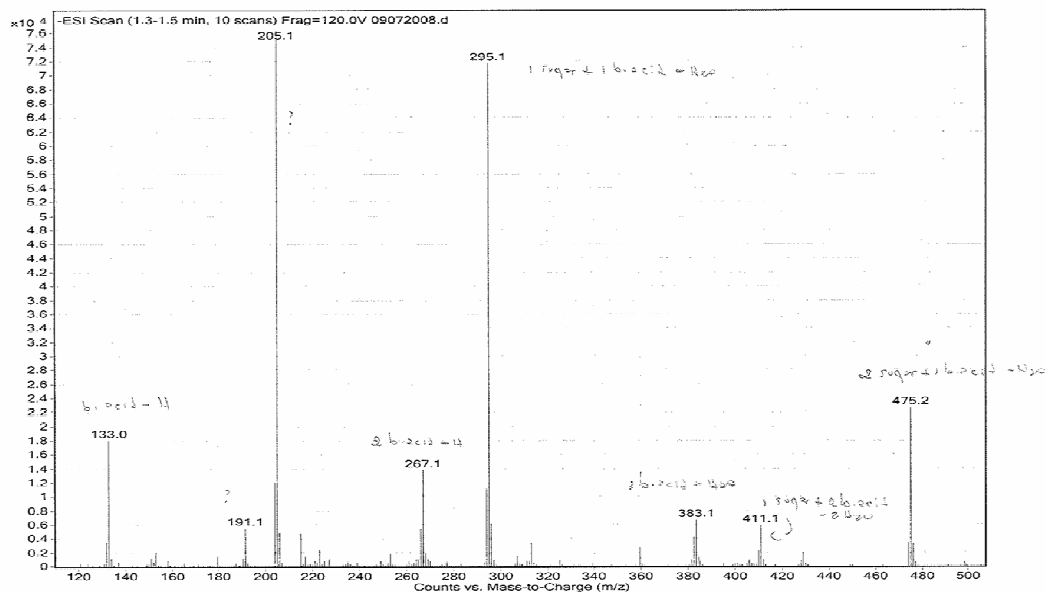


Figure 19. Example mass spectrum (ESI-MS) for the interaction of glucose **3b** and benzoboroxole **2a** in a 1:1 mixture of acetonitrile and water

A large peak at $M = 295.1$ m/z could be detected which can be assigned to a 1:1 binding between fructose/glucose and the benzoboroxole while one water molecule is released. Beside this peak the possible 2:1 binding between the boronic acid and the monosaccharide could be shown by a peak at $M = 411.1$ m/z. Surprisingly, also a 1:2 binding, thus two saccharides binding to one benzoboroxole could be observed with a peak at $M = 475.2$ m/z. Along with these peaks corresponding to the binding complexes also peaks for the individual components could be detected - mainly the formation of anhydrides associating two or three benzoboroxole units (boroxines). The results highlight that principally a 1:1 binding between the benzoboroxole and the monosaccharides is formed in solution and shows that to a less extent other binding stoichiometries are present. It can be assumed that in parallel to the results obtained by Norrild and Eggert the concentration of the interaction partners influences the stoichiometry of the complexes formed. Nevertheless, since the ionisation potentials of all formed compounds are not equal a quantitative conclusion is not possible by mass spectrometry unless appropriate internal standards are found.

4.1.4 Synthesis of compounds

Since just a few arylboronic acid derivatives for coupling to polymeric networks or direct polymerisation are commercially available, five different boronic acids are synthesised to gain combined with commercially available substances a variety of derivatives for different applications (Figure 20). These derivatives were synthesised during a research exchange with Prof. D. G. Hall at the University of Alberta in Edmonton, Canada. Figure 19 shows the different derivatives and divides between commercially available and in this work synthesised derivatives. The commercially available derivatives for the coupling to polymeric networks are 3-aminophenylboronic acid **1c**, 3-carboxyphenyl boronic acid **1b**, 5-Amino-2-hydroxymethylphenylboronic acid, HCl, dehydrate (3-aminobenzoboroxole) **2c** and the 3- or 4-vinylphenylboronic acid **1e** and **1f** as monomers for polymerisation. The synthesised derivatives are two polymerisable derivatives, the 3-methacrylamidophenylboronic acid **1d** and the corresponding benzoboroxole **2d**. Furthermore, for coupling 3-carboxy-2-hydroxymethylphenyl boronic acid (3-carboxybenzoboroxole) **2b** was synthesised and two different chiral benzoboroxoles 1,3-dihydro-1-hydroxy-3-(nitromethyl)-2,1-benzoxaborole **2e** (nitromethylbenzoboroxole) and 1,3-dihydro-1-hydroxy-3-(nitrile)-2,1-benzoxaborole **2f** (nitrilebenzoboroxole). The syntheses of these derivatives are already described. Nevertheless, for most derivatives the characterisations for glucose **3b** or fructose **3a** binding are not yet investigated.

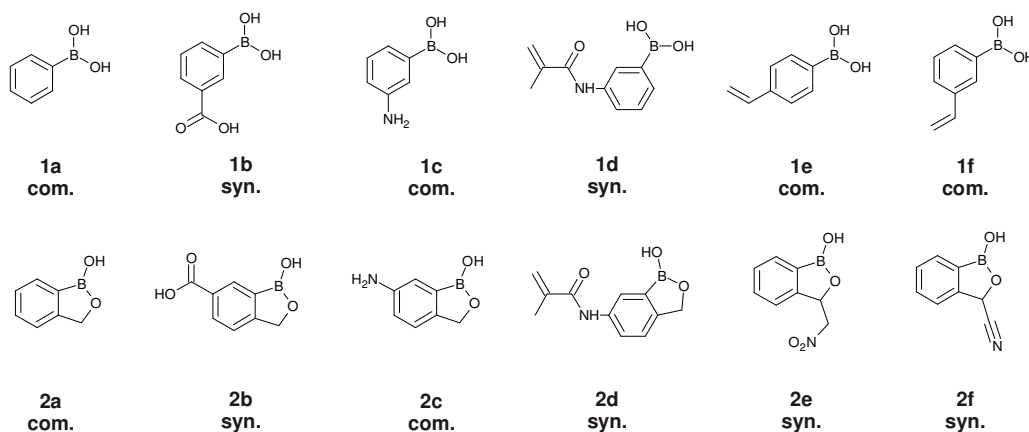


Figure 20. Different phenylboronic acid derivatives **1a-1f** and benzoboroxole derivatives **2a-2f** for coupling on or incorporation into polymeric networks; derivatives **2e** and **2f** are chiral derivatives (com. = commercially available; syn. = synthesised)

Based on a procedure by Pal *et al.*, the 3-carboxybenzoboroxole **2b** was synthesised starting from 3-bromo-4-methylbenzoic acid **28** (Figure 21).¹⁹⁴ To synthesise in a first step the corresponding boronic acid derivative **29** a halogen-metal exchange was performed by addition of

n-butyl lithium (BuLi) and subsequent trapping of the arylmetal intermediate with the electrophilic methyl borate.

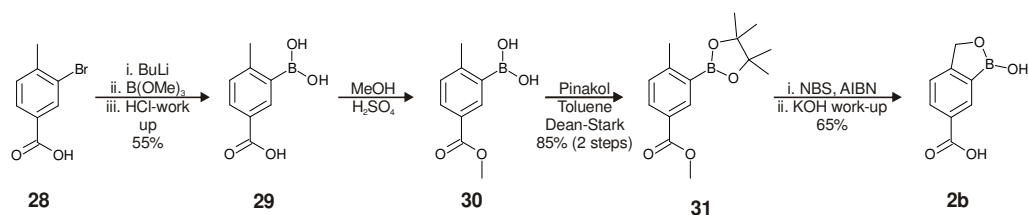


Figure 21. Synthesis route for 3-carboxybenzoboroxole **2b**

After acidic work-up 2-methyl-5-carboxy boronic acid **29** was yielded which was converted into the methanol carboxylic acid ester **30** and subsequent into the pinacol boronic acid ester **31**. Protected in both positions an α -bromination using N-Bromosuccinimide (NBS) and azobis(isobutyronitril) (AIBN) as radical starter in carbon tetrachloride were performed. After KOH-work up to substitute the α -bromine with a hydroxyl group the 3-carboxybenzoboroxole **2b** was yielded as a white powder.

To show the effect of a substitution in 3-position of the borolane ring two different derivatives **2e** and **2f** were synthesised (Figures 22 and 23; Figure 11 for numbering). Thus, the effect of electron withdrawing groups (EWG) attached to this ring could be verified as well as the effect of a chiral centre next to the boron.

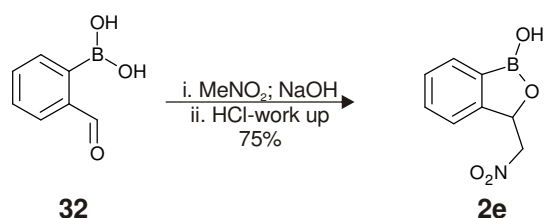


Figure 22. Synthesis route for 3-(nitromethyl)-benzoboroxole **2e** as chiral derivative starting from 2-formylphenylboronic acid **32**

The synthesis of the nitroderivative was performed by base-catalysed C-C bond formation (Henry-reaction) using nitromethane as the nitroderivative and 2-formylphenylboronic acid **32** as the starting arylboronic acid derivative.¹⁹⁸ The reaction was carried out at 15°C which tend to be more effective than at room temperature. After acidification the nitroderivate **2e** precipitated as a white powder which was recrystallised from water.

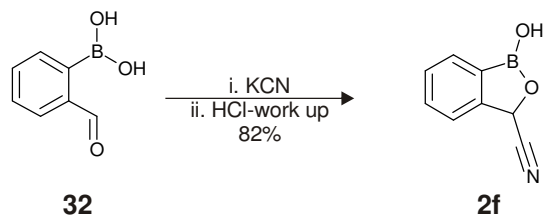


Figure 23. Synthesis route for 3-(nitrile)-benzoboroxole **2f** as second chiral derivative also starting from 2-formylphenylboronic acid **32**

As another chiral derivative a cyanobenzoboroxole **2f** was synthesised. Here, the 2-formyl boronic acid **32** was reacted with potassium cyanide at 10°C.²⁶⁶ After completion of the reaction the cyanobenzoboroxole **2f** was precipitated by acidification under appropriate safety.

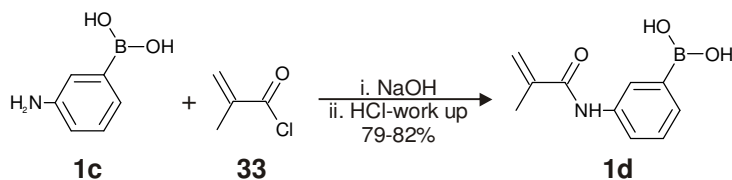


Figure 24. Synthesis of 3-methacrylamidophenylboronic acid **1d** starting from 3-aminophenylboronic acid **1c** and reaction with an acid chloride **33**

Despite the vinylphenyl boronic acid also methacrylamidophenyl boronic acid is described for the synthesis of boronic acid containing polymers. Therefore, the methacrylamidoderivatives for phenylboronic acid **1d** as well as benzoboroxole **2d** were synthesised (Figure 24).^{180,223,267} The synthesis was performed starting from a commercially available 3-aminophenylboronic acid **1c** which reacted with methacryloylchloride **33** at alkaline pH-values yielding 3-methacrylamidophenylboronic acid **1d** after slow acidification. The same synthesis was performed to yield **2d**.

4.1.5 Determination of binding constants using ITC

Isothermal titration calorimetry was used to characterise the binding between either glucose **3b** or fructose **3a** and different arylboronic acid derivatives **1a-1f** and **2a-2f** (Figure 20). In contrast to the ARS assay ITC yields the binding constants between the substances under investigation without any interference of a reporter substance. Moreover, as described above, the interaction is characterised also in terms of thermodynamic parameters such as enthalpy ΔH , the free energy ΔG and entropy ΔS .²⁵⁷ Data are not given as standard values as it is reported in recent literature having in mind that the system is in equilibrium. To obtain a first insight into the

binding of different synthesised as well as commercially available arylboronic acid derivatives to monosaccharides just the binding constants are compared. A detailed interpretation of the enthalpy ΔH , the free energy ΔG and entropy ΔS for the interaction of **3a** and selected derivatives is given in chapter 4.2.2.

As described already in the theoretical part of the thesis, the experiment can be designed via a so called *c*-value in which the expected binding constant has to be considered (see Chapter 2.4.4).²⁶¹ In the case of boronic acid - saccharide interaction the expected values are in the mM-range.²⁸ The concentrations needed for an appropriate *c*-value are too high since the heat of interaction would exceed the detection range of the used ITC device. To evaluate the data obtained by calorimetry it is therefore necessary to set the stoichiometry of the binding to a constant value which enables the determination of binding constants also at small *c*-values. In literature different binding structures for fructose and glucose to arylboronic acids (phenylboronic acid and *p*-tolylphenylboronic acid) are assigned by different spectroscopic methods and semi-empirical calculations as discussed in chapter 2.3.5. Fructose forms 1:1 and 1:2 complexes where in the case of the 1:1 binding tridentate or bidentate structures are favoured.²¹⁰ In case of glucose a 1:2 binding structure is favoured.²¹³ This is also possible for the boroxole - monosaccharide interaction as described already by mass spectroscopy (chapter 4.1.3).²⁷ Nevertheless, the binding stoichiometries are in these cases strongly dependent on the concentration ratio between the arylboronic acid and fructose. Since in the experimental design the saccharides are in a molar excess compared to the arylboronic acid derivative (35:1 in case of fructose and 40:1 in case of glucose) it is assumed that a 1:1 binding complex is most likely to occur. Therefore, all ITC raw data, which were corrected against the dilution experiments, were fitted with a 1:1 binding stoichiometry.

The ITC experiments were conducted at pH 7.4 to show the function of the arylboronic acid derivatives at this biological interesting pH-value. In general, the obtained binding constants are in agreement with the literature and different other methods such as NMR or the competitive ARS-assay.^{27,38,268} For the glucose - boronic acid interaction 20 mM of the boronic acid were inserted into the sample cell and a glucose solution with a concentration of 800 mM was added gradually. Since the concentration of the arylboronic acid derivative had to be quite high just some easy-soluble derivatives could be used in this experiment. These derivatives and their binding constants are listed in table 1.

Table 1. Binding constants for the interaction between different arylboronic acid derivatives and either glucose or fructose obtained by ITC at pH 7.4 in 0.1 M phosphate buffer.

Monosaccharide	Boronic acid	K / M^{-1} (ITC)	K / M^{-1} (Lit.)
D-Glucose 3b	1a	6 ± 1	4.6 (ARS) ³⁰
	1b	8 ± 1	
	1c	11 ± 1	3.1 (ITC, pH 6) ²⁶⁸ 27 (ITC, pH 8) ²⁶⁸
	2b	19 ± 1	
	2a	28 ± 1	31 (ARS) ³⁸ 17 (NMR, D ₂ O) ³⁸
	2f	52 ± 2	
	2e	67 ± 3	
D-Fructose 3a	1c	208 ± 3	11.5 (ITC, pH 6) ²⁶⁸ 137 (ITC, pH 8) ²⁶⁸
	1a	210 ± 2	160 (ARS) ³⁰
	1f	228 ± 11	
	1e	231 ± 4	
	1b	264 ± 10	
	2f	394 ± 7	
	2c	464 ± 10	
L-Fructose	2a	478 ± 13	
D-Fructose 3a	2b	481 ± 15	
	2a	508 ± 7	606 (NMR, D ₂ O) ³⁸
	1d	511 ± 6	
	2e	690 ± 16	
	2d	785 ± 40	

As expected there is a huge difference between the phenylboronic acid derivatives **1** and the derivatives of the benzoboroxole **2**. The binding constant of glucose to the phenylboronic acid **1a** is $6 M^{-1}$ and in agreement with data described by Springsteen *et al.*³⁰ They determined the binding constant between **1a** and glucose to be $4.6 M^{-1}$ by means of ARS. The derivatives **1b** and **1c** showed similar values in the same order of magnitude. In case of **1c** it can easily be explained since the amine-function does not affect the pK_a of the boronic acid derivative significantly. For **1b** it can be assumed that the effect is marginal, especially due to the small binding affinity. In contrast, the binding values for the benzoboroxole derivatives **2a**, **2c**, **2e** and **2f** to glucose are at least three times higher than the value for **1a**. This was also expected and is in line with the literature. For example, the binding constant of **2a** to glucose was determined by means of NMR and ARS-measurements to be between 17 (D₂O) and $31 M^{-1}$ (phosphate buffer, pH 7.4), respectively.^{27,40} With ITC measurements in phosphate buffer at pH 7.4 a binding constant of $28 M^{-1}$ was obtained. In comparison to **2a** different other substituents show to have an influence. Whereas a carboxyl-function in *meta*-position to the boron (**2c**) decreases the binding constant

slightly, EWGs such as nitrile- (**2f**) or nitro-groups (**2e**) attached to the borolane ring (R') increase the binding constant to glucose from 28 M^{-1} in case of **2a** to 52 or 67 M^{-1} , respectively. Two different assumptions can explain this behaviour. On one hand the electron withdrawing effect within the borolane ring can strengthen the acidity of the free hydroxyl-group attached to the boron leading to a lower $\text{p}K_{\text{a}}$ of the boroxole derivative. On the other hand, especially in case of **2e**, the oxygen atoms of the nitro-group can form additional hydrogen bonds to the saccharide which also enhances the binding affinity.

In case of fructose binding a similar picture is seen. In general, derivatives of phenylboronic acid **1** exhibit a lower binding constant to fructose than boroxole derivatives **2**. The binding constant of **2a** to fructose is 508 M^{-1} and thus more than two times higher than for **1a** (211 M^{-1}). Whereas substituents such as an amine- (**1b**) or vinyl-functions (**1e** and **1f**) does not show a significant change in binding constant, a carboxyl-function in *meta*-position to the boron increases the binding constant to a value of 260 M^{-1} which is explained by the lower $\text{p}K_{\text{a}}$ of **1b** compared to **1a** and **1c** (difference $\sim 0.8 \text{ p}K_{\text{a}}$ units).³⁸ For the vinyl-derivatives (**1e** and **1f**) the position of the substitution does not change the binding constant to a great extent. Furthermore, the vinyl-group is a low EDG and therefore the influence on the $\text{p}K_{\text{a}}$ of the boronic acid can be neglected. Surprisingly, the polymerisable methacrylamido-derivative **1d** shows a binding constant to fructose of 511 M^{-1} . This is a two-fold higher binding constant to fructose than detected for **1a** and is comparable to the binding constant of **2a** with fructose. In addition, the binding constant of the methacrylamido-derivative of benzoboroxole **2d** is with 748 M^{-1} also higher compared to the unsubstituted benzoboroxole **2a**. Hence, the methacrylamidogroup influences the binding. This leads to the conclusion that either the methacrylamidogroup acts as a significant EWG or due to the mesomeric effect the zwitterionic form of the methacrylamido-derivative acts as a possible coordinating group to the boron. Nevertheless, the responsible effect is hard to differentiate because Lowe *et al.* showed on one hand that the $\text{p}K_{\text{a}}$ of **1d** is 8.87 which is comparable to the $\text{p}K_{\text{a}}$ of **1a**. This would show that the electron withdrawing effect is not overwhelming.¹⁹³ On the other hand they showed that an intermolecular coordination of the zwitterionic form of **1d** could occur between pH 6 and 10. In a pH-titration experiment via ^{11}B -NMR spectroscopy they revealed a peak broadening which shifts significantly with higher pH-values. They explained the peak broadening with two present species of which one is the trigonal and the other the tetrahedral (= coordinated) form of the boron. Nevertheless, it cannot be distinguished if the coordination results from a coordination of hydroxyl groups of the solvent or from an intermolecular coordination of the zwitterionic form. In summary, both effects can contribute to the higher binding constant but an intermolecular coordination is more likely since the experiments are conducted at pH 7.4. Benzoboroxole derivatives which possess a residue in *meta*-position to the boron such as amine- (**2b**) or carboxy- functionalities (**2c**) show a slightly

smaller affinity constant than the underivatised benzoboroxole **2a**. The values are 464 and 481 M⁻¹, respectively. A lower binding constant compared to the underivatised benzoboroxole **2a** was also detected in case of **2c** for glucose. One possibility could be that the derivatisation of benzoboroxoles in *meta*-position with EWG leads to an effect of the borolane ring and consequently to a lower binding constant. Moreover, **2f** which exhibit an EWG at R' within the borolane ring showed a similar binding constant which is in contrast to the results obtained for glucose. Nevertheless, the nitro-derivative **2e** exhibits a very high binding constant (690 M⁻¹) to fructose which could be due to possible additional hydrogen bonds.

In conclusion, the binding of different phenylboronic acid (**1a-1f**) and benzoboroxole derivatives (**2a-2f**) to either **3b** or **3a** was investigated by ITC at pH 7.4 in 0.1 M phosphate buffer. It can be derived that the values are comparable to already described values in literature obtained by different other methods such as NMR-titration or the ARS-method. In general, it was found that the derivatives **2a-2f** exhibit higher binding constants than **1a-1f** for fructose and glucose. As expected the fructose binding constants are higher compared to glucose since the fructose-boronic acid interaction is known to be stronger. For the derivatives **1a-1f** a trend could be derived that EWGs attached to the phenyl ring can increase the binding constant to glucose or fructose as it is already described in the literature. In contrast, for the benzoboroxole derivatives it could be shown that EWGs attached to the phenyl ring cannot increase the binding constant. In fact, for the carboxy- and amine-derivative (**2a and 2b**) lower binding constants are detected for glucose as well as for fructose. Nevertheless, if the EWG is attached at R' in the borolane ring the binding constant to fructose or glucose can be increased. Since many different effects are involved in this type of chemistry in every case further experiments such as NMR binding-experiments or pK_a-measurements have to be performed to vary which type of effect results in a decrease or increase of binding strength. However, a panel of different arylboronic acids are synthesised and characterised for a later application.

4.1.6 Temperature dependent ITC

The influence of temperature on a binding reaction is of great interest because a deeper understanding into the thermodynamics can be gained. Furthermore, the temperature dependent measurement of the binding constant was classically used to determine the enthalpy ΔH_{vH} and the entropy ΔS_{vH} of a system by means of a van't Hoff plot ($\ln K$ vs. $1/T$).²⁶⁹ Also a temperature dependence of ΔH is used to determine the ΔC_p of a system under investigation. Therefore, the binding between fructose **3a** and either phenylboronic acid **1a** or benzoboroxole **2a** was investigated between 10 and 60°C by means of ITC (Table 2).

In a first comparison, the temperature dependency of the binding constants was evaluated (Figure 25). Since the esterification reaction between the saccharide and the arylboronic acid is exotherm, a temperature increase would decrease the binding affinity which is dependent on the principle of LeChatelier. Nevertheless, in case of **1a** this is not true because the binding constant seems to be independent from temperature and is around 200 M^{-1} . It has to be noted that there is a uncertainty since the values show a higher standard deviation with increasing temperature. For the interaction of **2a** with fructose a different behaviour was determined. Here, the binding constant decreases significantly with increasing temperature. At 10°C the obtained binding constant was 785 M^{-1} and at 60°C a binding constant of just 249 M^{-1} was detected.

Table 2. Obtained binding constants K between **1a** or **2a** and **3a** at pH 7.4 for different temperatures.

Temperature / °C	$K - \mathbf{1a} / \text{M}^{-1}$	$K - \mathbf{2a} / \text{M}^{-1}$
10	305 ± 18	805 ± 31
20	244 ± 18	585 ± 30
30	189 ± 11	396 ± 15
40	192 ± 21	311 ± 16
50	149 ± 14	261 ± 8
60	234 ± 40	256 ± 8

This change can be explained by the fact that an exothermic reaction is favoured at lower temperatures as the driving force. Nevertheless, it is surprising that the values decrease to about 250 M^{-1} which is in the region of the binding constant of **1a**. Therefore, there is a strong suspicion that the binding behaviour between **1a** and **2a** to **3a** is similar at higher temperatures. One possibility could be that the borolane ring opens at higher temperatures which would explain that the binding constants are comparable. In this case, **2a** acts like **1a** since the intramolecular coordination of the methylhydroxylgroup to the boron does not take place.

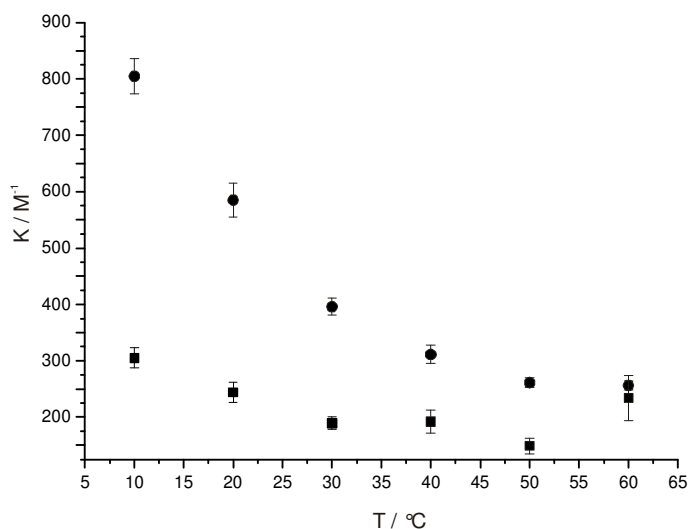


Figure 25. Binding constants determined at different temperatures for fructose binding to **1a** or **2a** at pH

7.4

As already described *via* temperature dependent ITC experiments it is possible to describe the evolution of entropy, enthalpy and Gibbs free energy (Table 3).

Table 3. Determined entropy $-T\Delta S$, enthalpy ΔH and Gibbs free energy ΔG for the interaction between fructose **3a** and **1a** or **2a** at different temperatures

T / °C	1a			2a		
	$\Delta G /$ kJ mol ⁻¹	$\Delta H /$ kJ mol ⁻¹	$-T\Delta S /$ kJ mol ⁻¹	$\Delta G /$ kJ mol ⁻¹	$\Delta H /$ kJ mol ⁻¹	$-T\Delta S /$ kJ mol ⁻¹
10	-13.4	-14.7	1.3	-15.7	-15.9	0.2
20	-13.5	-15.1	1.6	-15.6	-18.8	3.3
30	-13.0	-15.1	2.0	-15.0	-19.3	4.3
40	-13.1	-13.0	-0.1	-15.0	-19.3	4.3
50	-13.4	-15.0	1.7	-15.0	-18.0	3.1
60	-15.0	-12.1	-2.9	-15.3	-16.8	1.5

Especially interesting are the characteristics of the enthalpy ΔH at different temperatures. For the interaction of **1a** to fructose no observable dependency was detected. The values are differing in the range of the standard deviation around one value which is for ΔH around -15 kJ mol^{-1} . This goes along with the fact that this system does not show a real change due to the increase of temperature. It is also seen for the entropy and Gibbs free energy, that the changes are small with increasing temperature (Figure 26). In this regard a value for ΔC_p cannot be determined since the reaction is not dependent on the temperature. This was expected because of the small size of the molecules which does not allow for big changes in their conformation or structure. The interaction between **2a** and **3a** shows also a small but nevertheless strict change. Here, the interaction of **2a** and fructose shows a change in ΔH and ΔS which is often referred as entropy-enthalpy compensation, due to the fact, that the development of both mirrors.²⁷⁰ This results in a constant Gibbs free energy ΔG value but the contribution of enthalpy and entropy changes in a correlative way. Since this phenomenon is contrary discussed in literature, it should not be verified at this point.^{271,272} Nevertheless, the plot shows that the entropy and enthalpy does not change in a linear but rather in a parabolic way with a minimum in enthalpy or maximum of entropy around 35°C. It shows that this reaction has a changing heat capacity ΔC_p which is dependent on the temperature. Having a look at the development of binding constants of **2a** to fructose changing with temperature it can be assumed that also these values give an evidence for a ring opening of the borolane ring. Starting from 10°C with increasing temperatures, the term $-T\Delta S$ becomes more positive resulting in a compensation of the increasing ΔH .

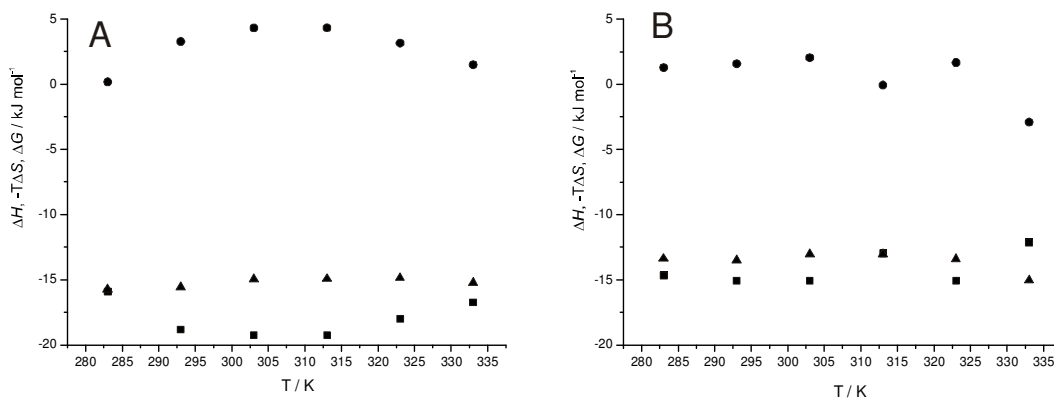


Figure 26. Evolution of ΔH , $-T\Delta S$ and ΔG dependent on the temperature for the interaction between benzboroxole **2a** (A) or phenylboronic acid **1a** (B) and fructose **3a**

Classically, to determine the thermodynamic parameters ΔH° and ΔS° a van't Hoff plot is generated (Figure 27).²⁷³ In this case, $\ln K$ is drawn against the reciprocal values of the temperatures. The enthalpy $\Delta H_{\text{vH}}^\circ$ can be calculated by the slope of the graph.

$$\frac{d \ln K}{d 1/T} = -\frac{\Delta H^\circ}{R} \quad (8)$$

The graph shows a linear correlation between $\ln K$ and the reciprocal temperature. In case of fructose-**2a** binding $\Delta H_{\text{vH}}^\circ$ was calculated to be $-21.95 \text{ kJ mol}^{-1}$. This is in good agreement with the values obtained by the ITC measurements for ΔH between 20 and 30 °C. The $\Delta H_{\text{vH}}^\circ$ value for the fructose-**1a** interaction is $-12.72 \text{ kJ mol}^{-1}$

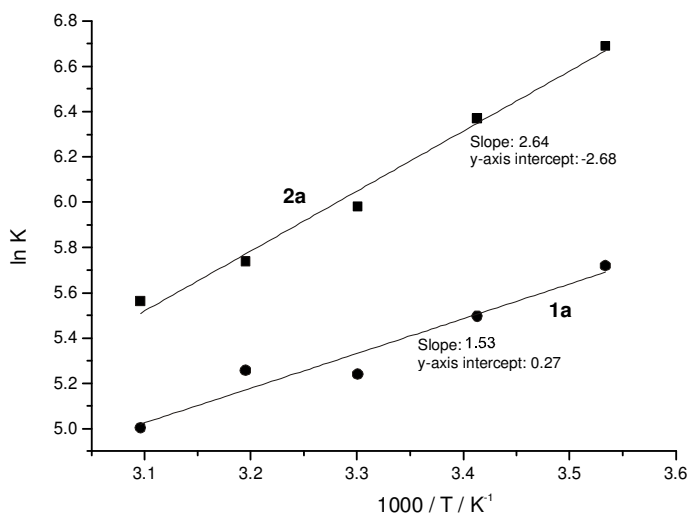


Figure 27. Van't Hoff – plot for the determination of $\Delta H_{\text{vH}}^\circ$ of the benzboroxole **2a** or phenylboronic acid **1a** interaction with fructose **3a**

4.1.7 Alizarin Red S as an electrochemical indicator for saccharide recognition

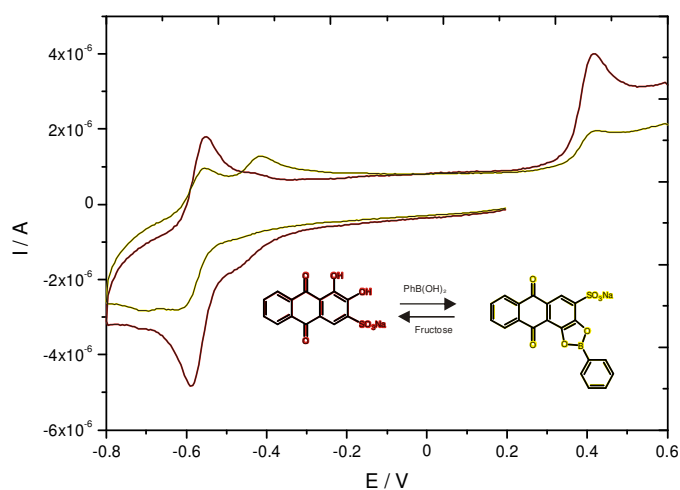


Figure 28. Electrochemistry of Alizarin Red S **3e**, its interaction with phenylboronic acid **1a** and displacement through fructose **3a** at pH 7.4; The red cyclic voltammogram corresponds to the free ARS, whereas the yellow was obtained after addition of **1a**

4.1.7.1 Abstract

*In addition to the well-established spectroscopic Alizarin Red S (ARS) assay for the determination of binding constants between arylboronic acids and different saccharides, the use of **3e** as a reporter in an electrochemical set-up was investigated. The electrochemical properties of ARS, the binding to phenylboronic acid **1a** and the competition with fructose in phosphate buffer at pH 7.4 were investigated by cyclic voltammetry (CV) (Figure 28). Two oxidation peaks for the neat ARS **3e** at the glassy carbon electrode were found at -0.54 and +0.42 V and one reduction peak at -0.64 V vs. Ag/AgCl, respectively. These peaks are characterised both as a 2-proton-2-electron transfer and corresponds to the oxidation and reduction of the anthraquinone or the ortho-quinone moiety of **3e**. After addition of **1a** a new oxidation peak occurred at -0.42 V which correlates with the ARS-**1a** interaction. The peak current increased with increasing phenylboronic acid concentration according to the release of **1a** and formation of the ARS-BA ester. After addition of fructose **3a** the peak current decreases again, in proportion to the fructose concentration, enabling the use of ARS as an electrochemical reporter for fructose detection in the concentration range between 20 mM and 100 mM.*

4.1.7.2 Introduction

Alizarin Red S (ARS) **3e** is a dye derived from anthraquinone which is used as a histochemical stain for calcium in biological samples.²⁷⁴⁻²⁷⁶ More recently, the interaction of ARS and arylboronic acids (BA) and their competition with saccharides or other *cis*-diol containing compounds **3** has also been used in a colourimetric assay for the determination of binding constants between the arylboronic acid derivative and the particular saccharide.^{30,251}

To monitor the ARS-PBA interaction, the change in absorbance or fluorescence can be observed by spectroscopic methods. The absorbance maximum of free ARS **3e** is at 530 nm (appears ruby-red) whereas the ARS-PBA complex has an absorbance maximum at 450 nm and appears orange-yellow. Fluorescence emission at 570 nm is only detectable for the ARS-PBA complex since an intramolecular fluorescence quenching mechanism occurs in the free ARS.²⁷⁷ Therefore, the concentrations of free and bound ARS dye can be simultaneously detected by spectroscopic measurements. Nevertheless, for application in portable sensor devices spectroscopic methods have their disadvantages due to the need of a precise optical assembly. Electrochemical detection is a promising alternative read-out method, mainly because of its relative technical simplicity and the ease of miniaturisation.

ARS is an anthraquinone derivative and is electrochemically active.²⁷⁸⁻²⁸⁰ It has been used as a redox mediator in different electrochemical configurations, for example for the detection of hydroxylamine or copper.²⁸¹⁻²⁸³ ARS was also used as an electrochemical reporter for arylboronic acids by James *et al.*²⁸⁴ They modified a glassy-carbon electrode with a boronic acid containing dendrimer-fiber hybrid. The adsorption of ARS was measured by means of cyclic voltammetry at pH 3 in a concentration range between 10 μ M to 1 mM. A possible application of their sensor for the detection of saccharides and other *cis*-diols in a competitive or displacement format was not reported. Hence, an electrochemical displacement assay for D-fructose at pH 7.4 was investigated.

4.1.7.3 Free ARS in solution

The redox behaviour of 0.144 mM ARS in phosphate buffer at pH 7.4 was investigated by cyclic voltammetry between -0.8 and 1 V on a glassy carbon electrode *vs.* Ag/AgCl. Starting at 0 V, with the initial scan in the negative direction, two oxidation peaks at -0.54 (P1) and +0.42 V (P3) could be detected in the first scan cycle. In addition, in the second scan cycle a new oxidation occurred at -0.04 V (P2). Moreover, two reduction peaks at -0.64 V (P1') and -0.24 V (P2') were recorded (Figure 29), whereas the second peak (P2') also just occurred in the second cycle.

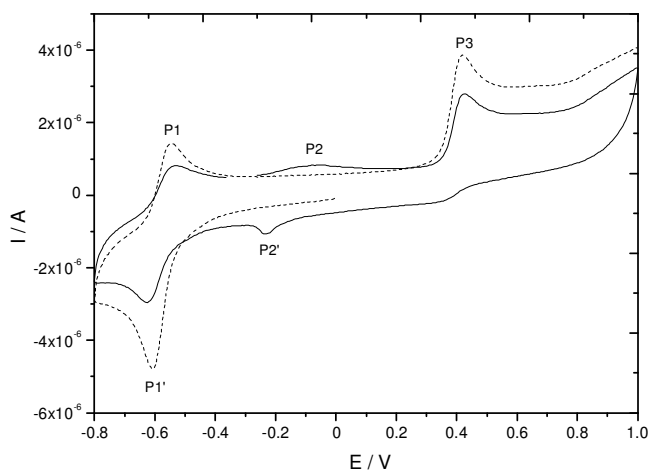


Figure 29. All measurements were performed at a scan rate of 0.1 V s^{-1} under oxygen exclusion; Cyclic voltammograms of 0.144 M ARS solution in 0.1 M phosphate buffer with 50 mM KCl at pH 7.4 at glassy carbon electrode ($\text{Ø}=3 \text{ mm}$) vs. Ag/AgCl (KCl = 3 M), solid line: positive scan direction; dashed line: negative scan direction

Alizarin Red S **3e** can be redoxactive at the position 9 and 10, *i.e.* the anthraquinone moiety at the central ring, giving the corresponding hydroquinone derivative **3e-A**, or at the catecholic moiety **3e-B** at positions 1 and 2 (Figure 30).

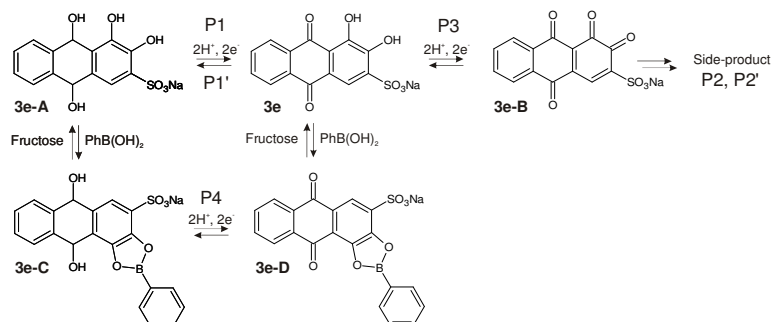


Figure 30. Reaction scheme of possible equilibria of ARS **3e** and corresponding reduction and oxidation processes

In the latter case, the oxidation product is a highly reactive ortho-quinone system. The first redox peaks P1 and P1' have a midpoint potential at -0.59 V and a peak separation of 0.1 V showed a quasi-reversible voltammetric response. The potential is in accordance with the literature for the redox reaction of anthraquinone.²⁸⁵ Here, the redox behaviour can be described by a 2-electron 2-proton reduction mechanism involving the oxygens at position 9 and 10. The oxidation of the catecholic moiety is described to be at much higher potentials. Consequently, the oxidation peak P3 at $+0.42 \text{ V vs. Ag/AgCl}$ can be assigned to this oxidation. Since no reduction peak could be observed, an irreversible reaction takes place which is related to the redox peaks P2 and P2' because these peaks does not occur in the first scan cycle. If the scan direction is changed

to positive, meaning that the oxidation of the ortho-quinone is the first process involved, the reduction peak P2' and P2 can directly be detected. Hence, the redox peaks P2 and P2' can be assumed to be related to the chemical reaction product from the reactive ortho-quinone species. Due to a decrease of all peak currents after the appearance of P2/P2' it is further assumed that a polymeric product of the ortho-quinone is formed which is adsorbed to the electrode. This is underlined by the finding, that the peak currents of both the oxidation peak P2 and the reduction peak P2' are strongly dependent on the upper return potential, since both peaks vanish if the upper return potential is below +0.4 V vs. Ag/AgCl (data not shown). For a deeper inside view, the scan rate dependency of P2/P2' was investigated. It could be shown that the peak currents of both P2 and P2' are proportional to the scan rate, which states for an adsorbed species. This result affirms the assumption of a polymeric product. In summary, it is an important finding of the study, that for the use of ARS as a quantitative electrochemical indicator in cyclic voltammetry, the starting potential has to be well below +0.4 V vs. Ag/AgCl and the initial scan direction has to be negative. In this case the interaction of the boronic acid with the ARS can be directly detected avoiding the obscuring effect of the adsorbed electroactive species responsible for P2/P2'.

4.1.7.4 Boronic acid – ARS interaction

In parallel to the spectroscopic ARS assay also here a solution of phenylboronic acid **1a** in ARS **3e** was added into the neat ARS solution. To avoid any adsorption process leading to redox peaks P2 and P2', the following sequence was applied: At first the electrode was conditioned at +0.2 V vs. Ag/AgCl for 15 s, followed by a negative scan to -0.8 V at a scan rate of 0.1 V s⁻¹. Then a positive scan from -0.8 V to +0.6 V was applied, using the same scan rate, and the measurement was stopped after the first oxidation cycle. After the addition of phenylboronic acid **1a**, a new oxidation peak P4 occurred at -0.42 V (P4) vs. Ag/AgCl alongside the already mentioned redox peaks P1, P1' and P3 (Figure 31).

Phenylboronic acid **1a** alone does not show any redox activity at these potentials. Thus, the new peak could be designated to the redox reaction of the anthraquinone moiety of the formed boronic acid-ARS ester (ARS-PBA), which is in parallel to the literature. The potential of the new oxidation peak P4 is slightly more positive which shows that the reduced state of the ARS-PBA **3e-C** ester is more stable than the reduced state of free ARS with a midpoint potential at -0.59 V.

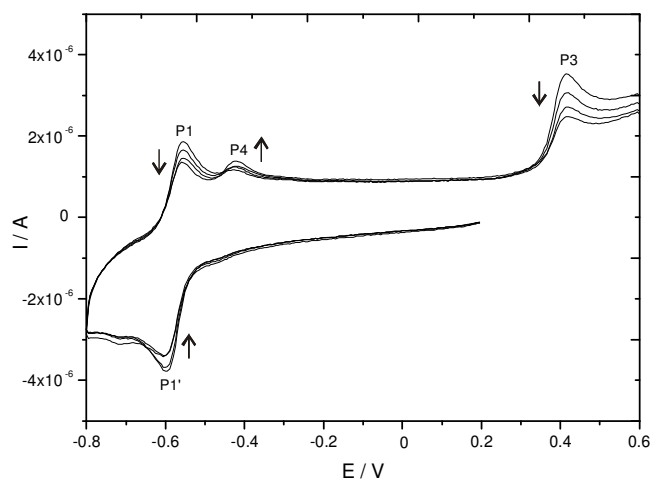


Figure 31. Cyclic voltammogram of ARS solution with increasing phenyl boronic acid **1a** concentrations

Further, the concentration dependence of the cyclic voltammogram with increasing boronic acid concentrations up to around 1 mM was investigated. In parallel to the spectroscopic ARS assay the peaks corresponding to the free ARS (P1; P1' and P3) decrease whereas the peak P4, which corresponds to the ARS-BA complex, increases. The effects of boronic acid addition on the individual peaks are different, however. The most reproducible signal change is gained at P3 (+ 0.42 V) which can be seen from the CV (Figure 31). Here, the experimental deviation for the peak current is only 2 % (n=3) and the signal change is higher compared to P1 and P1' leading to a better sensitivity. In contrast P1 and P1' show also a change but P1' has a higher experimental error (see Figure 29) which can be seen in the CV since the intensity follows not always the concentration of the boronic acid. Although the plot of the current change against the concentration of the boronic acid showed a similar slope and behaviour for P1 and P1', the reproducibility of P1 is better. In contrast, the formed ARS-BA complex (P4) does not show strict concentration dependence. In conclusion, the data obtained favours in all cases the use of the oxidation peaks P1 and P3 - at -0.54 V and +0.42 V, respectively - as analytical relevant signal to monitor the interaction between the ARS and boronic acids in different matrices.

4.1.7.5 Competition between ARS and fructose

Further a competition experiment was performed with fructose **3a** to prove the eligibility of the electrochemical behaviour of ARS **3e** as analytical signal for the quantitative detection of saccharides at pH 7.4. Phosphate buffer with a constant concentration of phenylboronic acid (1.5 mM) and ARS (0.1 M) was dispensed into the electrochemical cell and D-fructose was added in the range of 10 to 350 mM. The voltammograms showed similar redox peaks as in the case of pure BA-ARS interaction (Figure 32). The peaks P1, P1', P4 and P3 could again be detected. Again here, the peak change after addition of fructose **3a** was similar to the spectroscopic assay.

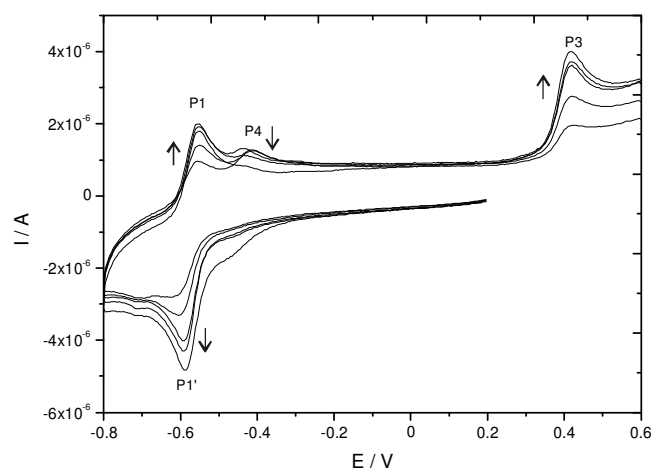


Figure 32. Cyclic voltammogram of ARS-PBA solution with differing fructose **3a** concentrations between 10 and 150 mM

The peaks P1, P1' and P3 showed an increase with increasing fructose concentration. This behaviour states for the release of ARS from the ARS-BA complex after displacement by fructose. This effect was also visually confirmed, as the colour of the solution changed from yellow to red. The peak P4 shows a decrease which is nevertheless not of analytical relevance. The plot of the current against the fructose concentration shows that the current change of P3 is higher compared to P1 and P1' which means that a higher sensitivity at +0.42 V is gained. In parallel to the results of the ARS-BA titration also P1' shows here a high experimental error and is therefore not suitable for an analytical signal. Under the reported experimental conditions, the detection range for fructose is between 20 mM and 100 mM. At higher fructose concentrations saturation occurs, *e.g.* no ARS can be displaced anymore (Figure 33).

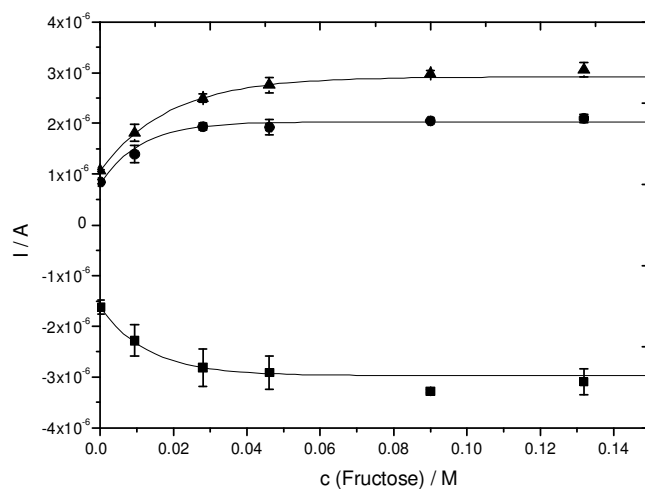


Figure 33. Current intensities ARS redox peaks vs. the added concentration of fructose **3a**; three repetitions, ▲: oxidation peak P3, ●: oxidation peak P1, ■: reduction peak P2.

4.1.7.6 Conclusion

The electrochemical behaviour of free ARS and of ARS in equilibrium with phenylboronic acid, resulting in the formation of a cyclic ARS-PBA ester, was investigated and used for fructose detection at pH 7.4. Using an optimised sequence of linear potential sweeps, free ARS showed a quasi-reversible redox reaction at the anthraquinone moiety (midpoint potential -0.59 V vs. Ag/AgCl) and an irreversible redox reaction followed by a chemical reaction at +0.42 V (assigned to the oxidation of the catechol moiety). The latter reaction leads to the formation of an electroactive, adsorbed species (midpoint potential -0.15 V) which obscured the further cyclic voltammograms of ARS. Reproducible, concentration dependent redox peaks at -0.54 and -0.64 V and +0.42 V which correlates with the ARS concentration in the BA-ARS equilibrium or in the competition equilibrium with fructose. In comparison to the spectroscopic read-out a comparable detection range (20-100 mM fructose) could be obtained. Thus, ARS can conveniently be used for saccharide recognition with boronic acid recognition entities in an electrochemical set-up at neutral pH-values which is essential for its use in biological matrices such as blood. Further investigations should be undertaken to (i) enhance the binding capability by using different arylboronic acid derivatives such as benzoboroxoles and (ii) to immobilise the ARS onto the electrode to provide an electrochemical sensor for saccharide recognition in different media.

4.1.8 Conclusion

In the chapter “4.1 Boronic acids in solution” the synthesis and characterisation of a variety of different boronic acid derivatives was described. Special attention was drawn to the benzoboroxole and derivatives thereof as saccharide recognition unit since this derivative opens the possibility for recognition of monosaccharides at pH 7.4. To understand the complexation between different monosaccharides and benzoboroxole $^1\text{H-NMR}$ spectroscopy and mass spectrometry were utilised. As expected and in line with the literature the benzoboroxole is able to complex with either D-fructose or D-glucose in 1:1, 2:1 and 1:2 complexes. The analysis of the $^1\text{H-NMR}$ spectra revealed that the complex formation is in terms of NMR time scale slow which can be derived through the formation of new peaks instead of a peak shift during titration experiments.

In regard to the later use of benzoboroxole or phenylboronic acid in polymeric networks different derivatives were synthesised and completed by commercially available arylboronic acids and benzoboroxoles. Among these, phenylboronic acid and benzoboroxole derivatives were chosen with similar substituents to derive different electronic effects. Here, carboxy- (**1** and **2b**), amine- (**1** and **2c**) and methacrylamido-derivatives (**1** and **2d**) were chosen due to their possibility to be coupled or incorporated into polymeric networks. The interaction to fructose and in some cases to glucose was monitored by ITC-experiments. To summarise, all benzoboroxole derivative exhibit a higher binding constant and just slight deviations of the binding strength due to electronic effects could be detected. Nevertheless, the binding constant of methacrylamidophenylboronic acid **1d** is in the same order of magnitude (about $500\text{-}700\text{ M}^{-1}$) compared to the benzoboroxole binding constant which can be due to the possibility of a zwitterionic form of the substituent. In addition also already reported racemic benzoboroxole derivative such as 3-(*nitromethyl*)- (**2e**) or 3-(*nitrile*)- (**2f**) substituents at R' (see Figure 11) were for the first time characterised in terms of their interaction with D-fructose or D-glucose. Temperature dependent ITC-measurements of the interaction between fructose and phenylboronic acid (**1a**) or benzoboroxole (**2a**) showed just an influence of temperature for the benzoboroxole. The binding constants drop with increasing temperature which is assumed to be an effect of an opening of the borolane ring. Nevertheless, due to just small changes in enthalpy no ΔC_p could be derived.

The last part of this chapter deals with the transfer of an already existing colourimetric assay for the detection of binding between saccharides and phenylboronic acid to an electrochemical set-up. Thus, the electrochemistry of Alizarin Red S (ARS), which is used as the electrochemical reporter substance, is analysed by cyclic voltammetry alone and in presence of phenylboronic acid. The binding of the ARS to the phenylboronic acid could be monitored and the change in current signals with increasing phenylboronic acid concentration could be followed.

The reverse reaction was induced by displacement with a model saccharide (here: D-fructose) showing a concentration dependency of the released ARS which can be used as an analytical signal for saccharide sensing. With this work, the already described and established ARS-assay was transferred for the first time to another transducing principle enabling its use to different application areas.

4.2 APPLICATIONS IN POLYMERIC NETWORKS

4.2.1 - General considerations

The intention of the present thesis was to provide different polymeric systems with boronic acid entities which bind saccharides at neutral pH-values. Thus, different arylboronic acid derivatives - especially benzoboroxoles **2** - are immobilised onto or incorporated into various polymeric networks to show their applicability as saccharide recognition elements (Figure 34). In this context two different directions are followed. On one hand the binding properties should be altered since on a polymeric backbone the binding behaviour alters significantly due to different secondary effects. On the other hand the selectivity of saccharides to arylboronic acid entities was targeted.

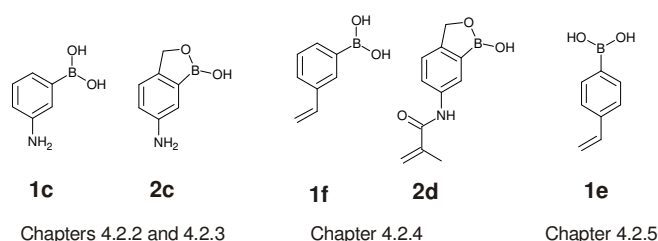


Figure 34. Different boronic acid derivatives in corresponding chapters

To alter the binding properties a nanoparticulate system was chosen since the surface-to-volume ratio of a nanoparticle enhances surface phenomena and leads therefore to an increase of possible secondary effects. Furthermore, a bottom-up approach leads to materials with defined properties. In this regard, a polystyrene-*co*-DVB-*co*-vinylbenzyl chloride latex was synthesised *via* a classical emulsion polymerisation and modified with either 3-aminobenzoboroxole **2c** or 3-aminophenyl boronic acid **1c**. The binding of D-fructose or D-glucose to these nanoparticulate receptor units was characterised by isothermal titration calorimetry (Chapter 4.2.2) and with Alizarin Red S **3e** as a reporter dye (Chapter 4.2.3). ITC measurements reveal all thermodynamically relevant parameter such as changes of enthalpy ΔH , free energy ΔG , entropy ΔS and the association constant K . The obtained data for the nanoparticulate system were compared to data obtained with free boronic acid ligands to verify different contributions to the binding. Hence, the binding is thermodynamically characterised. In a more practical approach ARS **3e** was chosen as a reporter dye to show the binding of D-glucose and D-fructose to the nanoparticulate receptor system. With a photometric readout the concentration dependency could be evaluated. Furthermore, it was investigated if the polymeric system can tolerate high temperatures which are employed to sterilise medical products.

To enhance the selectivity of arylboronic acids in polymeric systems the molecular imprinting approach with a known polymeric system was used. Here, a classical bulk polymer was synthesised using TRIM as the crosslinker and acetonitrile and toluene as porogen. Different polymerisable boronic acid derivatives were used. Joined by a diploma thesis prepared by Grüneberger the use of a polymerisable benzoboroxole **2d** was evaluated as functional monomer for binding of fructose down to pH 7.4 (Chapter 4.2.4). In comparison also 3-vinylphenylboronic acid **1f** was used as a common and well-described boronic acid functional monomer. After a medium optimisation the different polymers were tested for their binding to fructose at three different pH values to compare the performance of the different functional monomers. Another system describes the synthesis of the monosaccharide analogue *rac*-**3c** (Chapter 4.2.5). This structure was utilised as template molecules to imprint a defined, not mutarotation dependent boronic acid ester. The rebinding was tested with either D-fructose **3a** or D-glucose **3b**.

4.2.2 - Label-free detection of saccharide binding at pH 7.4 to nanoparticulate benzoboroxole based receptor units

4.2.2.1 Abstract

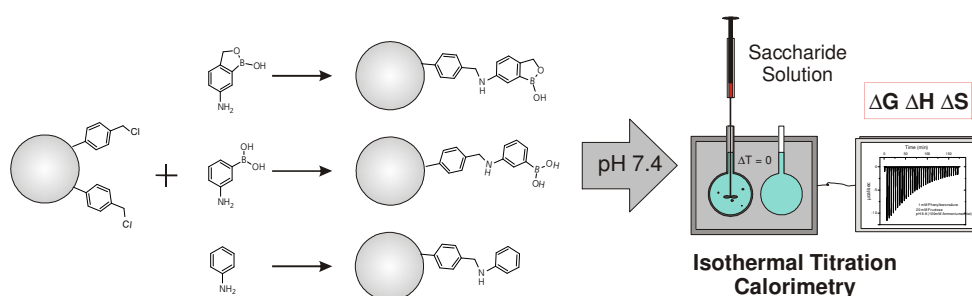


Figure 35. Graphical abstract for differently modified polystyrene nanoparticles and their fructose **3a** binding characterisation using ITC at pH 7.4

Nanoparticles modified with either 3-aminobenzoboroxole **2c** or 3-aminophenylboronic acid **1c** were prepared by nucleophilic substitution of a styrene-co-DVB-co-vinylbenzylchloride latex (25 nm) (Figure 35). Isothermal titration calorimetry (ITC) was used as a label-free detection method for the analysis of the binding between monosaccharides and these two differently derivatised nanoparticle systems at pH 7.4. It could be demonstrated that the association constant between these nanoparticle systems and fructose **3a** is more than two times higher compared to the binding constant obtained for the free arylboronic acid derivatives. Since ITC reveals moreover thermodynamical parameters such as the changes in enthalpy ΔH , free energy ΔG and entropy ΔS possible explanations for the higher binding constants can be derived in terms of entropy and enthalpy changes. The obtained thermodynamic parameters were interpreted to analyse entropy and enthalpy of the involved processes. In case of the modified nanoparticles the free energy of binding is dominated by the entropy term. This shows that besides the affinity found in “free” solubilised systems interfacial effects lead to a higher binding constant. For example, the binding constant for fructose to the benzoboroxole **2a** modified nanoparticles is 1150 M^{-1} which is twice as high as the binding constant of the free benzoboroxole.

4.2.2.2 Introduction

Since polymeric systems offer the possibility for a better binding as compared with soluble systems, the synthesis of benzoboroxole **2** modified nanoparticles (BX-NP) was described to employ these nanoparticles as multivalent receptor units for the binding of monosaccharides at pH 7.4. Due to the high surface-to-volume ratio of nanoparticles higher binding constants are targeted. In this regard also surface effects will have a higher influence. As a reference material, phenylboronic acid **1** nanoparticles (BA-NP) were synthesised. In this case the binding to monosaccharides was analysed by means of isothermal titration calorimetry as a label-free sensing method. To gain a better understanding of the thermodynamics of the binding reaction between boronic acids and fructose **3a**, firstly the free boronic acid ligands (benzoboroxole **2a**, phenylboronic acid **1a** and their corresponding amine-derivatives **2c** and **1c**) were examined. With this information the binding can be described in terms of contributions of enthalpy and entropy. Secondly, the different arylboronic acid modified nanoparticles were analysed in respect to their binding to fructose and compared to the free boronic acid derivatives. Consequently, the comparison of the different systems will then lead to more detailed view and understanding of processes involved in the binding between saccharides and arylboronic acids on the nanoparticles vs. in solution.

4.2.2.3 Results and Discussion

Particle characterisation

The raw latex was prepared by a classical, cationic emulsion polymerisation according to Paulke *et al.*²⁸⁶ The obtained nanoparticles had a mean diameter of 25 nm and a polydispersity index (PDI) under 0.1. The nanoparticles were subsequently modified by nucleophilic substitution with amino-derivatives of benzoboroxole **2c** and phenylboronic acid **1c** leading to a slightly brownish or yellowish diaphanous solution depending on the used arylboronic acid derivative (BX-NP and BA-NP; Figure 36). Furthermore, as reference nanoparticle, also aniline modified particles were synthesised in the same manner (Ref-NP). The amount of boron bound onto the nanoparticle surface was determined by ICP-OES after oxidative digest. The results are 0.2 mmol per mL nanolatex for the aminophenylboronic acid (BA-NP) and the aminobenzoboroxole (BX-NP). With a solid content of about 1 % of polymer particles in the latex, about 50,000 boronic acid molecules per particle can be assumed. Measurements regarding the size and the PDI of the modified latex showed that the coupling of boronic acids has a slight influence on the PDI (slightly over 0.1) showing a higher hydrodynamic diameter. This could be explained by the decrease of surface tension between the particles and its surrounding aqueous medium due to the boronic acids hydrophilicity. After modification the particles were dialysed against ultrapure water and the efficiency of washing was tested by measuring the eluate after ultrafiltration for

unbound boronic acid with Alizarin Red S (ARS). Only particles showing no colour change of the ARS solution were used for the ITC measurements.³⁰

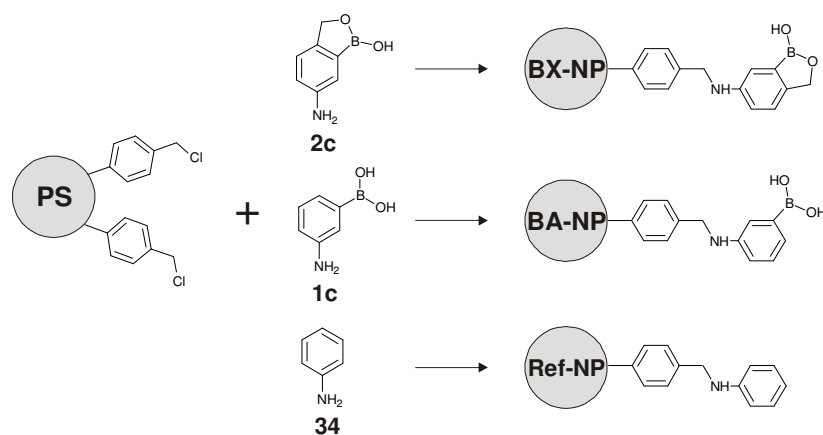


Figure 36. Synthesis of benzoboroxole **2** (BX-NP), phenylboronic acid **1** (BA-NP) and aniline **34** (Ref-NP) modified nanoparticles using the appropriate amino-derivatives **2c** and **1c** at pH 7.4 for nucleophilic substitution

Experimental design

As already mentioned the binding constants of for fructose with arylboronic acids are in the mmolar range.^{28,30} Hence, the stoichiometry of the reaction has to be fixed in order to analyse the obtained ITC data. In literature different binding structures for fructose **3a** to arylboronic acids are assigned by different spectroscopic methods and semi-empirical calculations.^{27,210} **3a** forms 1:1 and 1:2 complexes where in the case of the 1:1 binding a tridentate or bidentate structures are favoured.²¹⁰ The binding stoichiometries are in these cases strongly dependent on the concentration ratio between the arylboronic acid and fructose **3a**. Since in the experimental design **3a** is in a molar excess compared to the arylboronic acid derivative (35:1) a 1:1 binding complex is most likely to occur. Consequently, all ITC- binding experiments were analysed based on a 1:1 stoichiometry.

The binding behaviour of fructose to the nanoparticulate benzoboroxole (BX-NP) and phenylboronic acid (BA-NP) receptor units was investigated. The nanoparticles were dissolved in 20 mM phosphate buffer at pH 7.4 containing 0.5 % of cetyltrimethylammonium bromide (CTAB) and varying concentrations of fructose were added stepwise via the syringe of the ITC device. CTAB was added to ensure the dispersibility of the nanoparticles but it did not affect the binding behaviour (shown with free benzoboroxole **2a** and **3a**). To provide a comparison also free phenylboronic acid **1a**, benzoboroxole **2a** and their corresponding amine-derivatives **1c** and **2c** were examined for their binding to **3a** at pH 7.4. The unsubstituted as well as the amine-derivatives were chosen since amine-functions are known to coordinate to the boron centre. In solution the amine-functions are able to coordinate whereas coupled onto the particle the

possibility of coordination can be decreased. Consequently, the involved processes of saccharide binding to arylboronic acids (affinity) and effects of their coupling to nanoparticulate receptor units (apparent affinity) are evaluated.

Table 4. Thermodynamic parameters for the interaction between fructose **3a**, the arylboronic acid derivatives and the arylboronic acid modified particles (BA-NP and BX-NP) in phosphate buffer at pH 7.4 (*n.d.*=not detectable)

Receptor	K / M^{-1}	$\Delta H / kJ mol^{-1}$	$\Delta S / J mol^{-1} K^{-1}$
1a	210 ± 2	-14.2 ± 1.8	-3.0
2a	508 ± 7	-18.4 ± 1.5	-10.5
1c	208 ± 3	-15.1 ± 1.2	-6.0
2c	464 ± 10	-14.7 ± 1.4	1.7
BA-NP	590 ± 26	-1.2 ± 0.2	49.8
BX-NP	1150 ± 70	-3.0 ± 0.7	49.0
Ref-NP	<i>n.d.</i>	<i>n.d.</i>	<i>n.d.</i>

Thermodynamics of free arylboronic acids

In first experiments the affinity was characterised. 2 mM of the arylboronic acid derivatives were titrated against 75 mM fructose in phosphate buffer at pH 7.4. To analyse the raw data, the obtained curves were corrected against dilution experiments. The power q used to compensate the heat of dilution for 75 mM fructose **3a** into buffer is below $1 \mu cal sec^{-1}$. As expected, the binding of **3a** to the arylboronic acids is exothermic. The power q used for heat compensation is (with $26 \mu cal s^{-1}$) in case of the benzoboroxole-fructose interaction two-fold higher than the fructose-phenylboronic acid interaction. In general, the binding values match other publications in which the binding constants are determined by other physical methods such as absorption or fluorescence of Alizarin Red S as a reporter dye. The benzoboroxole-fructose association constant was found to be $508 M^{-1}$ and is more than two times higher compared to phenylboronic acid (Table 4, Obtained ITC raw data: Appendix A1). The higher affinity of the benzoboroxole to saccharides is in agreement with obtained data by ARS-competition experiments or NMR spectroscopy and can be assigned to the hemilabile hydroxyligand which releases ring strain due to the favoured hybridisation change of the boron atom. In comparison the binding constants of the corresponding amine-phenylboronic acid do not vary to a great extent from the phenylboronic acid and are about $210 M^{-1}$. This is due to the comparable pK_a -values of both derivatives (8.8 for phenylboronic acid; 8.9 for aminophenylboronic acid). For the aminobenzoboroxole the value is about $50 M^{-1}$ smaller but is in the same order of magnitude.

To gain a deeper insight ΔH and ΔS were further analysed for the unsubstituted arylboronic acids. The measured enthalpy ΔH is mainly dependent on the binding enthalpy ΔH_{bind} and the ionisation enthalpy ΔH_{ion} which is dependent on the number of protons n_H released or taken up from the buffer.^{258,287}

$$\Delta H = \Delta H_{bind} + n_H \Delta H_{ion} \quad (9)$$

In case of the interaction between the boronic acid and a saccharide the main process which contributes to the measured enthalpy ΔH will be the esterification by the formation of a covalent bond. Therefore, with -14.2 and -18.4 kJ mol⁻¹, the values for ΔH are in the same order of magnitude for both phenylboronic acid and benzoboroxole with fructose. In addition an ionisation step could contribute to the measured enthalpy. Hydroxylanions are coordinating to the boron saturating the electron deficiency and releasing the ring strain of the formed cyclic saccharide ester by hybridisation change from sp² to sp³ of the boron. This process contributes to the higher ΔH at higher pH values. The lower binding constants found at pH 7.4 for the phenylboronic acid show that the ionisation does not take place to a high degree.

In case of the benzoboroxole the complex formation is slightly different resulting in higher binding enthalpies than in case of phenylboronic acid. On one hand the higher binding enthalpies are favoured due to the already saturated electron deficiency and decreased ring strain occasioned by the intramolecular bond with the hydroxyl group. Therefore, the binding of *cis*-diols towards the benzoboroxole is easier to achieve. Hall and *co*-workers stated that the closed anhydride form of the benzoboroxole **2a** is present at pH 7.4 also upon binding towards *cis*-diols. This phenomenon contributes to the overall ΔH . Unfortunately, the ionisation enthalpy ΔH_{ion} of the number of protons n_H cannot be detected easily for this system. The use of different buffers with known ionisation enthalpies will have a high influence on the binding strength due to possible coordination effects to the boron. In general, the negative values for ΔH indicate that the binding is in all cases enthalpically favoured.

The overall changes of entropy ΔS are contributed by different factors such as solvation, conformational and rotational restrictions and ionisation. In case of such small receptor-ligand pairs the value for ΔS_{Rot} is believed to be minor compared to values obtained for protein-ligand binding. However, for nanoparticulate receptor units the influence can be high. For the ionisation entropy the same descriptions than for ΔH_{ion} are valid meaning that the benzoboroxole exhibit a higher ionisation potential than the boronic acid. In addition, contributions from the water shell around saccharides can be monitored.²⁸⁸ The formed boronic acid ester has to be dissolved and the water molecules are then again arranged around the free hydroxyl groups. Furthermore, one

reason for the higher entropy value is that in the benzoboroxole **2a** the 4th ligand comes from "inside" (the intramolecular hydroxyl) as opposed to a hydroxyl anion from the solvent water.

Apparent affinity of nanoparticulate receptor units

Nanoparticles were chosen to realise a high surface-to-volume ratio to enhance possible surface effects. In literature the interaction between a saccharide and a polymeric system containing boronic acid residues is described to have contributions from different effects.²⁸⁹ Here, the measured enthalpy ΔH is described as a summation of the esterification ΔH_{ester} , the dilution enthalpy ΔH_{Dil} , the unspecific binding $\Delta H_{Surface}$ and the enthalpy which refers to polymer rearrangements $\Delta H_{Polymer}$.

$$\Delta H = \Delta H_{ester} + \Delta H_{Dil} + \Delta H_{Surface} + \Delta H_{Polymer} \quad (10)$$

In the described case the contribution of the polymer rearrangement $\Delta H_{Polymer}$ can be seen as small because the nanoparticles are prepared with the addition of 2.5 mol-% divinylbenzene crosslinked and are therefore compact. Furthermore the nanoparticles are stored in aqueous media and reorientation processes due to a swelling or shrinking of the polymer backbone do not take place.

The amount of dilution enthalpy ΔH_{Dil} was measured by different dilution experiments. Here, the boronic acid modified latices as well as aniline modified latex were titrated against buffer but no pronounced heat evolution was detected (Figure 37, A1). This shows that no rearrangement processes of the surface are taking place. Just the titration of fructose in buffer showed exothermic dilution behaviour of about 0.05 $\mu\text{cal/s}$ which again can be explained by the special structure between saccharides and water (Figure 37, A3). The unspecific binding $\Delta H_{Surface}$ was determined by the titration of aniline modified latex against fructose (Figure 37, A2). It is known from literature that the hydrophobic face of the carbon ring of saccharides can bind to aromatic systems and undergo a π -CH-interaction. This is for example described for saccharide binding proteins which possess a tyrosine unit for this hydrophobic interaction. In the case of the nanoparticles under investigation a small endothermic heat signal was detected. As far as the enthalpy terms reflects the interaction of a ligand to a receptor relative to the interaction with the solvent a reorientation of the solvent is more likely to occur than a binding of fructose to the hydrophilic particles. To summarise, in all cases the impact is quite low that just the esterification dictates a high exothermic heat during the titration experiment. Nevertheless, the titration experiments with modified latex were corrected against both dilution and unspecific binding.

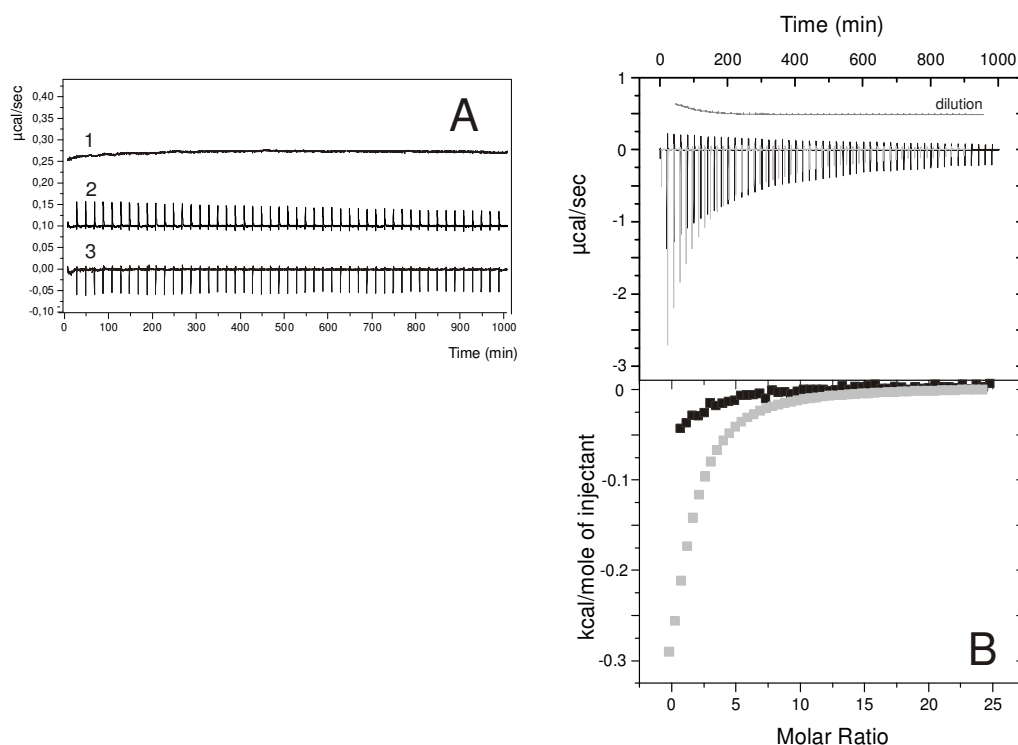


Figure 37. A. Control experiments performed with aniline modified nanoparticles (Ref-NP) titrated against buffer (20 mM phosphate) (1) and 75 mM fructose **3a** (2), and **3a** against buffer alone (dilution experiment, 3). **B.** Isothermal titration calorimetry experiments with benzoboroxole (gray) and phenylboronic acid (black) modified nanoparticles (BX-NP and BA-NP) titrated against 75 mM at pH 7.4 in 20 mM phosphate buffer. The data were corrected against the dilution experiments

The results of the calorimetric binding studies of the two modified latices are in agreement with the results obtained from free ligand studies (Table 4, Figure. 37B). Here, the benzoboroxole modified latex exhibit an almost two-fold higher affinity to fructose than the arylboronic acid modified one. The values are also in the mmolar regime - for the benzoboroxole containing latex a value of 1150 M^{-1} is obtained, for the boronic acid latex a value of 640 M^{-1} is found. This is almost twice as high as for the free boronic acid derivatives which could be explained with the fact that the fructose molecules are bound by a second neighbouring boronic acid entity after release from the first one. This effect is described for many systems where the receptor is immobilised because the intrinsic affinity of the receptor is not the only contribution. Moreover, secondary effects due to the high concentration of ligands per volume unit leads to multivalent surface binding known as apparent affinity. Furthermore it can be derived, that for the nanoparticle system the entropy term is the driving force for the high binding (Figure 38). The values are about $47 \text{ kJ mol}^{-1} \text{ K}^{-1}$. This positive value may be explained with effects which are contributed by the double layer of the nanoparticle and rearrangements can occur. This process is accompanied by the release of water and ions from the layer leading to a positive entropy contribution which is enhanced due to the high surface concentration of boronic acids. The loss of

entropy accompanied by the loss of conformational freedom of the saccharide is small compared to the first described process. Furthermore, the control experiments with the aniline modified latex shows no detectable heat signal. This underlines that just the binding of fructose to the immobilised boronic acid entities are responsible for the entropy change but not any unspecific interaction.

Further, the enthalpies ΔH with -3 kJ mol^{-1} in case of the benzoboroxole latex and -1.3 kJ mol^{-1} contribute to the binding strength. The same trend as for the free ligand can be seen meaning that the benzoboroxole has a higher enthalpy value contributed from the possible ionisation enthalpy ΔH_{ion} at this pH value. Nevertheless, the values for ΔH are smaller than for the boronic acids in solution which could again be assigned to the fact that the boronic acids are now immobilised. Consequently, two different assumptions can be made. Firstly, the high concentration of locally immobilised boronic acids contributes to a different binding behaviour such as multivalency and rebinding processes. Secondly, negative or positive cooperation of neighbouring boronic acids can lead to a different enthalpy contribution.

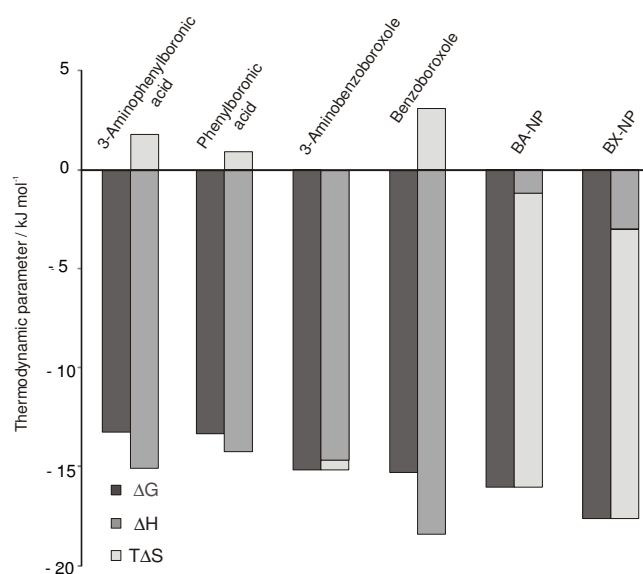


Figure 38. Enthalpic and entropic contributions to the Gibbs free energy of fructose **3a** binding to free 3-aminophenyl boronic acid **1c**, phenylboronic acid **1a**, 3-aminobenzoboroxole **2c**, benzoboroxole **2a** and to the nanoparticles decorated with phenylboronic acid (**BA-NP**) and benzoboroxole (**BX-NP**)

4.2.2.4 Conclusion

In this chapter, benzoboroxole **2** carrying nanoparticles were synthesised and characterised for the binding of fructose at pH 7.4. It could be shown that the coupling of the benzoboroxole **2c** leads to an enhanced binding constant due to possible multivalent binding events. Via the use of isothermal titration calorimetry as a label-free sensing method the

interaction between arylboronic acid derivatives free in solution or immobilised onto nanoparticles and monosaccharides was monitored. The special *O*-hydroxymethyl phenylboronic acid (benzoboroxole **2**) was chosen as the boronic acid entity for carbohydrate sensing at pH 7.4. In first experiments the free non-immobilised boronic acid derivatives - benzoboroxole and phenylboronic acid - were examined for their binding to fructose. It could be shown that the benzoboroxole exhibits, for instance, a two times higher binding affinity to fructose than the phenylboronic acid with a binding constant of 508 M^{-1} . The thermodynamic parameters enthalpy ΔH and entropy ΔS for this system showed that the binding of monosaccharides to the chosen boronic acid derivatives is mainly enthalpically driven. In parallel the nanoparticle system with immobilised 3-aminobenzoboroxole **2c** or 3-aminophenylboronic acid **1c** shows a much smaller enthalpical contribution to the binding of fructose but a high entropic contribution due to the processes which are taking place during the binding of the saccharide. In general the binding of fructose to these boronic acid modified nanoparticles is more than two times enhanced due to the small spatial distribution of boronic acid units on the nanoparticle surface. It could be shown that the immobilisation and high spatial concentration of ligands can result in higher apparent binding constants below the binding constants found in solution. Hence, the choice of polymer and its morphology, the possibility for multiple modification sites in a small volume fragment and the high yield of modified surface area influences the involved processes and materials with high affinity can be obtained.

4.2.3 Benzoboroxole-modified nanoparticles for the recognition of glucose at neutral pH

4.2.3.1 Abstract

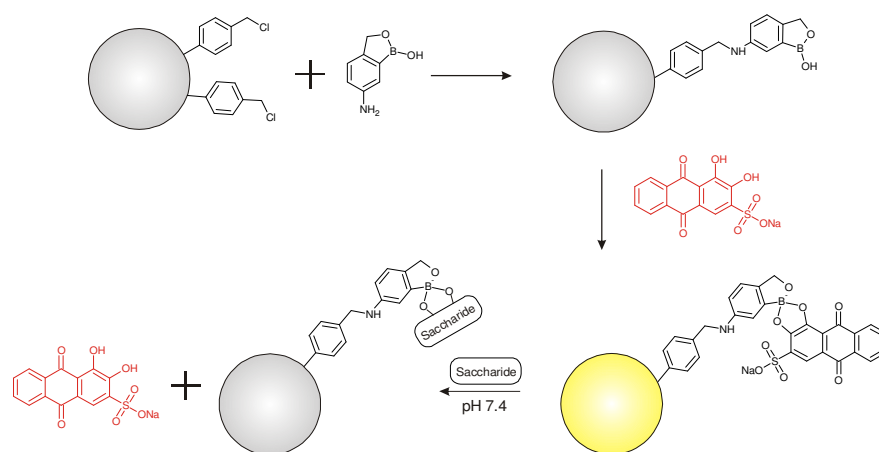


Figure. 39. Preparation of benzoboroxole modified nanoparticles (**BX-NP**), their loading with ARS **3e** and subsequent binding of monosaccharide such as fructose **3a** at pH 7.4

*Benzoboroxole modified nanoparticles were prepared starting from a polystyrene-co-vinylbenzylchloride latex by nucleophilic substitution with 6-amino-1-hydroxy-2,1-benzoxaborolane **2c** (Figure 39). It is known that benzoboroxole **2** binds to saccharides at pH 7.4 due to the intramolecular coordination of a hydroxyl group coordinating as a donor group, which compensates the electron deficiency of the boron. These benzoboroxole modified nanoparticles were tested with regard to their aqueous saccharide binding ability utilising Alizarin Red S **3e** as a reporter dye. Consequently, the pH value was chosen to be 7.4 as the targeted key feature. It was shown that the binding of fructose as well as glucose can be determined by UV-Vis spectroscopy in a concentration range from 20 mM to 400 mM which is of clinical relevance. The binding constants determined by the analysis of competitive binding for the benzoboroxole modified nanoparticles were 2354 M^{-1} for fructose and 580 M^{-1} for glucose. Furthermore, the temperature stability up to $121\text{ }^{\circ}\text{C}$ of these nanoparticles was tested and it could be shown that 95% of the initial binding capacity could be conserved.*

4.2.3.2 Introduction

It was shown in the previous chapter 4.2.2 that the modification of styrene latex of 25 nm with aminobenzoboroxole **2c** leads to a high binding constant due to different secondary effects such as the high spatial concentration of ligands leading to a cooperative binding. Nevertheless, it was not possible to detect the interaction of the nanoparticles with glucose since the measurements hit the restrictions of the employed ITC device. Thus, the binding of fructose and glucose at pH 7.4 to the opalescent yellowish latex particles was shown by displacement of Alizarin Red S **3e** (ARS), a reporter dye assay previously described by Wang and *co-workers*. In addition, a photometric assay can conveniently be used and exhibit a higher practical relevance compared to calorimetry. Also, the temperature stability of these materials was tested under usual conditions for sterilisation of medical products.

4.2.3.3 Results and Discussion

Measurements were performed at pH 7.4 in 20 mM phosphate buffer to show the ability of these nanoparticles to bind saccharides at a biological relevant pH-value. To ensure the colloidal stability 0.5% of cetyltrimethyl ammonium bromide (CTAB) was added. To show the effect of sugar binding at pH 7.4 towards the nanoparticles, the ARS - displacement assay was chosen as an easy method which directly shows the binding of ARS to boronic acid entities. In this assay the *cis*-diol containing ARS - dye is incubated with benzoboroxole - modified nanoparticles which results in a colour change from red (indicating the free dye) to yellow. Due to the presence of CTAB the red colour of the ARS solution was changed to a purple which could be explained by the interaction of the quaternary amine present in CTAB with the sulphate group of the ARS. After addition of the boronic acid containing nanoparticles a colour change to orange was observed which indicates the boronic acid - ARS interaction.

The absorption spectra show a broad adsorption maximum at $\lambda = 573$ nm which is described for the free ARS (Figure 40, A). Upon addition of the benzoboroxole-containing latex a decrease in intensity can be observed which indicates the binding of ARS to the boronic acid entities going along with a decrease of the free ARS at 573 nm. This is accompanied by an increase of absorbance below 500 nm where the boronic acid - ARS complex absorbs.

Saccharide binding experiments were performed with Alizarin Red S **3e** loaded nanoparticles. Therefore, the peak maximum at $\lambda = 466$ nm reflects the ARS - benzoboroxole complex formed. If fructose **3a** is now added stepwise the absorbance of the ARS - benzoboroxole complex decreases and the absorbance of the free ARS at 573 nm increases (Figure 40, B). This shows the ability of fructose to displace the reporter dye and to form a complex with the benzoboroxole entity on the nanoparticle surface at pH 7.4. This finding is in

line with a work of Cannizzo *et al.* in which they synthesised boronic acid modified nanoparticles and measured the binding of fructose to these particles at pH 8.8.²⁹⁰

Furthermore, the binding of glucose **3b** to the nanoparticles was investigated at pH 7.4. In the case of the benzoboroxole modified nanolatex the addition of glucose resulted in a small but traceable change in absorbance intensity at $\lambda = 466$ nm (Figure 40, C). This shows that glucose can also compete with ARS for the binding to benzoboroxole. However, the changes determined are not as high as for fructose since the affinity is lower.^{28,211}

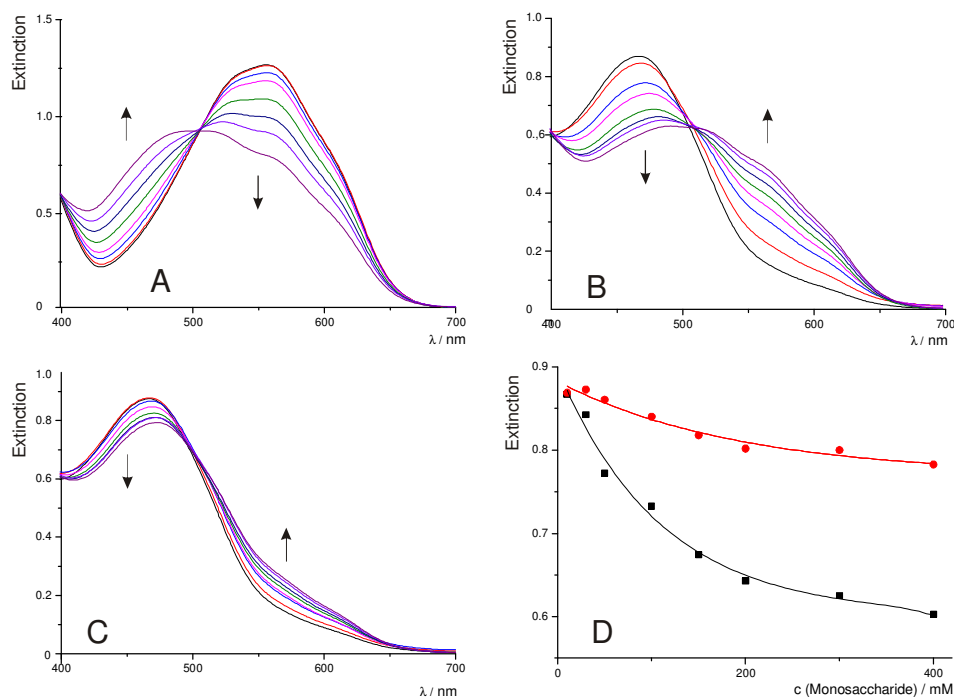


Figure 40. A-C. Absorption spectra of the benzoboroxole modified nanoparticles and their binding to ARS **3e** (A) and fructose **3a** (B) or glucose **3b** (C) in phosphate buffer at pH 7.4. **A.** Increasing nanoparticle concentration, **B.** and **C.** Competition assay with fructose, in which the ARS - loaded nanoparticles are titrated against increasing fructose/glucose concentrations; **D.** Concentration dependence of the absorption at 466 nm for fructose (squares) or glucose (dots) after displacement of **3e**

To describe the binding of glucose **3b** and fructose **3a** to the benzoboroxole modified nanoparticles the saturation curves as well as the binding constants were determined. The saturation curves could be fitted with an exponential plot as seen in Figure 40, D. The sensitivity in the linear range of the curves (until 200 mM) was detected to be 2.5 times higher in case of fructose. To determine the binding constants for the saccharide - boronic acid interaction, the binding constant between the benzoboroxole and ARS was needed. The binding constant between free benzoboroxole and ARS is described in literature to be 1200 M^{-1} .²⁷ Using different deviations the binding constants for fructose and glucose were calculated with respect to this system (see Appendix for theoretical explanation).²⁷ Fructose exhibits an approximately five times higher

binding constant to the benzoboroxole modified nanoparticles with 2354 M^{-1} than glucose with 579 M^{-1} (Appendix Figures A2 and A3). In comparison with values obtained in solution with free benzoboroxole **2a** the trend that **3a** exhibit a higher binding constant to **2a** is similar. In contrast, however, for benzoboroxole, fructose is bound only four times tighter than glucose. In solution the factor is about 20 depending on the method used (ITC or ARS). One possibility for the higher binding constants can be the greater local concentration of boronic acids onto the surface of the nanoparticle meaning that a saccharide molecule, when released, can rebind more effectively to a neighbouring boronic acid entity. This is known and described in literature as apparent affinity.³¹

In order to show the possibility for these nanoparticles to work in systems in which a sterile environment is essential, the particles were treated for 20 minutes at $121 \text{ }^\circ\text{C}$ (Figure 41). Then, the solutions were again tested for their ability to bind ARS. For this experiments the ARS solution was mixed with both treated and untreated latex and it was shown that the complex formation seen at 450 nm is comparable. The comparison shows that almost 95% of the initial binding capacity can be preserved in case of the benzoboroxole.

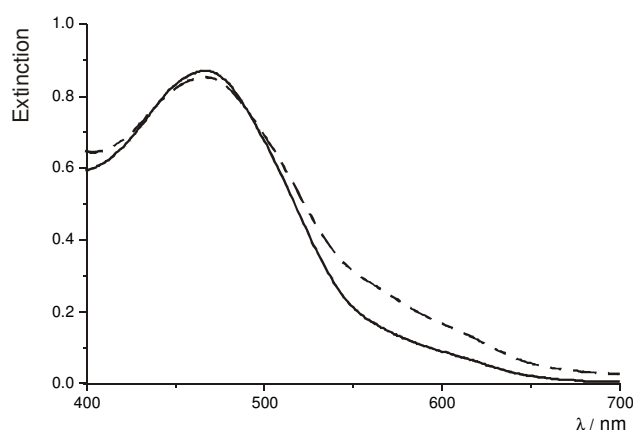


Figure 41. Absorption of the benzoboroxole modified latex at pH 7.4 with ARS before (solid line) and after (dashed line) heat treatment

4.2.3.4 Conclusion

Saccharide binding nanoparticles were synthesised which bind fructose and even glucose at pH 7.4 in phosphate buffer in the mM range. The benzoboroxole **2** was chosen because it has a binding strength towards *cis*-diol containing compounds at neutral pH values than arylboronic acids. The binding of glucose **3b** and fructose **3a** to these nanoparticles was demonstrated with ARS as reporter dye and binding constants could be determined. The binding constant between the benzoboroxole modified nanoparticles and fructose was 2354 M^{-1} and with glucose 579 M^{-1} . To show the temperature stability of the particles obtained the solution was incubated for 20 minutes at $120 \text{ }^\circ\text{C}$ and the binding of ARS to the particles was tested. It could be shown that more than 95% of the initial benzoboroxole entities have again the possibility to bind Alizarin Red S

3e. In this regard these nanoparticles have the ability to be used in systems in which a sterilisation is essential prior their usage. These systems can either be in medical applications or in biotechnological systems such as fermentation. Through the high surface area and the higher apparent binding constants to saccharides these particles have the ability to be used in such types of systems.

4.2.4 Molecular imprinting of fructose using a polymerisable benzoboroxole: Effective Complexation at pH 7.4

This chapter was supported by a diploma thesis from Franziska Grüneberger.

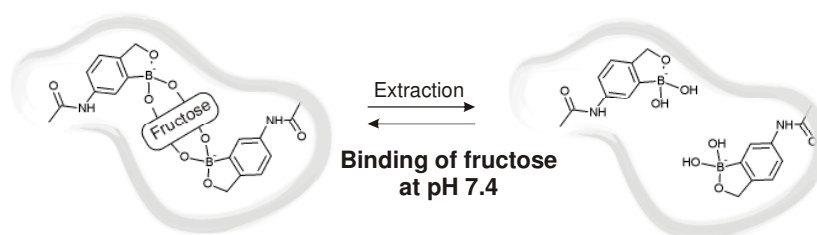


Figure 42. Schematic drawing of a molecularly imprinted polymer for fructose employing a polymerisable benzoboroxole **2d** for effective fructose recognition at pH 7.4

4.2.4.1 Abstract

Covalent molecularly imprinted polymers against *D*-fructose **3a** employing different arylboronic acid derivatives as functional monomer and trimethylpropane trimethacrylate (TRIM) as the crosslinking agent were prepared by a conventional radical bulk polymerisation. Special focus was set on the prepared imprinted polymer using 3-methacrylamidobenzoboroxole **2d** (MIP-BX(Fru)) as functional monomer (Figure 42). Batch binding studies were conducted in aqueous buffers containing 10% methanol at three different pH values starting from pH 11.4 down to 7.4 to study the ability of the used functional monomers to act at a physiologically relevant pH-value. The unbound fructose fraction was analysed by scintillation measurements with ^3H -labelled fructose. The data were compared to a pinacol **3d** imprinted polymer (MIP-BX(Pin)) using the same functional monomer. A fructose **3a** (MIP-BA(Fru)) and pinacol **3d** (MIP-BA(Pin)) imprinted polymer employing the corresponding 3-vinylphenyl boronic acid ester **1f** were also synthesised. Furthermore, a polymer just containing the crosslinker and 1:1 acetonitrile-toluene as porogen was provided as a control polymer to detect the amount of unspecific binding to the polymeric backbone. MIP-BX(Fru) and MIP-BA(Fru) bind comparably fructose at pH 11.4. At lower pH-values the binding capability of MIP-BX(Fru) is paramount compared to MIP-BA(Fru). Furthermore, cross-reactivity studies at pH 7.4 were performed with *L*-fructose, sucrose, glucose and sorbitol showing the shape-selectivity of the MIP-BX(Fru). A medium optimisation revealed that binding of the MIP-BX(Fru) is best in 0.1 M phosphate buffer at pH 7.4.

4.2.4.2 Introduction

As described in the previous chapters arylboronic acids exhibit different affinities to different saccharides. Thus, the interaction between the boronic acid entity and the saccharide is just dependent on the affinity but selectivity is not addressed. Consequently, a different system was chosen to address selectivity since one attribute for receptors is the recognition of one target molecule from a variety of different molecules. To obtain this the molecular imprinting approach was chosen since this technique provides the opportunity to tailor-made artificial receptors in an easy fashion.

The synthesis of benzoboroxole-containing covalently imprinted polymers using fructose **3a** as a model template is described. As the functional monomer 3-methacrylamido-benzoboroxole **2d** was synthesised and employed due to its known ability to bind saccharides at a physiological pH-value. For comparison purposes, the appropriate pinacol-imprinted (MIP-BX(Pin)) and also the fructose (MIP-BA(Fru)) and pinacol (MIP-BA(Pin)) imprinted polymers with 3-vinylphenyl boronic acid **1f** as functional monomer were synthesised. Accordingly, batch binding experiments were performed at pH 11.4, 8.7 and 7.4 to show the binding behaviour of these molecularly imprinted polymers at different pH-values. Moreover, the binding of fructose to a control polymer was also tested in order to assess the amount of unspecific binding. The shape-selectivity of the MIP-BX (Fru) was investigated by competition analysis between D-fructose and a background of 2.5 mM L-fructose, glucose **3b**, sucrose or sorbitol **9**.

4.2.4.3 Results and Discussion

Synthesis

Since benzoboroxole was described as a potential binding agent for monosaccharides in aqueous media at pH 7.4 a corresponding polymerisable derivative **2d** was synthesised and used as functional monomer.

For the covalent imprinting approach it is necessary to synthesise the functional monomer - template complex before its polymerisation. In the case of saccharide imprinting using arylboronic acids the particular boronic acid ester has to be synthesised (Figure 43). Depending on the saccharide under investigation different binding complexes between the arylboronic acid and the saccharide are revealed and proposed in the literature. In the special case, the binding of fructose to arylboronic acids has a high binding strength due to the *syn*-periplanar arrangement of its hydroxylgroups and was investigated by means of NMR spectroscopy. Norrild and Eggert studied the esterification in solution between fructose and p-tolylboronic acid varying the ratio between fructose and the boronic acid derivative. By applying a 2:1 ratio between boronic acid

and fructose in DMSO they found different 1:1 (60%) binding complexes and one 2:1 complex (33%).²¹⁰ Since a stoichiometric pure 2:1 binding complex for fructose is envisaged, esterification methods such as simple mixing are not sufficient enough. Therefore, azeotropic distillation in anhydrous dioxane was chosen for the synthesis of the fructose benzoboroxole ester **4a** and fructose vinylphenyl boronic acid ester **4b** since the removal of the released water forces the reaction into the direction of the 2:1 boronic acid ester. Using this ester as functional monomer - template complex in molecular imprinting is believed to result in higher binding constants and superior selectivity also described by other authors. A conversion of about 80% in each case was reached. Furthermore the synthesis was started with the desired 2:1 ratio between the arylboronic acid derivative and fructose avoiding the removal of unreacted boronic acid. The pinacol arylboronic acid esters **4c** and **4d** were also prepared by azeotropic distillation.

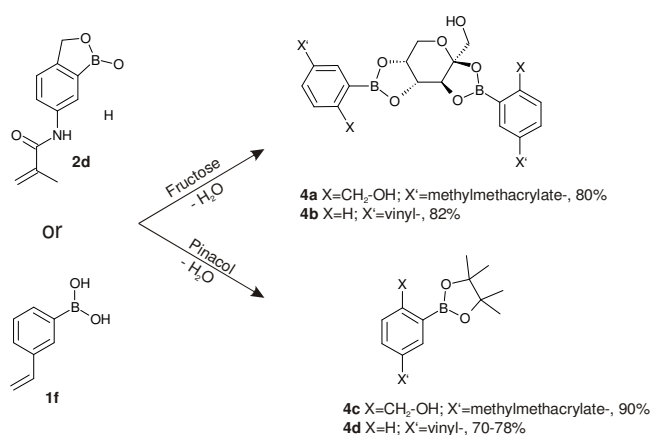


Figure 43. Synthesis of different 3-methacrylamidobenzoboroxole and vinylphenylboronic acid esters for incorporation into a molecularly imprinted polymer

The characterisation of the products was easy in case of the phenylboronic acid esters and the analytical data matched data already reported.³⁹ In contrast, the characterisation of the 3-methacrylamido-benzoboroxole ester **4a** is more complicated. As reported earlier, the esterification of benzoboroxole with different substituted saccharides leads to a peak broadening in the aromatic region due to either slow exchange times or due to the formation of different possible binding complexes.²⁷ Thus, NMR experiments with D-fructose and benzoboroxole were performed in deuterated phosphate buffer at pH 7.4 and at equimolar concentration (Figure 44).

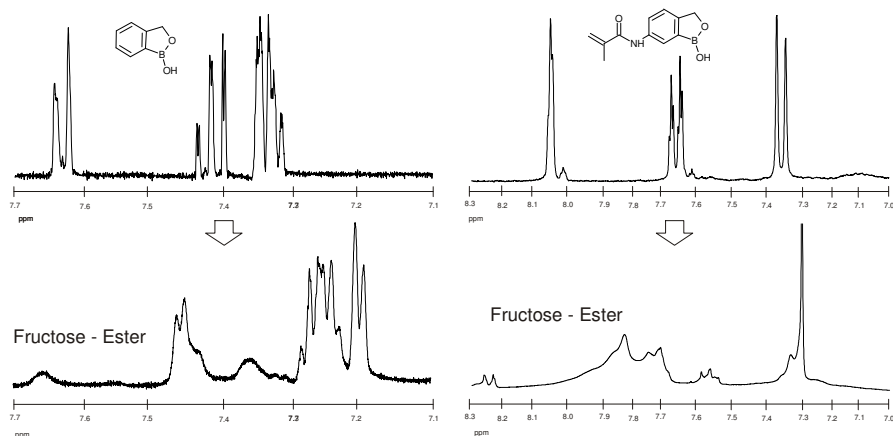


Figure 44. NMR spectroscopy of neat benzoboroxole **2a** and 3-methacrylamidobenzoboroxole **2d** and their formed fructose esters

Beside new peaks at 7.2 and 7.4 ppm which can be assigned to the formed benzoboroxole ester also huge peak broadening could be observed. In line with these results, the synthesised polymerisable benzoboroxole ester **4a** also showed a peak broadening which leads to the assumption that the ester was formed. In combination with mass spectrometry and IR data it is concluded that the fructose-benzoboroxole ester **4a** was synthesised.

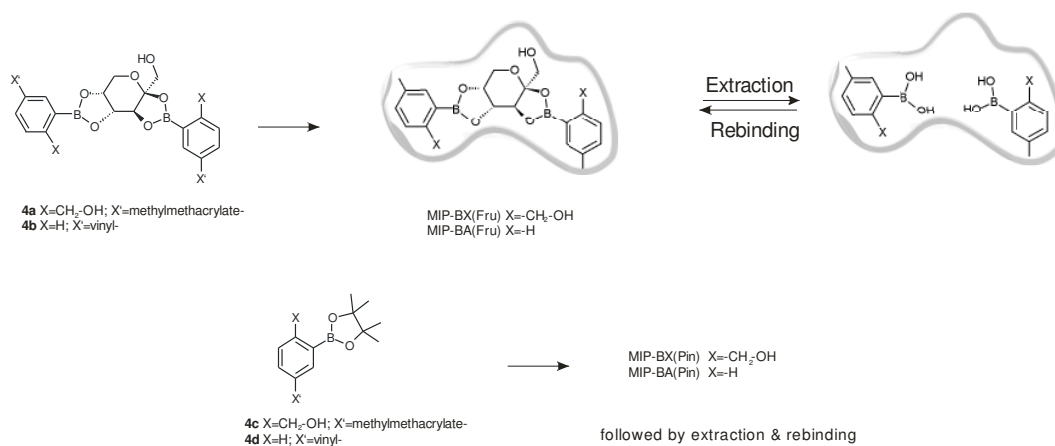


Figure 45. Synthesis scheme of the four different molecularly imprinted polymers MIP-BX(Fru), MIP-BA(Fru), MIP-BX(Pin) and MIP-BA(Pin) starting from the corresponding esters **4a** - **4f**

The synthesised template-functional monomer complexes were then polymerised with trimethylolpropane trimethacrylate (TRIM) as the crosslinking agent. Four polymers were synthesised: two fructose imprinted polymers with esters **4a** or **4b** and two pinacol imprinted polymers with **4c** or **4d** as control polymers (Figure 45). It was not possible to synthesise a polymer without the template molecule since the solubility of the bare arylboronic acid derivatives in the pre-polymerisation mixture was not sufficient. Thus, a bare control polymer

(CP) without any boronic acid content was synthesised to evaluate the interaction of the polymeric backbone with the targeted substances.

After the polymerisation in a two step - process the template was removed by simple washing in MeOH/water mixtures until no further fructose was detected in the washing solution using a colourimetric anthrone assay (data not shown).²⁹¹

The ground and sieved polymer particles in the size of 25 - 50 μm (which were also used for batch binding studies) were characterised by means of nitrogen sorption measurements. Here, the specific surface area (BET) and the pore volumes of either mesopores (BJH) or micropores (HK) were analysed. The data are found in table 5. For comparison also a control polymer (CP) containing just crosslinker was analysed.

Table 5. Summarised pore volumes obtained by nitrogen sorption measurements

Polymer	BET surface area / $\text{m}^2 \text{g}^{-1}$	BJH-mesopore / mL g^{-1}	Poresize BJH / nm	HK-micropore volume / mL g^{-1}	Poresize HK / nm
MIP-BX(Fru)	436	0.21	1.9	0.21	1
MIP-BX(Pin)	360	0.24	2	0.18	1
MIP-BA(Fru)	332	0.29	1.8	0.16	1.2
MIP-BA(Pin)	360	0.28	1.9	0.18	0.9
CP	482	0.42	4.7	0.23	0.9

The values obtained for the surface area and pore volumes are differing between the boronic acid containing polymers and the control polymer devoid of it. The control polymer shows the highest BET surface area of 482 m^2/g whereas the surface areas of the imprinted polymers are between 332 and 436 m^2/g . The values reflect the synthetic procedure since the overall monomer concentration is slightly lower for the control polymer. The polymeric structure in the mesopore regime shows also the same trend. The control polymer which consists just of crosslinker shows with 0.42 mL/g the highest pore volume which is up to two times higher compared to the imprinted polymers. In terms of pore size the imprinted polymers exhibits a pore size around 2 nm whereas the control polymer shows a value of 4.7 nm. Thus, a mass transfer of solvent and saccharides can be present in both cases but due to the size slightly favoured in the control polymer. The values for the HK-measurements displaying the micropores show that there is no huge difference between the polymers.

Medium optimisation

Before starting batch binding experiments the medium was especially optimised for the recognition of fructose at pH 7.4 (Figure 46).

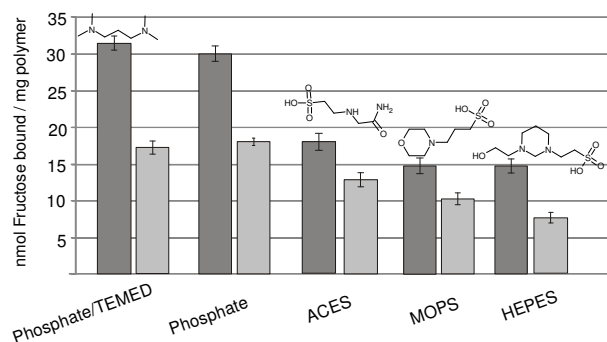


Figure 46. Media optimisation for 2 mM fructose at pH 7.4 with 10 % MeOH; MIP-BX(Fru) (dark bars); MIP-BX(Pin) (light bars)

Arylboronic acids have a sp^2 -hybridised boron atom which exhibit a vacant p-orbital. This can interact with Lewis-bases leading to a different binding behaviour.^{155,160} Therefore, a medium optimisation was conducted and the MIP-BX(Fru) compared to the MIP-BX(Pin) was tested with different buffer compositions at pH 7.4. In a first step the type of *co*-solvent was compared. 10% of either methanol or acetonitrile were added to 0.1 M phosphate buffer. The experiments were performed with 2 mM initial fructose concentration. The rebinding capacity of 2 mM fructose was 23 nmol per mg polymer and thus, inferior in the case of acetonitrile compared to methanol with almost 30 nmol. Two hypotheses can explain this behaviour: (i) acetonitrile is able to interact with the polymer and could be responsible for a morphology change of the polymer; (ii) the binding of one fructose releases in case of a 2:1 (boronic acid:fructose) binding four methanol molecules which favours the reaction entropically. Therefore, methanol was used as *co*-solvent in the subsequent buffer optimisation. Beside phosphate buffers consisting of substituted sulfonic acids - namely ACES, MOPS and HEPES were also chosen. Moreover, to show the effect of possible nitrogen coordination, a phosphate buffer containing 1 % tetramethylethylenediamine (TEMED) was used. In general, the binding of fructose in sulfonic acid containing buffers is lower as compared with binding in phosphate buffer. Among the sulfonic acid buffers the binding in ACES is higher compared to MOPS and HEPES due to the possible coordination of the primary amide. The binding of fructose to the imprinted polymers is comparable if either a neat or a TEMED containing phosphate buffer was used. Since the imprinting factor (IF) – the difference between the MIP-BX(Fru) vs. MIP-BX(Pin) – is in both cases about 1.9, just the neat phosphate buffer was used for the following binding studies at pH 7.4.

Binding studies

The binding of fructose to the differently imprinted polymers at different pH values was determined by batch binding studies. The binding studies were performed according to earlier works in our group.³⁹ Therefore 1 mL fructose solutions in the concentration range of 0.1 - 5 mM

were added to 10 mg of the polymer. To detect the unbound fraction ^3H -radiolabelled fructose was used and scintillation measurements were undertaken. The bound fractions were then calculated. The investigations were started in 0.1 M carbonate solution pH 11.4 with 10% methanol. Furthermore, the binding pH was lowered down to pH 8.7 and pH 7.4 to show the ability of the MIP-BX(Fru) to bind at neutral pH values as well. In the latter cases a 0.1 M phosphate buffer with 10% of methanol was chosen according to the above described optimisation studies.

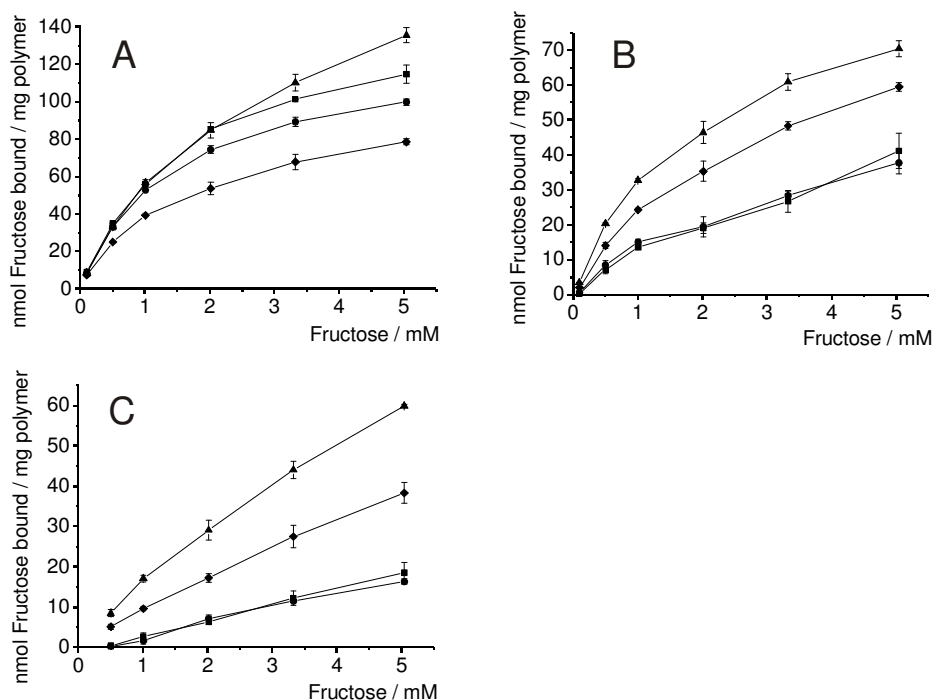


Figure 47. Batch binding experiments for different fructose binding MIPs at different pH-values. **A-C:** Concentration dependency for fructose binding to MIP-BX(Fru) (▲), MIP-BA(Fru) (■), MIP-BX(Pin) (◆) and MIP-BA(Pin) (●); **A:** carbonate solution, pH 11.4, 10 % MeOH; **B:** phosphate buffer, pH 8.7, 10 % MeOH; **C:** phosphate buffer, pH 7.4, 10 % MeOH

The batch binding studies at pH 11.4 revealed high capacities of the synthesised MIP-BX(Fru) and MIP-BA(Fru) of 135.6 and 114.7 nmol per mg polymer, respectively (Figure 47, A). The theoretical binding capacities of both fructose-imprinted MIP polymers are about 200 nmol per mg polymer. Therefore, about 60 % of the possible binding pockets are accessible at an initial fructose concentration of 5 mM. The binding behaviour of both MIP-BX(Fru) and MIP-BA(Fru) is comparable and can be explained by the overwhelming concentration of hydroxyl ions in solution at this alkaline environment which strongly favours fructose complexation regardless of the monomer structure. Thus, the coordination of hydroxyl ions from solution is the predominant action for saturating the electron deficiency of the boron. Consequently, the methylhydroxylgroup in the benzoboroxole derivative **2d** plays a negligible role in terms of binding strength.

Nevertheless, there is a pronounced difference between the MIP-BX(Pin) and MIP-BA(Pin). In case of the MIPs with vinylphenylboronic acid **1f** the difference is (with 15 nmol/mg polymer) comparably small. In contrast, the difference in capacity of the MIP-BX(Fru) and the MIP-BX(Pin) is four times higher (about 60 nmol/mg) showing that imprinting efficiency is higher. One possibility could be that the methylhydroxylgroup increases the affinity due to steric hindrances within the smaller binding pocket obtained for the MIP-BX(Pin).

The binding to the control polymer synthesised just with TRIM as the crosslinker shows no binding to fructose (at different pH-values) at all concentrations studied. This is in line with the literature since TRIM is a favoured crosslinking agent for the recognition of saccharides. Nevertheless, due to the higher pore size of the control polymer (more than two times measured by BJH-sorption isotherms) it shows that the binding of fructose is not dominated by the polymer morphology. Taking into account the lower binding of fructose to the MIP-BX(Pin) it can rather be explained by the presence of boronic acid entities and their right arrangement showing the desired imprinting effect.

The rebinding of fructose at pH 8.7 gives a different outcome (Figure 47, B). Here, a clear difference between MIP-BX(Fru) and MIP-BA(Fru) can be seen. The capacity at an initial concentration of 5 mM is about 70 nmol/mg polymer for MIP-BX(Fru) whereas for the MIP-BA(Fru) a binding of only 40 nmol/mg polymer is reached. Thus, the binding difference is about 30 nmol/mg polymer. Here, most likely a mixture between intra- and intermolecular coordination of the boron is present. Two findings support this assumption. Firstly, the rebound concentration of fructose to the MIP-BX(Fru) is decreasing with decreasing pH-value. This could be due to a lower coordination of hydroxyl ions from the solution to the boron. Secondly, MIP-BX(Fru) exhibit a higher binding capacity compared to MIP-BA(Fru) which shows that an intramolecular coordination of the hydroxylgroup to the boron occurs.

Furthermore, in the case of the MIP-BX(Fru) and MIP-BX(Pin) there is still a significant difference between both polymers for fructose binding. The difference in capacity at 5 mM initial fructose concentration is about 12 nmol/mg polymer. The binding isotherms of fructose to the MIP-BA(Fru) and MIP-BA(Pin) at pH 8.7 are almost similar and show no difference.

At pH 7.4 the advantage of intramolecular coordination provided by the benzoboroxole units becomes evident (Figure 47, C). The polymers bearing vinyl phenylboronic acid exhibit a small binding ability with just about 18.5 nmol/mg polymer at 5 mM initial fructose concentration and no differentiation between the fructose and pinacol imprint was seen. At this concentration the MIP-BX(Fru) is still able to bind 60 nmol/mg polymer which is a factor of 3.2 compared to the MIP-BA(Fru). The MIP-BX(Pin) binds 40 nmol/mg polymer at 5 mM fructose resulting in a difference of about 20 nmol/mg polymer. The decreasing difference in capacity between the MIP-BX(Fru) and MIP-BX(Pin) with decreasing pH-values underlines the effect of the possible free

hydroxylgroup in *ortho*-position to the boron which can lead to an additional hydrogen bonding to the saccharide. Since this effect could also be present during the polymerisation, it is just possible in the MIP-BX(Fru).

Cross reactivity

Since molecular imprinting aims to be selective for a targeted analyte the cross-reactivity has also to be investigated. To verify the imprinting selectivity in this case, the affinity between boronic acids and different saccharides in solution has to be considered. In general, the affinity is dependent on the pK_a of the arylboronic acid derivative as well as of the structure of the saccharide. Moreover, in case of aqueous environment the tautomeric form of the saccharide is also one of the key factors regarding binding strength. The binding strength of fructose is comparably high due to the high presence of about 25 % of the β -D-fructose furanose species (water, 31° C). The binding to this form is preferred due to the presence of a *syn*-periplanar hydroxyl pair (C2-C3). Compared to glucose the binding strength is much higher because the binding of the pyranose-isomer (α -D-glucopyranose) is just present with 0.14 % in deuterated water at 27 °C. Taking these limitations into account, the cross-reactivity was evaluated with L-fructose since the discrimination of enantiomers is described for many different molecular imprints. Beside L-fructose, D-glucose, sucrose and sorbitol were used as competitors. Competition between D-fructose of varying concentrations and the competitor with a constant concentration of 2.5 mM was chosen (Appendix Figure A4; at equimolar concentration shown in Fig. 48). Since just the D-Fructose is ^3H -labeled the amount of bound competitor was obtained by calculating the difference between bound D-Fructose to the imprinted polymers in the presence or without competitor. Therefore, the difference of the binding with and without competitor reflects the displacement of fructose showing the degree of cross selectivity.

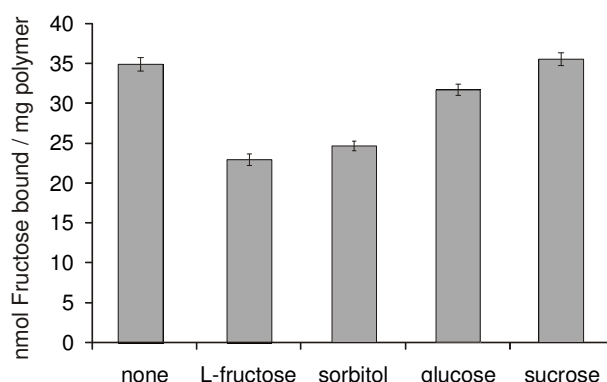


Figure 48. D-fructose binding to MIP-BX(Fru) at pH 7.4 in phosphate buffer in presence of competitors at equimolar concentration

As expected, the degree of competition is dependent on the strength of the saccharide - boronic acid interaction (Figure 45). D-glucose **3b** and sucrose influence the binding of D-fructose to the MIP-BX(Fru) slightly whereas L-fructose and sorbitol have a higher impact. It is noteworthy that the extent of competition between sorbitol and L-fructose are comparable even their binding constants to arylboronic acids vary just by a factor of two. It is derived that more than 90 % of D-fructose is still bound in the presence of D-glucose or sucrose (more than 95 %) as competitors. In contrast, sorbitol and L-fructose act as competitors since less D-fructose could bind to the polymer. 36 nmol D-fructose per mg polymer are bound without competitor, whereas just around 24 nmol D-fructose are bound with equimolar addition of either L-fructose or sorbitol. Consequently, 2/3 of the possible binding cavities are occupied by D-fructose and just 1/3 by either L-fructose or sorbitol at equimolar concentrations. Moreover, at smaller D-fructose concentrations than the concentration of the competitor also high amounts of D-fructose are bound to the MIP-BX(Fru) (see Appendix A4).

The degree of saccharide competition can be estimated in a more quantitative way. The separation factor α can be derived which describes the interaction of a targeted molecule with a stationary phase compared to a competitor. The values for L-fructose and sorbitol are 2 and 2.5 at an equimolar concentration of D-fructose to the competitor, respectively. These values show that L- and D- fructose can be distinguished in a normal batch binding experiment, which is equal to one plate in terms of chromatography. The α -values for D-glucose and sucrose are 10.7 and 71 underlining the small impact and degree of competition with these saccharides.

4.2.4.4 Conclusion

For the first time a molecularly imprinted polymer with 3-methacrylamido-benzoboroxole **2d** as functional monomer for the binding of fructose was prepared. In comparison to earlier reports for fructose recognition, the binding pH could be lowered and a favoured rebinding in comparison to the MIP-BX(Pin) could be observed. It was shown that the MIP-BX can be used for saccharide recognition at pH 7.4 in aqueous environment which was so far not reported for unprotected saccharides such as fructose. Hence, the benzoboroxole still poses a paramount performance in terms of binding at pH 7.4 even in case of change of polymer morphology, *e.g.* from a nanoparticulate system to a highly rigid and crosslinked polymer.

4.2.5 Biomimetic monosaccharide analogues – (Easy) Synthesis, characterisation and application as template in molecular imprinting

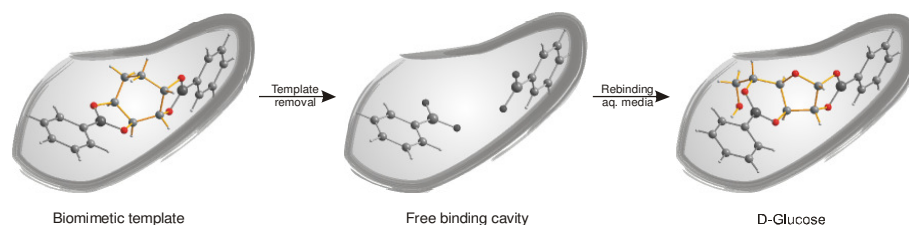


Figure 49. Schematic drawing of the imprinting process of biomimetic monosaccharide analogues and binding with glucose to these polymers; Crystal structures are new or published data

4.2.5.1 Abstract

Biomimetic monosaccharide analogues derived either from cyclopentadiene or 1,3-cyclohexadiene were conveniently synthesised via cis-dihydroxylation under Upjohn's condition using Narasaka's modification with addition of phenylboronic acid. The intermediately synthesised diboronic acid esters of 1,2,3,4-tetrahydroxycyclopentane and -hexane were crystallised and the obtained new crystal structures were in-silico overlapped with already published crystal structures of diboronic acid esters of D-glucose or D-fructose. Their structural superimposition showed a good agreement reflecting on their stereochemistry. For fructose the R-enantiomer of the tetrahydroxy compounds showed a good alignment whereas the S-enantiomer had a good alignment with the boronic acid ester of glucose. To further investigate the applicability of the synthesised structures, rac - 1,2,3,4-tetrahydroxycyclohexane (which was yielded by oxidative cleavage of the diboronic acid ester) was used as a template for molecular imprinting since the geometric properties of the six-membered ring were slightly better compared to the five-membered ring. For covalent molecular imprinting 4-vinylphenylboronic acid was chosen as the functional monomer and the corresponding boronic acid ester of the tetrahydroxy cyclohexane was polymerised with TRIM as the crosslinker and a 1:1 mixture of acetonitrile and toluene as the porogen (yielding MIP-Biomim). The rebinding of fructose and glucose was tested with ³H-labelled saccharides at pH 11.4 with addition of 10 % methanol. The data were compared to a pinacol imprinted polymer (MIP-Pin) employing the corresponding 4-vinylphenyl boronic acid ester. It could be shown that fructose as well as glucose can bind to the MIP-Biomim and a clear difference can be seen with the MIP-Pin which shows that the imprinting process was successful. Furthermore, the comparison between the binding isotherms for fructose and glucose suggests different binding behaviour and characteristics which reflects the internal boronic acid - saccharide interaction.

4.2.5.2 Introduction

So far, mainly the interaction between boronic acid entities and fructose was chosen as a model system. Nevertheless, more important is the interaction between arylboronic acids and glucose due to the high interest in artificial receptors for glucose monitoring.²⁵ One problem which arises is the complicated interaction between glucose and the boronic acid since not a defined binding structure is obtained.²¹³ This makes template mediated approaches for the synthesis of artificial receptors such as molecular imprinting quite difficult. From a molecular point of view the need for a defined functional monomer - template complex is mandatory for the imprinting efficiency. To address this problem a two-step synthesis of biomimetic saccharide-like structures by employing the Sharpless-dihydroxylation to cyclopentadiene or cyclohexadiene was introduced.²⁹² By choosing Narasaka's modification a *trans*-alignment of the two *cis*-diols is addressed which corresponds to the fructose and glucose form which bind to boronic acids. To prove and to verify the structural relationship between these mimics and glucose or fructose two new crystal structures of the associated arylboronic acid esters were characterised and *in-silico* overlapped with already published boronic acid esters of fructose and glucose.^{188,293} Thus, a core atom set was selected and *via* molecular superimposition the root mean square distance of the overlapped structures was calculated. With these results one derivative was chosen to act as template in the molecular imprinting approach. The efficiency was tested by rebinding with radiolabelled D-fructose and D-glucose.

4.2.5.3 Results and Discussion

Synthesis of the biomimetic substances

The synthesis of carbohydrate mimic compounds was performed using the Upjohn alkene dihydroxylation procedure in which osmium tetroxide is employed as oxidative agent and N-methylmorpholine N-oxide (NMO) as the cooxidant (Figure 50).²⁹² As substrates cyclopentadiene **35** and 1,3-cyclohexadiene **36** were chosen since cyclic saccharide structures of glucose or fructose can either be in a five- or six-membered ring corresponding to the furanose or pyranose form, respectively. In comparison to the most prevalent binding forms of fructose and glucose to boronic acids the *cis*-diols have to be in a *trans*-alignment. Therefore, Narasaka's modification for the *cis*-dihydroxylation was chosen because phenylboronic acid acts as (i) agent for the electrophilic cleavage for the osmate ester and as (ii) protecting group.²⁹⁴ As protecting group, the phenylboronic acid helps firstly to overcome the problem of overoxidation and secondly as stereo-delegating group since after the monoboronic acid ester is formed the second dihydroxylation is favoured from the opposite site of the ring. This leads to the wanted *trans*-alignment of the *cis*-diol units. After the synthesis of the diboronic acid esters

(1R*,2R*,3R*,4R*)-cyclopentane-1,2,3,4-tetraol-1,2:3,4-bis(phenylboronate) **rac-4e** and (1R*,2R*,3R*,4R*)-cyclohexane-1,2,3,4-tetraol-1,2:3,4-bis(phenylboronate) **rac-4f** the biomimetic saccharide analogue **rac-3c** was obtained by oxidative cleavage with hydrogen peroxide in an ethyl acetate/acetone mixture of **rac-4f**. The synthesis was performed as described by Gysper *et al.* and the analytical data matched the described data.²⁹²

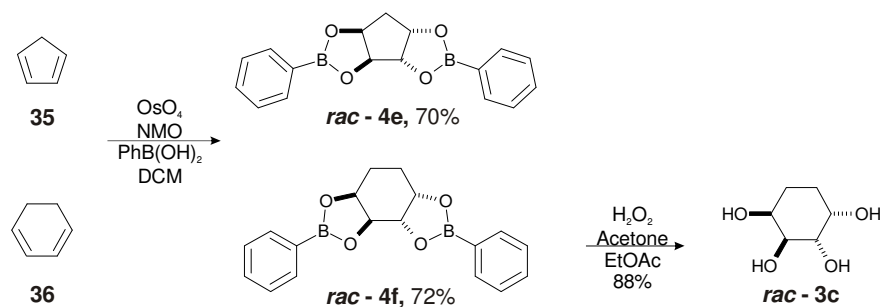


Figure 50. Synthesis of the biomimetic analogue **rac-3c** starting from cyclic dienes **35** and **36**

Crystal structures

Crystals of the diboronic acid ester derivatives **4e** and **4f** suitable for X-ray analysis were obtained from a DCM solution by slow evaporation of the solvent. The X-ray structures for both compounds unambiguously confirmed the formed diboronic acid esters (Figures 51). Crystallographic data as well as details of the crystal structure solution and refinement are summarised in Table A3 (Appendix). **4e** crystallises in the non-centrosymmetric space group $Pna2_1$. Because of the presence of glide planes, both enantiomers can be found in the crystal packing. **4f** crystallises in the centrosymmetric space group $P2_1/a$ as racemate, too.

Since crystal structures reveal the geometrical properties of the molecules, several key parameters were compared to show the difference between the biomimetic structures and glucose or fructose. It was important to compare the structures to glucose or fructose bound to phenylboronic acid since the complex formation of boronic acid esters is quite complicated. For example, for fructose it was derived by NMR experiments that the binding form to boronic acids is the β -D-fructofuranose which is present in aqueous solution to 25%.²¹⁰ For glucose it was concluded that the preferred binding form is the α -D-glucopyranose.²¹³ For a diboronic sensor prepared by Shinkai *et al.* with an anthracene bridge between the two boronic acid residues it was shown that glucose binds initially as a pyranose and converts to the thermodynamically more stable furanose form.²¹⁴ Therefore, crystal structures were chosen which possess equal structures than revealed by NMR. It should be mentioned at this stage that the boron in the compared crystal structures of the diboronic acid esters is sp^2 -hybridised. Nevertheless, for the later application in

aqueous basic environment the hydroxyl groups can coordinate to the boron leading to sp^3 -hybridisation of the boron. It is assumed that this hybridisation change is equal for all diboronic acid esters and hence, the superimposition of the sp^2 -hybridised structures (which are found in crystal structures) is valid to show the degree of analogy.

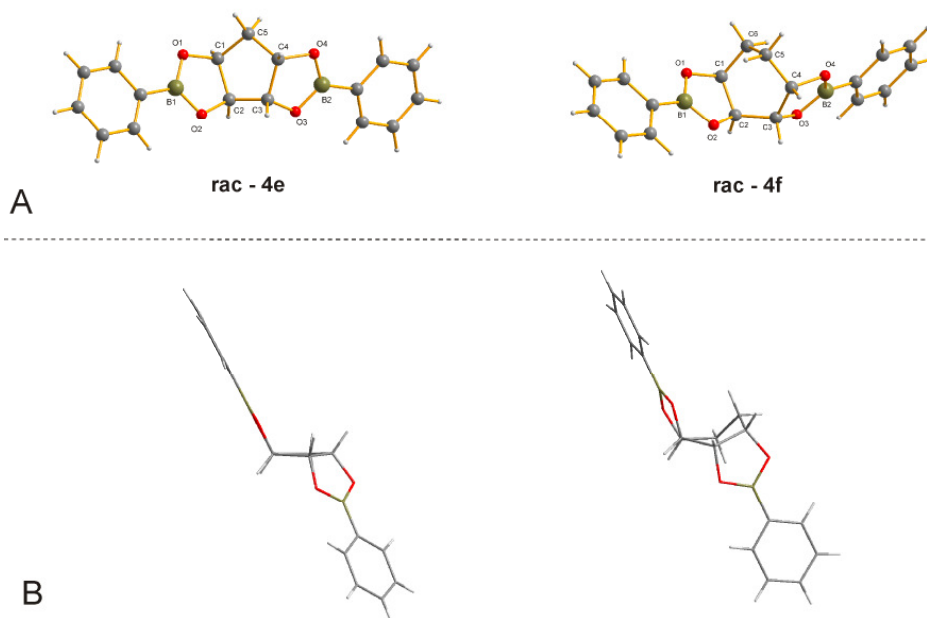


Figure 51. Molecular structure of the diboronic acid ester *rac-4e* and *rac-4f*: A) top view and B) side view. Shown here: *S*-enantiomer

Hence, parameters that reflect the structural arrangement of the boronic acid functionalities which are later fixed in the polymeric network are chosen to gain a deeper understanding on a molecular scale. These key parameters include the distance between the boron atoms, different torsion and bond angles, and the position between different planes of the molecule.

The cyclopentane ring of *4e* is almost planar with a maximal deviation from the best plane of 0.041(2) Å (C4) whereas the cyclohexane ring of *4f* occurs in a twisted boat conformation (Figure 1B). In comparison to the already published glucose and fructose boronic acid esters in which the glucofuranose or the fructopyranose are in an out-of-plane or also twisted boat conformation, respectively, structure *4f* exhibits a higher similarity. This goes along with the dihedral angles between the planes of both boron ring planes. The dihedral angle accounts for the spatial arrangement of the two functional monomers to each other. This angle is for the structure *4e* about 38° whereas for *4f* this value is nearly twice as high (79°). The values for the glucose or fructose phenylboronic acid esters vary between 58° and 74°, respectively. In *4e*, each of both boronic acid ester rings are also nearly planar with maximal deviations of the best plane of 0.020

(2) Å (C2) and 0.047(2) Å (C3). The five ring moieties are folded with respect to the cyclopentane ring forming dihedral angles of 62.7(1)° and 61.6(1)°. The phenyl groups are only slightly torsioned around the boron ring system with 2.6(4)° (C7-C6-B1-O2) and 3.8(4)° (C17-C12-B2-O3). The dihedral angle between the nearly planar boron ring (B1/O1/O2/C1/C2; maximal deviation from the best plane 0.095(1) Å) and the C1/C2/C3/C6 plane in **4f** is 61.8(1)°. The other boron ring (B2/O3/O4/C3/C4) forms with the C2/C3/C4/C5 plane a dihedral angle of 62.4(1)°. In analogy to **4e**, both boron ring moieties are folded along the C-C bonding of the central cycloalkane ring system in opposite directions. The B...B distance is with 5.4 to 5.5 Å in all crystal structures comparable showing that the saccharide mimic and the natural saccharides have almost the same size and the almost equal alignment of the hydroxyl groups. Thinking about the molecular imprinting approach, the size and alignment of hydroxyl groups has to match since a 2:1 binding stoichiometry is envisaged for a possible cooperative binding. The O-B-O angles are also in the same order of magnitude (**4e**: 114.5(2)° and 113.9(2)°; **4f**: 112.8(2)° and 113.0(2)°) and show a compressed sp²-hybridised angle due to cyclic ring formation in non-aqueous environment. This value is typical and described for normal boronic acid ester formation with 1,2-*cis*-diols. In contrast, the bond angle of the O-B-O bond at C3 and C5 of the glucofuranose is about 124° due to the 1,3-boronic acid ester. From the structural comparison it can be derived that both structures show a good alignment to fructose and glucose itself. Furthermore, also the compared boronic acid esters **4e** and **4f** showed high similarities for example in the B...B distance and the attachment of phenylboronic acids, which supports the use of the biomimetic monosaccharide analogue as templates in template-mediated receptor synthesis such as molecular imprinting.

Table 6. Selected geometric parameters of crystal structures **4e**, **4f**, glucose and fructose boronic acid ester

Parameters	4e	4f	Glucose boronic acid ester	Fructose boronic acid ester
B...B distance / Å	5.440(4)	5.447(3)	5.529(3)	5.430(3)
Bond angle O1-B1-O2 /°	114.5(2)	112.8(2)	123.7(2)	113.4(2)
Bond angle O3-B2-O4 /°	113.9(2)	113.0(2)	113.6(2)	113.7(2)
Dihedral angle between both boron ring planes /°	37.9(1)	78.6(1)	57.3(1)	73.6(1)

Structural superimposition

To verify the similarity between the synthesised structures *rac*-**3c** and glucose or fructose in a quantitative way, their corresponding diboronic acid esters **4e** and **4f** were superimposed with already published structures of the diboronic acid esters of glucose and fructose.

The comparison was started by defining a core atom set which contained 22 atoms (Figure 52, A). The atoms of both phenylboronic acid parts were chosen and in addition to that also four atoms within the cycle of the saccharide. With this selection, the difference in ring size of either the pyranose or the furanose form has no influence. Furthermore, especially in the case of the glucose boronic acid ester, the published binding conformer is an α -D-glucofuranose in which a six-membered cyclic boronic acid ester (ester with 1,3-diol) is formed whereas in all other cases just a five-membered ring (ester with 1,2-diol) is formed.

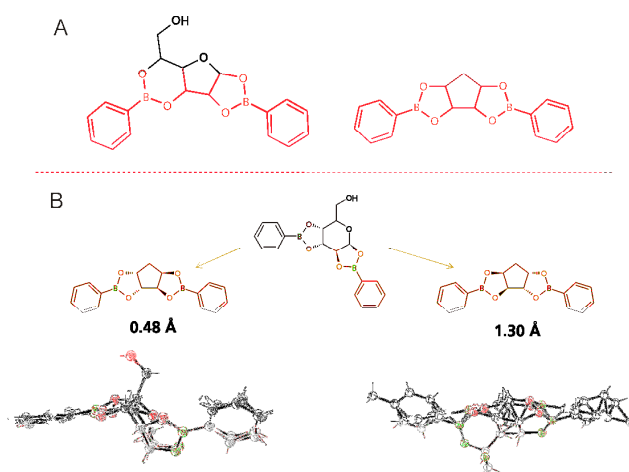


Figure 52. **A:** Defined core atom set highlighted in red using for example glucopyranose boronic acid ester and the compound **4e**; **B:** Structural superimposition of the fructofuranose boronic acid ester with *S*-**4e** and *R*-**4e**.

For the structural superimposition the Kabsch method for best rotation of vector sets has been used.²⁹⁵⁻²⁹⁷ This method was so far applied for the 3-dimensional protein structure alignment.²⁹⁸⁻³⁰⁰ The program written for superimposition of saccharides is a small octave script. The measure for the similarity of two molecules is the root mean square (rms) - distance of the core atoms (Table 7).

Table 7. Results of the rms-distance after structural overlap between the biomimetic saccharide analoga and glucose or fructose phenylboronic acid esters

Enantiomer	Glucose boronic acid ester ²⁹³ / Å	Fructose boronic acid ester ¹⁸⁸ / Å
<i>S-4e</i>	0.44	1.34
<i>R-4f</i>	1.30	0.48
<i>S-4e</i>	0.46	1.50
<i>R-4f</i>	1.52	0.20

Due to the racemic synthesis of the saccharide mimic boronic acid esters **4e** and **4f**, both enantiomers *all-S* and *all-R* were used to calculate the superimposition. Surprisingly, it was found that the *S*-enantiomer has a better overlay with the glucofuranose whereas the *R*-enantiomer has a better overlap with the fructopyranose (Table 7). With 0.2 Å the smallest mean square distance is found for the overlap between the *R-4f* and the fructopyranose. In this case, the *R-4f* is about 0.28 Å better than the *R-4e* derivative.

Molecular imprinting

To show the validity of the saccharide-like biomimetic structures, one derivative *rac-3c* was chosen to act as a template for molecular imprinting (Figure 53). In this regard, **4f** was hydrolysed using acetone/hydrogen peroxide to yield tetrahydroxy cyclohexane *rac-3c*. According to earlier works in our group the imprinting was performed with TRIM as the crosslinking agent, 1:1 acetonitrile toluene as the porogen and classically AIBN as the radical initiator.^{39,157} 4-Vinylphenyl boronic acid was used as the functional monomer and the corresponding diboronic acid ester **4g** was synthesised using azeotropic distillation in anhydrous dioxane. The polymerisable ester was then polymerised with the crosslinker to yield a bulk polymer which was mechanically destroyed and sieved to obtain particles in the range between 25-50 µm. The template was removed by repetitive washings with MeOH/water. It was not possible to obtain a non-imprinted polymer since the solubility of the 4-vinylphenyl boronic acid was not sufficient in the monomeric mixture. Therefore, as a control polymer a pinacol imprint was synthesised using the corresponding pinacol vinylphenyl boronic acid.

The binding of fructose **3a** and glucose **3b** to the polymer was determined by batch binding studies with ³H-labelled glucose or fructose between 0.1 and 5 mM over night. **3a** and **3b** were chosen to show the ability of the polymer to bind to both monosaccharides since the racemic template showed a good structural overlap to both monosaccharides. The polymer particles were centrifuged, the unbound fraction was determined by scintillation measurements and the fructose bound to the polymer was calculated. In parallel to earlier imprinting efforts in our group the batch binding studies were performed at pH 11.4 in carbonate solution with 10 % methanol since

this showed the best performance for saccharide binding to this polymer. The obtained binding curves are shown in figure 54.

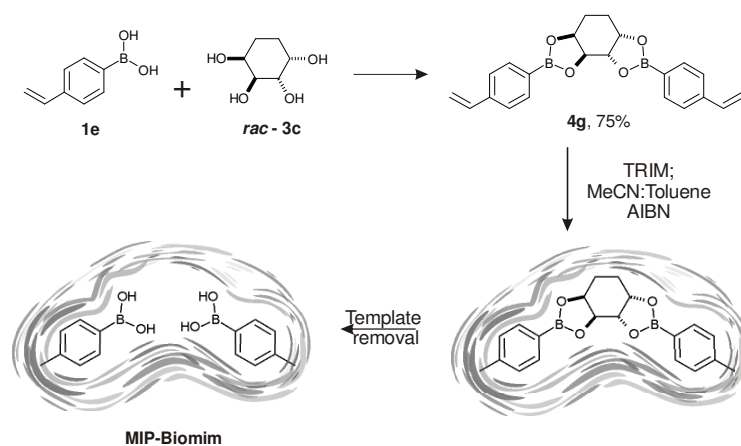


Figure 53. Molecular imprinting scheme

The binding curves for the MIP-Biomim with fructose showed a high capacity with 110 nmol per mg polymer. These are almost 55 % of the theoretical binding pockets that are accessible for a rebinding of fructose which is comparable to other polymers since the binding site distribution is irregular. Furthermore, in case of fructose binding just the R-enantiomer of **3c** should act as a template molecule since the structural overlay revealed a better superimposition. The comparison of the fructose binding curves of the MIP-Biomim and MIP-Pin shows a clear difference of 40 nmol per mg polymer at saturating fructose concentration of 5 mM. This higher binding of fructose to the MIP-Biomim compared to the MIP-Pin is reflected by an “imprinting factor” (for rebinding) of about 1.6. The values show that fructose binds preferably to the MIP-Biomim but nevertheless, also a high binding can be observed to the MIP-Pin. It can be explained by the possibility of fructose to bind in either a 1:1 or 2:1 binding complex to arylboronic acids. Furthermore, the tridentatic 1:1 binding complex is favoured especially in alkaline, aqueous environments.²¹⁰ Consequently, the fructose can bind either to the well-defined binding pockets in a 2:1 manner since the optimal binding site should exhibit two boronic acid entities, or to single boronic acids attached to the polymeric network. Hence, the difference in binding of both polymers is comparably small.

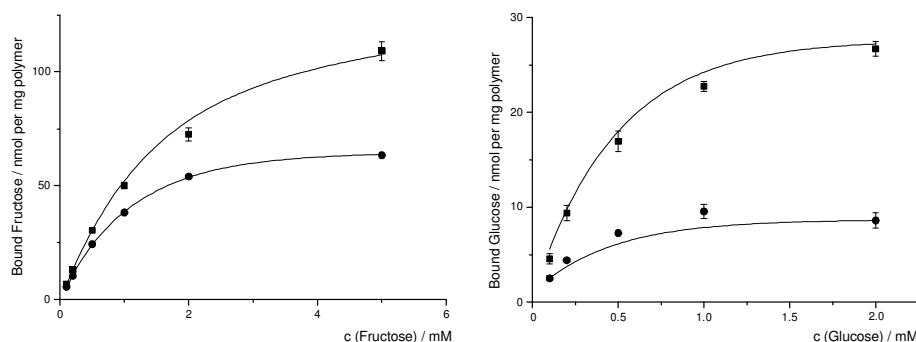


Figure 54. Binding isotherms obtained by batch binding of fructose (A) or glucose (B) to either MIP-Biomim or MIP-Pin at pH 11.4

In case of glucose rebinding a different picture is seen. Here, the binding at saturation to the MIP-Biomim is 25 nmol per mg polymer and hence just one fourth of the binding capacity obtained by fructose rebinding. This can be explained by the lower binding constant for glucose with arylboronic acids. In case of phenylboronic acid and glucose the binding constant at pH 7.4 is about 6 M^{-1} whereas the binding constant with fructose is about 200 M^{-1} obtained by ITC measurements (data shown in chapter 4.1.5). Since the overall bound saccharide at 5 mM initial saccharide concentration differs just by a factor of four, whereas the ratio of binding constants is more than 20 times, the difference in binding constant alone cannot explain the behaviour. Furthermore, the possibility of a 2:1 binding between the incorporated boronic acid functional monomers and glucose can display a higher binding constant leading to the observed binding behaviour. This can further be confirmed by comparing the binding of the MIP-Biomim and MIP-Pin with glucose. Here, an “imprinting factor” of about 2.5 can be derived which is higher compared to the fructose binding. This makes clear that the binding characteristics of glucose or fructose to the vinylphenylboronic acid within the polymer are different in terms, for example, of selectivity or capacity.

4.2.5.4 Conclusion

The applicability of biomimetic monosaccharide analogues was tested via *in-silico* superimposition of crystal structures and the use of one derivative in the molecular imprinting for saccharide recognition. The data revealed that a synthetic two-step protocol yields tetrahydroxy-compounds which can be used as saccharide mimics since their overlay showed an excellent alignment to either glucose or fructose. It was found that the stereochemistry of the tetrahydroxy-compounds brings a better overlay to fructose or to glucose. In terms of molecular imprinting, the synthesised compounds show a possibility to overcome the problem of a non-defined template-functional monomer complex using saccharides as template molecules and arylboronic acid

derivatives as functional monomers. In this manner it was possible to create the first molecular imprint in a TRIM matrix based on boronic acids capable of binding glucose in aqueous media at pH 11.4. Further studies, especially through the use of enantiomeric pure analogues will gain a deeper insight into this system targeting a higher selectivity for just one saccharide. Nevertheless, since the biomimetic analogue is of small size an easy stereo-controlled synthesis was so far not yet found.

4.2.6 Conclusion

In this chapter a variety of boronic acid derivatives were used to act as binding units within different polymeric systems. Especially derivatives of benzoboroxole **2** were chosen to enable these different polymeric systems to bind saccharides at neutral pH-values. This envisages their use in biological or medicinal application scenarios.

It could be demonstrated by ITC experiments that the binding of saccharides to functionalised nanoparticles is mainly entropically driven which states for secondary effects such as multivalent binding or reorientation processes. This leads to a higher apparent binding constant compared to the free boronic acid ligand without immobilisation. It opens possibilities to use such kind of nanoparticles as coatings for sensors or as filling materials in membranes for extraction, sensing and binding of *cis*-diol containing substances. Either ITC or UV-Vis spectroscopy (ARS) could be used as detection methods for the binding of saccharides to the nanoparticle system (Chapters 4.2.2 and 4.2.3). The ITC-experiments showed the advantage to characterise the binding by thermodynamical means and to provide a label-free sensing method. Nevertheless, it was not possible to obtain data for glucose binding because of limitations of the used ITC system due to the weak binding affinity of glucose to the boronic acid. Therefore, the reporter dye ARS was used as a competitor which reflects the binding to the boronic acid entity by colour changes. In this regard also the binding of glucose to these modified nanoparticles could be monitored. The combination with electrochemistry (chapter 4.1.9) opens the possibility for creating an electrochemical sensor for different *cis*-diol containing analytes for recognition at pH 7.4. However, ARS has to be immobilised for a later sensor application.

As mentioned above in these systems the cross reactivity is governed by the affinity of the *cis*-diol containing compound to the boronic acid derivate. In this direction, molecular imprinting was chosen as one possibility to improve selectivity which was demonstrated in chapter 4.2.4 and 4.2.5. Both described polymeric systems bind the targeted monosaccharides selectively. In chapter 4.2.4 the main focus was to bind fructose at pH 7.4 by 3-methacrylamidobenzoboroxole **2d** as functional monomer. The performance of this polymer to bind fructose was compared to a polymer which was prepared in parallel to Rajkumar *et al.* with vinylphenylboronic acid **1f** as functional monomer. The main focus of chapter 4.2.5 was to provide biomimetic template molecules for a more defined interaction with boronic acids as functional monomer. Recognition of glucose was focussed since glucose itself does not give a defined template-functional monomer complex. In parallel also here the system by Rajkumar *et al.* was resynthesised and the biomimetic saccharide analogue was used as template molecule. In this system it was shown that the imprinted polymers using boronic acid derivatives as functional monomer are able to bind the targeted monosaccharides. For example the imprinting factor for glucose recognition to the MIPs generated in chapter 4.2.5 is 2.5 whereas the IF (in terms of rebinding) for fructose recognition to

the same MIP is just 1.6. Nevertheless, the binding capacity of the MIP for fructose or glucose recognition is mainly driven by the affinity of the monosaccharide to the boronic acid. In this regard the overall capacity for fructose is about four times higher compared to glucose. Therefore, the affinity governs the capacity and hence the performance of the binding reaction.

Considered as a whole, new materials for saccharide recognition were synthesised and characterised. It was concluded, that the chemical nature and the morphology of polymers have an influence on the binding reaction. The coupling of binding units onto a polymeric backbone also influences the binding since multivalent binding on a high surface area can be achieved. Multivalent binding sites can be considered as one of the key to enhance binding reactions with low binding constants. For example, lectins have binding constants in the mmolar range. Nevertheless, the binding to targeted structures such as cell-walls in case of pathogen-host interaction is an interplay of a variety of different binding sites which results in a strong overall binding. Nevertheless, the binding of boronic acids to *cis*-diol containing compounds is in these systems the dominant factor. There are some approaches, for example by Pal *et al.*, in which boronic acids are also used as primary recognition units. However, in addition also the backbone in this case of a peptidic structure was varied to gain binders for the Thomson-Friedenreich antigen. Therefore, beside the primary interaction also secondary interactions, for example hydrophobic interaction found in lectins, have to be considered to gain binding units with higher specificity. In addition, a more sophisticated polymerisation method could form a binding pocket in a more specific way than the free radical polymerisation. Also the kinetics of the polymerisation can be tuned and orientation processes of monomers to the template or targeted molecule can occur more precisely. Furthermore, in addition to the boronic acid entities also different other functional monomers could be used to gain binding pockets with cooperative interactions.

In this thesis entitled “Saccharide Recognition - Boronic acids as Receptors in Polymeric Networks” different aspects of boronic acid synthesis, their analysis and incorporation or attachment to different polymeric networks and characterisation thereof were investigated.

The following key aspects were considered:

- Provision of a variety of different characterised arylboronic acids and benzoboroxoles
- Attachment of certain derivatives to nanoparticles and the characterisation of saccharide binding by means of isothermal titration calorimetry and displacement assay (ARS) to enhance the association constant to saccharides at pH 7.4
- Enhancement of selectivity in polymeric systems by means of molecular imprinting using fructose as template and a polymerisable benzoboroxole as functional monomer for the recognition at pH 7.4 (Joined by a diploma thesis of F. Grüneberger)
- Development of biomimetic saccharide structures and the development of saccharide (especially glucose and fructose) binding MIPs by using these structures as template molecules.

In the first part of the thesis different arylboronic acid derivatives were synthesised and their binding to glucose or fructose was investigated by means of isothermal titration calorimetry (ITC). It could be derived, which is in parallel to the literature, that derivatives bearing a methylhydroxyl-group in *ortho*-position to the boron (benzoboroxole) exhibit in most cases a two-fold higher association constant compared to the corresponding phenylboronic acid derivative. To gain a deeper understanding NMR spectroscopy and mass spectrometry with the benzoboroxole and glucose or fructose was performed. It could be shown that the exchange rate in terms of NMR time scale is quite slow since in titration experiments new peaks appeared. Via mass spectrometry of a mixture between benzoboroxole and glucose or fructose, different binding stoichiometries could be detected showing that the binding of saccharides is comparable with their binding to phenylboronic acid. In addition, the use of Alizarin Red S as an electrochemical reporter was described for the first time to monitor the saccharide binding to arylboronic acids not only with spectroscopy. Here, the redox behaviour and the displacement were recorded by cyclic voltammograms.

In the second part different applications of boronic acids in polymeric networks were investigated. The attachment of benzoboroxoles to nanoparticles was investigated and monitored by means of isothermal titration calorimetry and a colourimetric assay with Alizarin Red S as the report dye. The investigations by isothermal titration calorimetry compared the fructose binding of arylboronic acids and benzoboroxoles coupled to these nanoparticles and “free” in solution. It could be shown that the attached derivatives showed a higher binding constant due to an increasing entropy term. This states for possible multivalent binding combined with a higher water release. Since ITC could not characterise the binding of glucose to these nanoparticles due to experimental restrictions the glucose binding at pH 7.4 was shown with ARS. Here, the displacement of ARS by fructose and also glucose could be followed and consequently these nanoparticles can be used for saccharide determination. Within this investigation also the temperature stability of these nanoparticles was examined and after normal sterilisation procedures (121°C, 20 min.) the binding behaviour was still unchanged.

To target the selectivity of the used polymeric networks, molecular imprinting was used as a technique for creating artificial binding pockets on a molecular scale. As functional monomer 3-methacrylamidobenzoboroxole was introduced for the recognition of fructose. In comparison to polymers prepared with vinylphenylboronic acid the benzoboroxole containing polymer had a stronger binding at pH 7.4 which was shown for the first time. In addition, another imprinted polymer was synthesised especially for the recognition of glucose and fructose employing biomimetic saccharide analogues as template molecule. The advantage to use the saccharide analogues is the defined template-functional monomer complex during the polymerisation which is not the case, for example, for glucose-boronic acid interaction. The biomimetic character was proven through structural superimposition of crystal structures of the analogues with already described crystal structures of boronic acid esters of glucose and fructose. A molecularly imprinted polymer was synthesised with vinylphenylboronic acid as the functional monomer to show that both glucose and fructose are able to bind to the polymer which was predicted by the structural similarity of the analogues.

The major scientific contributions of this thesis are

- *the determination of binding constants for some, not yet reported saccharide – boronic acid / benzoboroxole pairs,*
- *the use of ARS as electrochemical reporter for saccharide detection,*
- *the thermodynamic characterisation of a saccharide binding nanoparticle system containing benzoboroxole and functioning at pH 7.4,*
- *the use of a polymerisable benzoboroxole as functional monomer for saccharide recognition in neutral, aqueous environments*
- *and the synthesis and utilisation of biomimetic saccharide analogues as template molecules especially for the development of a glucose binding MIP.*

6.1 Reagents

Styrene (ReagentPlus grade), cyclopentadiene, 1,3-cyclohexadiene, Alizarin Red S (ARS), trimethyl borate, n-butyllithium, pinacol (2,3-dimethyl-2,3-butanediol), 3-vinylphenylboronic acid, methacryloylchloride (97 %), trimethylolpropane trimethacrylate (techn.) (TRIM), D-glucose, sucrose and sorbitol, N-methylmorpholine N-oxide (NMO) and aniline were purchased from Sigma-Aldrich, N-bromosuccinimide, 3-bromo-4-methylbenzoic acid from Alfa-Aesar, nitromethane, vinylbenzylchloride (>90 %), divinylbenzene (techn. grade), PEG 6000, sodium phosphate, nitrobenzene from Fluka, 2,2'-azobis(2-methylpropionamide)dihydrochloride (V-50) from Wako Chemicals, cetyltrimethylammonium bromide (CTAB) from Roth, 2-formylphenylboronic acid, phenylboronic acid and 3-aminophenylboronic acid, monohydrate from Frontier Scientific, 2-hydroxymethylphenylboronic acid, dehydrated (benzoboroxole) and amino-2-hydroxymethylphenylboronic acid, HCl, dehydrated (aminobenzoboroxole) from Combi-Blocks, D-fructose from Merck, D-fructose and D-glucose [^3H -(G)] from Biotrend. As scintillation liquid Rotiszint from Carl Roth was purchased. L-fructose was purchased by TCI Europe. Solvents for polymerisation were dried before use or purchased as anhydrous grades. All boronic acids which are commercially available were either obtained by Frontier Scientific or Combi-Blocks. All other substances were used without further purification.

6.2 Binding analysis via NMR spectroscopy

To perform the NMR spectroscopic measurements an aqueous solution of 0.10 M monobasic phosphate buffer was prepared and adjusted to pH 7.4 which was evaporated under reduced pressure and redissolved in D_2O . The pH value was again adjusted to pH 7.4 and it was observed that due to the hygroscopic nature of D_2O a small amount of water was always present. Benzoboroxole **2a** (50 mg, 0.4 mmol) was dissolved in deuterated phosphate buffer solution to yield a solution of 15 mM. In addition a monosaccharide solution (fructose **3a** or glucose **3b**) was prepared also in deuterated phosphate buffer with a concentration of 150 mM (27 mg, 0.15 mmol/mL). To 700 μL of the **2a** solution different amounts of the monosaccharide solution were added and NMR measurements were performed. The saccharide concentration range was between 8 and 26 mM. Measurements were performed on a Varian i600.

6.3 Mass spectrometry of boroxole – saccharide interaction

For the mass spectrometry with electrospray ionisation the benzoboroxole **2a** (13 mg, 0.1 mmol) and the monosaccharide (1.8 mg, 0.01 mmol; either glucose **3b** or fructose **3a**) were dissolved in a 1:1 mixture of deionised water and acetonitrile (HPLC-grade). Furthermore, samples were prepared in a buffered solution at pH. 7.4 of ammonium acetate. The samples were analysed by means of low resolution ESI-MS.

6.4 Synthesis of different arylboronic acid and benzoboroxole derivatives

6.4.1 Synthesis of 5-Carboxy-2-methylphenylboronic acid **29**

3-Bromo-4-methylbenzoic acid **28** (1.0 g, 4.7 mmol) were dissolved in 12 mL of dry THF. This mixture was cooled down to -100°C in a mixture of methanol and liquid nitrogen. Then, *n*-BuLi (8 mL, 1.4 M in hexane, 11.2 mmol, 2.4 eq.) was added slowly via a syringe giving a clear yellowish solution. The temperature of the solution was maintained to be below -90°C and the reaction was conducted for about 1h follow by the slow addition of trimethyl borate (1.8 mL, 25.5 mmol, 5 eq.). The mixture was again stirred for 1h at -100°C and then warmed up to room temperature overnight. The solvent was evaporated under reduced pressure, the residue dissolved in diethyl ether and subsequent acidified using 1M HCl to pH 4-5. The crude product precipitated and could be extracted via further addition of diethyl ether. The combined organic phases were washed with brine, dried over MgSO_4 and evaporated to dryness. For purification the product was dissolved in hot THF and precipitated by addition of cold *n*-hexane giving the pure product **29** as a white-yellowish solid with a yield of 55 %.

Analytical data corresponds to data published by Pal *et al.*

$^1\text{H-NMR}$ (300 MHz, acetone- d_6): δ (ppm) 8.24 (d, 1H), 7.84 (dd, 1H), 7.21 (dd, 1H), 2.51 (s, 3H).

$^{13}\text{C-NMR}$ (300 MHz, acetone- d_6): δ (ppm) 168.1, 148.7, 135.9, 131.0, 127.6, 22.7. HRMS-ESI: Calculated $\text{C}_8\text{H}_8\text{BO}_4$ 179.05102, Found: 179.05093

6.4.2 Synthesis of 5-Methoxycarbonyl-2-methylphenylboronic acid **30**

Carboxy-2-methylphenylboronic acid **29** (2.5 g, 13.8 mmol) were dissolved in about 75 mL MeOH and 350 μL of H_2SO_4 . The solution was stirred under reflux overnight. The reaction was stopped by addition of water and extraction of the product was performed by ethyl acetate. The combined organic phases were dried over MgSO_4 and evaporated to yield **30** a yellowish solvent which was used without any further purification.

6.4.3 Synthesis of 1,1,2,2-Tetramethyl-1,2-ethanediol-(5-methoxycarbonyl-2-methylphenyl) boronate ester **31**

0.9 g (4.5 mmol) of 5-Methoxycarbonyl-2-methylphenylboronic acid **30** are dissolved with pinacol **3d** (6.7 mmol, 1.5 eq.) in dry toluene. The reaction was heated over night to reflux using a Dean-Stark water trap. After reaction the solvent was removed under reduced pressure and the crude product was purified by recrystallisation from hexane - ethyl acetate to yield **31** in a yield of 85 % over two steps.

$^1\text{H-NMR}$ (300 MHz, Acetone- d_6): δ (ppm) 8.49 (m, 1H), 8.05 (m, 1H), 7.32 (m, 1H), 4.98 (m, 3H), 1.44 (m, 12H); HRMS (ESI): Calculated $\text{C}_{14}\text{H}_{19}\text{BO}_4$:262.13764; Found: 262.12663

6.4.4 Synthesis of 3-Carboxybenzboroxole **2b**

The pinacol ester **31** (400 mg, 1.45 mmol) was dissolved in CCl_4 , freshly recrystallised *N*-Bromosuccinimide (from water, 256 mg, 1.45 mmol) and a small amount of AIBN. After 4h of reaction time the solvent was removed under reduced pressure (under appropriate care) and the residual was dissolved in diethyl ether and filtered to remove the undissolved side-products. The filtrate was extracted with 15% aqueous KOH for three times and the combined aqueous layer were stirred for 1h at room temperature. Before acidification below pH 2 with 6M HCl the reaction mixture was cooled down to 0°C . During acidification the product precipitated and was

collected through filtration. The crude was purified via recrystallisation from water to yield the carboxybenzoboroxole **2b**. Yield: 65 %

$^1\text{H-NMR}$ (300MHz, acetone- d_6): δ (ppm) 8.39 (d, 1H), 8.08 (dd, 1H), 7.50 (dd, 1H), 5.04 (s, 2H); $^{13}\text{C-NMR}$ (300MHz, acetone- d_6): δ (ppm) 168.1, 159.9, 132.9, 132.7, 130.5, 122.3, 71.2; HRMS (ESI): Calculated $\text{C}_8\text{H}_6\text{BO}_4$: 177.03537; Found: 177.03619

6.4.5 Synthesis of 1,3-dihydro-1-hydroxy-3-(nitromethyl)-2,1-benzoxaborole (nitrobenzoboroxole) **2e**

According to a synthesis procedure by Snyder *et al.* 2-formylphenylboronic acid (1.0 g, 6.7 mmol) and 0.28 g (7.03 mmol, 1.05 eq.) of sodium hydroxide were dissolved in a minimum of distilled water. The mixture was cooled down to 15°C and 360 μL (407.1 mg; 6.6 mmol) of nitromethane were added slowly. The reaction was stirred at 15°C for 2h followed by acidification with HCl to pH 2-3. The slightly yellow crude was collected and recrystallised from water to yield 75% the pure **2e**.

$^1\text{H-NMR}$ (300 MHz, acetone- d_6): δ (ppm) 7.77 (m, 1H), 7.55 (m, 1H), 7.43 (m, 2H), 5.86 (m, 1H), 5.22 (m, 1H), 4.52 (m, 1H); HRMS (ESI): Calculated $\text{C}_8\text{H}_7\text{BNO}_4$: 193.05464; Found: 192.04744

6.4.6 Synthesis of 1,3-dihydro-1-hydroxy-3-(nitrile)-2,1-benzoxaborole (nitrilebenzoboroxole) **2f**

1.5 g (10 mmol) of 2-formylphenylboronic acid are dissolved in distilled water and cooled down to 10°C. Then, 0.67 g (10.3 mmol) of potassium cyanide are added (under appropriate care). After a reaction time of 30 minutes at 10°C the reaction was slowly acidified under extreme care (fumehood) yielding **2f** as a $^1\text{H-NMR}$ pure product (Yield: 82%).

$^1\text{H-NMR}$ (300 MHz, acetone- d_6): δ (ppm) 7.80 (d, 1H), 7.63 (m, 2H), 7.51 (m, 1H), 6.26 (s, 1H); MS (ESI): 159.04982 Found: 158.04

6.4.7 Synthesis of 3-methacrylamidobenzoboroxole **2d**

1.5 g (10.9 mmol) 5-amino-2-hydroxymethylphenylboronic acid **2c** and 1.75 g (43.8 mmol) sodium hydroxide were dissolved in a small amount water to yield an almost saturated solution which was stirred for 10 minutes at 0 °C. Then 1.6 mL (22 mmol) of methacryloyl chloride **33** was slowly added via a syringe pump and vigorous stirring within one hour maintaining the 0 °C. After four hours the solution was acidified very slowly using concentrated HCl avoiding unwanted polymerisation. The pale yellow precipitate which appeared during the acidification was filtered off yielding **1d** as pale yellow crystals which were pure by $^1\text{H-NMR}$. Yield: 79-82 %

$^1\text{H-NMR}$ (300 MHz, DMSO): δ (ppm) 8.06 (m, 1H) 7.67 (m, 1H), 7.34 (m, 1H), 5.80 (s, 1H), 5.50 (s, 1H), 4.95 (s, 2H), 1.96 (s, 3H). $^{13}\text{C-NMR}$ (300 MHz, DMSO): δ (ppm) 166.71, 148.97, 140.33, 137.67, 123.52, 122.26, 121.25, 119.78, 69.68, 18.69. MS (ESI+): $m/z = 217.12$ (M^+), 218.10 ($\text{M}+\text{H}^+$), 240.10 ($\text{M}+\text{Na}^+$).

6.4.8 Synthesis of 3-methacrylamidophenylboronic acid **1d**

In analogy to **2d**, 3-methacrylamidophenylboronic acid **1d** was synthesised in the same manner (beside 1eq. NaOH less).

$^1\text{H-NMR}$ (300 MHz, DMSO): δ (ppm) 8.08 (m, 1H), 7.94 (m, 1H), 7.74 (m, 1H), 7.49 (m, 1H), 7.27 (m, 1H), 5.81 (s, 1H), 5.48 (s, 1H), 1.95(s, 3H). $^{13}\text{C-NMR}$ (500 MHz, DMSO): δ (ppm)

166.49, 140.26, 137.99, 129.22, 127.33, 126.43, 122.27, 119.68, 18.67. MS (ESI+): $m/z = 206.10$ (M+H⁺), 228.28 (M+Na⁺).

6.5 Determination of Binding constants using Isothermal Titration Calorimetry – Temperature-dependent ITC measurements

The binding experiments were performed in an ultrasensitive ITC instrument (Microcal VP-ITC, Microcal Northhampton, USA) at 25°C, for temperature-dependent measurements between 10-60°C. All solutions were degassed for five minutes under reduced pressure. The receptor solution (boronic acid derivative) was then inserted into the sample cell (total volume was 1.461 mL). For the determination of binding constants between glucose and the boronic acid a ratio of 40:1 (800 mM : 20 mM) was chosen, in case of fructose 37.5:1 (75 mM : 2 mM). The syringe of the ITC device was purged three times with the ligand solution and then filled with the same solution. Then the sample cell was equipped with the syringe and the injection started after the thermal equilibrium was reached. The first injection was 2 μL and followed by 49 injections of 5 μL . For every measurement the appropriate reference power was set. The solvent used was either 0.1 mM or 0.02 mM monobasic phosphate buffer. Each titration experiment was complemented by an additional control experiment, designed to measure the heat of dilution. The ligand was injected into the buffer without receptors. The data analysis was performed using the Origin 7 VP-Viewer software after subtraction of the dilution experiment yielding the thermodynamic parameters K , ΔH and ΔS . Owing to the restriction of the experimental setup (described below) the stoichiometric ratio was set to 1 for fitting the obtained integrated heats with the data analysis software.

6.6 Electrochemical behaviour of ARS in saccharide-boronic acid interaction

Following the procedure of Wang and *co-workers* a 0.1 mM ARS (purchased from Sigma Aldrich) solution (Solution A) was prepared in 0.1 M sodium phosphate monobasic buffer containing 50 mM KCl. The pH was adjusted to 7.4 with NaOH. 2 mL of solution A were dispensed into the 2 mL electrochemical cell. A cyclic voltammogram was recorded using a three-electrode set-up with a glassy carbon disc electrode ($\varnothing=3$ mm), a Ag/AgCl (3 M KCl) reference electrode and a Pt wire as the counter electrode. The potential was scanned between -0.8 V and +0.2 V with a scan rate of 0.1 V s^{-1} .

For the analysis of the phenylboronic acid- ARS interaction, phenylboronic acid was dissolved to a final concentration of 15 mM, in buffer of pH 7.4, containing 0.1mM ARS (solution B). The formation of the boronic acid-ARS ester occurred within a few seconds (as indicated by the colour change to orange-yellow). Solution B was added stepwise to the electrochemical cell containing solution A and a voltammogram was recorded after each injection and purging with argon for three minutes. Before each measurement the glassy carbon electrode was polished with aluminium oxide powder (0.05 μm).

To perform the displacement assay solution B was further diluted to 3.1 mM (solution C) in which then fructose was dissolved resulting in a 2 M fructose solution (solution D). The experiments were conducted similar to the phenylboronic acid - ARS interactions. Here, solution C was firstly inserted into the chamber and solution D was added stepwise covering the range between 10 and 150 mM.

6.7 Label-free detection of saccharide binding at pH 7.4 to nanoparticulate benzoboroxole based receptor units

6.7.1 Synthesis of nanoparticles

Within a 250 mL round-bottom flask equipped with a dropping funnel, magnetic stirrer and argon/vacuum manifold 0.66 g (1.82 mmol) CTAB and 0.21 g PEG 6000 were suspended into 122.5 mL of an aqueous monobasic phosphate solution (100 mM). After solvation 1.07 mL (9.35 mmol) styrene, 1.36 mL (9.35 mmol) vinylbenzylchloride and 92.5 μ L (0.66 mmol) divinylbenzene were added. In order to remove oxygen, the mixture was stirred at room temperature and flushed with argon after applying a vacuum. This was repeated five times to assure that no oxygen is present during polymerisation. After that the pre-polymerisation mixture was heated to 75 °C and initiated by the addition of 17.5 mL aqueous solution containing 100 mg V-50. The polymerisation was carried out at 75 °C over 18 h resulting in an opalescent solution. The freshly prepared latex was purified by dialysis against ultrapure water until the conductivity of the water was below 1 μ S/cm.

6.7.2 Modification of the latex

The latex was modified in the following manner. The purified latex was diluted to its half concentration and titrated with 0.1 N aqueous NaOH to pH 7.4. After that the amine-containing ligand (here: aminophenylboronic acid, aminobenzoboroxole and aniline) was added without previous solubilisation. The aminobenzoboroxole hydrochloride had to be titrated with 0.1 M NaOH prior to adding it to the mixture. The mixture was stirred for three days at room temperature to get an appropriate yield. To 15 mL of the raw latex 230 mg (1.5 mmol) aminophenylboronic acid monohydrate, 290 mg (1.5 mmol) aminobenzoboroxole and 140 μ L (1.5 mmol) aniline were added, respectively. The modified latex was dialysed against ultra pure water and checked for unbound boronic acid (colour change with Alizarin Red S (ARS)).

6.7.3 Characterisation of the latex

The size distribution of the nanoparticles was characterised by dynamic light scattering using a Brookhaven Particle Analyzer. The boron content, which is proportional to the amount of immobilised boronic acids, was detected by ICP-OES. 200 mg of the particle solution were dissolved in 5 mL nitric acid and distilled water was added up to a final volume of 50 mL. An ICP OES instrument (Optima 2100 DV, from Perkin Elmer, USA) was used for the measurement. The calibration was done with a commercially available standard kit from Merck (Boron ICP Standard Kit, Merck, Darmstadt, Germany).

6.7.4. ITC-experiments

The ITC-experiments were conducted in analogy to 6.5. In case of the determination of binding constants between the nanoparticles and fructose, 0.5% of CTAB was added to ensure the colloidal stability of the nanoparticles.

6.8 Boroxole-modified nanoparticles for the recognition of glucose at neutral pH

6.8.1 Latex synthesis

Synthesis and characterisation of the latex see 6.7

6.8.2 ARS-assay with nanoparticles

For all absorption measurements a Jasco V-570 spectrophotometer was used. The binding studies were performed as described in literature. A solution of 0.144 mM ARS in 20 mM phosphate buffer with 0.5% CTAB was freshly prepared. A titration experiment was performed in which the boronic acid modified latex suspended in the ARS solution was added stepwise to the ARS solution to keep the concentration of ARS constant and varying the range of boronic acid concentration. The absorption was measured after each addition and an equilibration time of at least three minutes. To 2 mL of the neat ARS-solution volumes between 10 and 100 μ L of the boronic acid solution (with 0.2 mmol per mL nanolatex) was added. The saccharide binding experiments were performed in the same manner. The boronic acid - ARS solution was mixed with different saccharide concentrations showing a concentration spectrum from 10 to 400 mM. In each experiment the absorption spectrum was recorded between 400 and 700 nm.

6.8.3 Temperature stability

The temperature stability was tested with 15 mL of the modified latex. They were transferred into a beaker and sterilised for 20 minutes at 121 °C in an autoclave. The binding was of the treated latex was then tested again with alizarin red in the above mentioned manner.

6.9 Molecular imprinting of fructose using a polymerisable benzoboroxole: Recognition at pH 7.4

6.9.1 Synthesis of fructose ester 4a - 4d

Fructose ester synthesis (**4a** and **4b**) was carried out as described by Wulff et al.¹⁵⁶ D-fructose (2.5 mmol) was esterified with the desired boronic acid **2d** or **1f** (5 mmol) in 80 mL of dioxane solution in presence of nitrobenzene (10 μ L) under argon atmosphere. The water generated was removed by azeotropic distillation (88°C) from the reaction mixture. The residual solvent was removed in vacuo. Purification was performed by dissolution of the ester in DCM.

Analytical data **4a**: Yield: 80.5% ¹H-NMR (300 MHz, CDCl₃): δ (ppm) 8.31 – 7.51 (m, 6H), 5.79 (s, 2H), 5.45 (s, 2H), 5.03 (s, 4H), 2.04 (s, 6H). As discussed in the Results and Discussion part, strong peak broadening was observed, which makes the analysis difficult. ¹³C-NMR (300 MHz, CDCl₃): δ (ppm) 167.22, 166.92, 149.80, 140.56, 136.85, 129.25, 126.83, 123.82, 123.45, 120.14, 103.60, 73.25, 72.56, 72.22, 71.12, 70.80, 66.04, 61.58, 18.68. IR: ν 3276 cm⁻¹ (s), 2927 cm⁻¹ (m), 1655 cm⁻¹ (m), 1614 cm⁻¹ (m), 1524 cm⁻¹ (m), 1398 cm⁻¹ (s), 1214 cm⁻¹ (w), 1054 cm⁻¹ (s), 980 cm⁻¹ (s), 914 cm⁻¹ (m), 822 cm⁻¹ (s), 754 cm⁻¹ (s) MS (ESI): m/z = 577.27 (M+H⁺)

Analytical data **4b**: Yield: 82 % ¹H-NMR (500 MHz, CDCl₃): δ (ppm) 7.89 (m, 2H), 7.73 (m, 2H), 7.57 (m,2H), 7.38 (m, 2H), 6.74 (dd, 2H J = 10.9, 17.6 Hz), 5.81 (ddd, 2H, J = 0.4, 7.5,

17.6 Hz), 5.28 (dd, 2H, $J = 8.5, 11.1$ Hz), 5.12 (dd, 1H, $J = 2.4, 8.4$ Hz), 4.85 (d, 1H, $J = 2.4$ Hz), 4.71 (dd, 1H, $J = 1.6, 8.4$ Hz), 3.98 (d, 1H, $J = 13.7$ Hz), 3.85 (dd, 1H, $J = 5.1, 12.1$ Hz), 3.78 (dd, 1H, $J = 2.1, 13.8$ Hz), 3.67 (d, 1H, $J = 12.1$ Hz). $^{13}\text{C-NMR}$ (500 MHz, CDCl_3): δ (ppm) 137.23, 137.09, 136.56, 136.38, 134.56, 134.34, 133.11, 132.89, 130.08, 129.52, 128.28, 128.16, 114.46, 114.21, 105.01, 72.69, 72.60, 72.43, 65.99, 61.88. MS (ESI+): $m/z = 405, 40$ ($\text{M}+\text{H}^+$), 427.19 ($\text{M}+\text{Na}^+$), 443.18 ($\text{M}+\text{K}^+$).

Pinacol esters (**4c** and **4d**) were synthesised analogously. Pinacol (590 mg, 5 mmol) was esterified with the equimolar boronic acids **2d** or **1f** in 180 mL of toluene in presence of nitrobenzene (10 μL) under argon atmosphere. Generated water was removed by azeotropic distillation (84°C) and finally solvent was removed *in vacuo*.

Analytical data **4c**: Yield: Pale yellow solid, 90% $^1\text{H-NMR}$ (300 MHz, CDCl_3): δ (ppm) 8.24 (m, 1H), 8.01-7.48 (m, 3H), 5.79 (s, 1H), 5.46 (s, 1H), 4.67 (s, 2H), 2.06 (s, 12H). $^{13}\text{C-NMR}$ (300 MHz, CDCl_3): δ (ppm) 166.44, 143.45, 140.76, 136.72, 129.63, 129.24, 127.66, 122.92, 119.81, 117.74, 84.43, 65.44, 24.79, 18.68; MS (ESI+): $m/z = 340.20$ ($\text{M}+\text{H}^++\text{Na}^+$). IR: ν 3310 cm^{-1} (m), 2979 cm^{-1} (m), 2931 cm^{-1} (w), 1664 cm^{-1} (m), 1529 cm^{-1} (s), 1343 cm^{-1} (s), 1142 cm^{-1} (s), 1068 cm^{-1} (m), 967 cm^{-1} (w), 855 cm^{-1} (w)

Analytical data **4d**: Yield: 70-78 %, oil $^1\text{H-NMR}$ (300 MHz, CDCl_3): δ (ppm) 7.84 (s, 1H), 7.70 (m, 1H), 7.52 (m, 1H), 7.34 (m, 1H), 6.73 (dd, 1H, $J = 10.9, 17.6$ Hz), 5.79 (dd, 1H, $J = 0.9, 17.6$ Hz), 5.24 (dd, 1H, $J = 0.9, 10.9$ Hz), 1.36 (s, 12H). $^{13}\text{C-NMR}$ (500 MHz, CDCl_3): δ (ppm) 136.86, 136.76, 134.18, 132.72, 128.85, 127.91, 113.86, 83.83, 24.86. MS (ESI+): $m/z = 230.19$ (M^+), 231.19 ($\text{M}+\text{H}^+$).

6.9.2 Synthesis of polymers

For polymer synthesis a modified approach was applied where 2 mmol of the desired boronic acid ester **4a** and **4b** and thermal initiator AIBN (295 mg, 1.8 mmol) were dissolved in 9 mL THF for **4a** or 9 mL acetonitrile/toluene 1:1 for **4b**.³⁹ After addition of crosslinker TRIM (9 g, 8.5 mL), the mixture was mixed well and purged with argon for 10 min. Polymerisation was initiated and carried out at 65°C for 48 h and afterwards increased up to 95°C for 24 h. The synthesised polymer monoliths were crushed and ground in a ball mill (MM200, Retsch) for 2 min at 30 Hz. Polymer powder was wet sieved (mesh 25 μm) using acetone. The template molecule fructose was removed from polymers by washing with methanol and water. The polymer particles were dried *in vacuo* and stored at room temperatures. The corresponding pinacol imprinted polymers were synthesised in the same manner.

6.9.3 Batch rebinding studies

Batch rebinding experiments were accomplished at three different pH values: pH 11.4 (0.1 M sodium carbonate solution + 10% methanol), pH 8.7 and 7.4 (0.1 M phosphate buffer + 10% methanol respectively). Fructose stock solutions of 10.0 mM were prepared with each of these buffers and doped with ^3H -fructose. Finally, to 10 mg of polymer, fructose stock solution and buffer was added to yield 1 mL fructose solutions of 0.1 to 5 mM. The mixtures were incubated over night at 20°C and centrifuged (9000 g) for 10 min. 500 μL of the supernatant were discharged to a separate vessel and 5 mL of scintillation solution (Rotiszint® eco plus) were added. Radioactivity was measured in Scintillation counter LS 650 (Beckmann Coulter) and unbound fructose could be calculated with a calibration curve.

6.9.4 Competitive binding

Competitive binding studies were done with MIP-BX(Fru) at pH 7.4 with different sugars/sugar alcohol: L-fructose, sorbitol, glucose and sucrose. The same solutions as for batch binding experiments were used, completed with different 50 mM sugar solutions. For the experiments, fructose stock solution, buffer solution and 50 μ L of the desired sugar solution were added to 10 mg of polymer to yield a 1 mL reaction mixture. Fructose concentrations varied from 0.1 to 4.5 mM and the competitive sugar/sugar alcohol had constant concentrations of 2.5 mM. Incubation, centrifugation and detection were done the same way as for simple binding experiments.

6.9.5 Adsorption/Desorption measurements

The porosity of the MIPs was determined by nitrogen adsorption/ desorption porosimetry on a Fisons Sorptomat 1900.

6.10 Biomimetic monosaccharide analoga – (Easy) Synthesis, characterisation and application as template in molecular imprinting

6.10.1 X-Ray Analysis

The X-ray analyses were performed on an Imaging Plate Diffraction System IPDS-2 (Stoe) at 210 K with graphite-monochromated Mo-K α radiation ($\lambda = 0.71073 \text{ \AA}$). The data were corrected for Lorentz, polarisation and extinction effects. The structures were solved with SHELXS-97 using direct methods and refined against F^2 by means of full-matrix least-squares procedures with SHELXL-97. The non-hydrogen atoms were refined anisotropically. All hydrogen atoms could be located from the difference Fourier maps, and allowed to ride on their parent atoms with $U_{\text{iso}}(\text{H})=1.2U_{\text{eq}}(\text{C})$. For the visualisation of the structures the graphic programs DIAMOND was used. CCDC-123456 (*rac-4e*) and CCDC-123456 (*rac-4f*) contain the supplementary crystallographic data for this paper. These data can be obtained free of charge from the Cambridge Crystallographic Data Centre via www.ccdc.cam.ac.uk/data_request/cif.

6.10.2 General procedure for synthesis of (1R*,2R*,3R*,4R*)-Cyclopentane-1,2,3,4-tetra-1,2:3,4-bis(phenylboronate) *rac-4e* and (1R*,2R*,3R*,4R*)-Cyclohexane-1,2,3,4-tetra-1,2:3,4-bis(phenylboronate) *rac-4f*

According to Gypser *et al.*, 4.6 g (38 mmol) N-methylmorpholine N-oxide (NMO) and 4.5 g (38 mmol) phenylboronic acid were dissolved in approximately 40 mL CH_2Cl_2 in a 250 mL round-bottom flask. At least 50 mg (0.0025 equivalents per alkene linkage) of OsO_4 were added under appropriate safety. Subsequently, the 19 mmol of the cyclodiene (cyclopentadiene **35**: 1.3 g, 1.6 mL; 1,3-cyclohexadiene **36**: 1.5 g; 1.8 mL) were dissolved in 35 mL of CH_2Cl_2 and added slowly via a dropping funnel. The reaction was conducted for 5 h at room temperature until it was quenched via addition of a 10 % bisulfite solution. After stirring for 2 h the reaction mixture was extracted with CH_2Cl_2 and dried over MgSO_4 . Evaporation yielded a brownish solid which was recrystallised from 10:1 hexane/ethyl acetate giving the diboronic acid ester **4e** and **4f** as colourless solids. The analytical data matched the already reported. For X-ray crystals a concentrated solution in DCM was slowly evaporated. Cyclopentadiene was cracked prior use via distillation.

Analytical data **4e**: Yield: Colourless solid, 70%; ¹H-NMR (300 MHz, CDCl₃): δ ppm 7.90 (m, 2H), 7.58 (m, 2H), 7.47 (t, 4H, *J*=7.2Hz), 5.24 (dd, 2H, *J*=5.7Hz, *J*=11.6Hz), 5.24 (dd, 2H, *J*=5.7Hz, *J*=11.6Hz), 5.11 (d, 2H, *J*=6.2Hz), 2.59 (t, 2H, *J*=5.6Hz); ¹³C-NMR (300 MHz, CDCl₃): δ ppm 135.4, 132.3, 128.4, 88.0, 81.6, 42.8.

Analytical data **4f**: Yield: Colourless solid, 72%; ¹H-NMR (300 MHz, CDCl₃): δ ppm 7.89 (m, 4H), 7.57 (m, 2H), 7.46 (t, 2H, *J*=7.2Hz), 5.03 (q, 2H, *J*=1.6Hz), 1.84 (br s, 4H); ¹³C-NMR (300 MHz, CDCl₃): δ ppm 135.0, 131.7, 127.9, 74.9, 73.8, 29.7, 21.8.

6.10.3 Oxidative cleavage of **4f**

The oxidative cleavage of **4f** was performed by dissolving 1 g (3.1 mmol) of **2b** in a minimum of 1:1 ethylacetate - acetone mixture. Then 1.5 equivalents of a 30 % hydrogen peroxide solution were added and the mixture was stirred for at least two hours until the product precipitated as a colourless solid. **Rac-3c** was collected via filtration and pure by ¹H-NMR.

¹H-NMR (300 MHz, DMSO-*d*₆): δ ppm 4.33 (m, 2H), 4.17 (d, *J*=5.0 Hz, 2H), 3.66 (br s, 2H), 3.53 (br s, 2H), 1.43-1.53 (m, 4H); ¹³C-NMR (300 MHz, DMSO-*d*₆): δ ppm 72.2, 67.8, 26.1. MS (ESI): Calculated: 148.07356; Found: 148.07

6.10.4 Synthesis of functional monomer template complex **4g**

The boronic acid ester **4g** for polymerisation was synthesised in according to earlier reported synthesis in our group of a fructosyl-vinyl phenylboronic acid. For that 0.5 g (6.7 mmol) of **rac-3c** and 1.9 g (13.4 mmol) of 4-vinyl phenylboronic acid were dissolved in anhydrous dioxane. A small amount of nitrobenzene was added to avoid unwanted polymerisation of the monomers. The mixture was heated up and the generated water was removed by azeotropic distillation. The residual solvent was removed in vacuo and the residue was washed out with CH₂Cl₂ to dissolve the formed boronic acid ester. The ester was pure by ¹H-NMR. Yield: 75%.

¹H-NMR (300 MHz, CDCl₃): δ ppm 8.19 (d, 2H, *J*=8.0Hz), 7.80 (d, 2H, *J*=8.1Hz), 7.55 (d, 2H, *J*=8.0Hz), 7.45 (d, 2H, *J*=8.0Hz), 6.78 (m, 4H), 5.88 (t, 2H, *J*=18.2Hz), 5.36 (dd, 2H, *J*=11.1Hz, *J*=14.6Hz), 4.93 (dd, 2H, *J*=7.9Hz, *J*=25.9Hz), 1.78 (br s, 4H); ¹³C-NMR (300 MHz, CDCl₃): δ ppm 141.5, 140.7, 136.8, 135.9, 135.2, 125.7, 115.5, 74.9, 73.7, 55.7, 21.8.

To provide a comparison the pinacol 4-vinylphenylboronic acid ester was synthesised via azeotropic distillation in anhydrous toluene.

Analytical data: Yield: Colourless solid, 85%; ¹H-NMR (300 MHz, CDCl₃): δ ppm 7.84 (d, 2H, *J*=8.1Hz), 7.45 (d, 2H, *J*=8.0Hz), 6.79 (m, 1H), 5.85 (dd, 2H, *J*=0.9Hz, *J*=17.6Hz), 5.32 (dd, 1H, *J*=0.8Hz, *J*=10.9Hz), 1.38 (s, 12H); ¹³C-NMR (300 MHz, CDCl₃): δ ppm 140.1, 136.8, 135.8, 135.0, 125.4, 114.8, 83.7, 24.8.

6.10.5 Molecular imprinting

To obtain molecularly imprinted polymers 660 mg (2 mmol) of **4g**, 7.4 mL TRIM and 268 mg AIBN were dissolved in 9 mL of a 1:1 mixture of toluene – acetonitrile. After removal of oxygen using argon the polymerisation was started at 65 °C for 48 h. The polymer was cured at 100 ° for additional 24 h. The polymer monolith was then mechanically destroyed and ground in a ball mill (MM200, Retsch) for 2 min at 30 Hz. The yielded polymer powder was wet sieved in acetone to obtain particles between 25 and 50 μm. The template was removed by repeated washing in MeOH-water until no template could be recovered in the washing solution. The control polymer with pinacol was synthesised in the same manner.

6.10.6 Batch rebinding

The batch binding studies were carried out in carbonate solution at pH 11.4 (0.1 M sodium carbonate solution + 10% methanol) according to Rajkumar *et al.* To 10 mg of the polymers fructose or glucose (doped with ³H-labelled fructose or glucose) concentrations between 0.1 mM and 5 or 2 mM, respectively, were added. These solutions were incubated over night at 20 °C under vigorous stirring followed by centrifugation of the polymer particles. 500 µL of the supernatant were used and mixed with 5 mL scintillation solution to measure the radioactivity of the unbound saccharide part.

- (1) Garfield, E. *Current Contents* **1988**, 3-9.
- (2) Bazin, H. *Actualite Chimique* **2009**, 20-27.
- (3) Rissanen, K. In *Analytical Methods in Supramolecular Chemistry*; Schalley, C. A., Ed.; Wiley-VCH: Weinheim, 2007.
- (4) Chruszcz, M.; Domagalski, M.; Osinski, T.; Wlodawer, A.; Minor, W. *Current Opinion in Structural Biology* **2010**, *20*, 587-597.
- (5) Konteatis, Z. D. *Expert Opinion on Drug Discovery* **2010**, *5*, 1047-1065.
- (6) Kurpiewska, K.; Lewinski, K. *Central European Journal of Biology* **2010**, *5*, 531-542.
- (7) Strandberg, B.; Dickerson, R. E.; Rossmann, M. G. *Journal of Molecular Biology* **2009**, *392*, 2-32.
- (8) Lehn, J. M. *Pure and Applied Chemistry* **1978**, *50*, 871-892.
- (9) Lehn, J. M. *Science* **1993**, *260*, 1762-1763.
- (10) Lehn, J. M. *Supramolecular Chemistry: Concepts and Perspectives*; Wiley-VCH: Weinheim, 1995.
- (11) Oshovsky, G. V.; Reinhoudt, D. N.; Verboom, W. *Angewandte Chemie International Edition* **2007**, *46*, 2366-2393.
- (12) Thévenot, D. R.; Toth, K.; Durst, R. A.; Wilson, G. S. *Biosensors and Bioelectronics* **2001**, *16*, 121-131.
- (13) Tadigadapa, S.; Mateti, K. *Measurement Science & Technology* **2009**, *20*, -.
- (14) Zhou, Q. F.; Lau, S. T.; Wu, D. W.; Shung, K. *Progress in Materials Science* **2011**, *56*, 139-174.
- (15) Schrader, T.; Hamilton, A. D. *Functional Synthetic Receptors*; Wiley-VCH: Weinheim, 2005.
- (16) Rebek, J. *Pure and Applied Chemistry* **1996**, *68*, 1261-1266.
- (17) Fernandez-Gonzalez, A.; Guardia, L.; Badia-Laino, R.; Diaz-Garcia, M. E. *Trac-Trends in Analytical Chemistry* **2006**, *25*, 949-957.
- (18) Sansone, F.; Baldini, L.; Casnati, A.; Ungaro, R. *New Journal of Chemistry* **2010**, *34*, 2715-2728.
- (19) Dickert, F. L.; Hayden, O. *TrAC Trends in Analytical Chemistry* **1999**, *18*, 192-199.
- (20) Bier, F. F.; Schumacher, S. *Public Health Forum, In Press, Corrected Proof*.
- (21) Alper, J. *Science* **2001**, *291* 2338-2343.
- (22) Allender, C.; Mosbach, K. *Biosensors & Bioelectronics* **2009**, *25*, 539-542.
- (23) Zhu, W. B.; Wu, F. Y. *Progress in Chemistry* **2009**, *21*, 1241-1253.
- (24) Boraston, A. B.; Bolam, D. N.; Gilbert, H. J.; Davies, G. J. *Biochemical Journal* **2004**, *382*, 769-781.
- (25) Turner, A. P. F.; Chen, B. N.; Piletsky, S. A. *Clinical Chemistry* **1999**, *45*, 1596-1601.
- (26) Walker, D. B.; Joshi, G.; Davis, A. P. *Cellular and Molecular Life Sciences* **2009**, *66*, 3177-3191.
- (27) Berube, M.; Dowlut, M.; Hall, D. G. *Journal of Organic Chemistry* **2008**, *73*, 6471-6479.
- (28) James, T. D.; Phillips, M. D.; Shinkai, S. *Boronic Acids in Saccharide Recognition*; 1 ed.; The Royal Society of Chemistry: Cambridge, 2006.
- (29) Jin, S.; Cheng, Y. F.; Reid, S.; Li, M. Y.; Wang, B. H. *Medicinal Research Reviews* **2010**, *30*, 171-257.
- (30) Springsteen, G.; Wang, B. H. *Tetrahedron* **2002**, *58*, 5291-5300.
- (31) Nieba, L.; Krebber, A.; Pluckthun, A. *Analytical Biochemistry* **1996**, *234*, 155-165.
- (32) Alexander, C.; Andersson, H. S.; Andersson, L. I.; Ansell, R. J.; Kirsch, N.; Nicholls, I. A.; O'Mahony, J.; Whitcombe, M. J. *Journal of Molecular Recognition* **2006**, *19*, 106-180.
- (33) Schumacher, S. In *Handbook of Molecular Imprinting: Advanced Sensor Application*; Lee, S.-W., Kunitake, T., Eds. 2011.
- (34) Wulff, G.; Sarhan, A. *Angewandte Chemie-International Edition* **1972**, *11*, 341-&.
- (35) Wulff, G.; Sarhan, A.; Gimpel, J.; Lohmar, E. *Chemische Berichte-Recueil* **1974**, *107*, 3364-3376.
- (36) Wulff, G.; Sarhan, A.; Vesper, W.; Grobeeinsler, R. *Chemiker-Zeitung* **1976**, *100*, 288-288.
- (37) Wulff, G.; Sarhan, A.; Zabrocki, K. *Tetrahedron Letters* **1973**, 4329-4332.
- (38) Yan, J.; Springsteen, G.; Deeter, S.; Wang, B. H. *Tetrahedron* **2004**, *60*, 11205-11209.
- (39) Rajkumar, R.; Warsinke, A.; Mohwald, H.; Scheller, F. W.; Katterle, M. *Talanta* **2008**, *76*, 1119-1123.

- (40) Hall, D. G.; Dowlut, M. *Abstracts of Papers of the American Chemical Society* **2006**, 231, -.
- (41) Fischer, E. *Ber. Dtsch. Chem. Ges.* **1894**, 27, 2985-2993.
- (42) Koshland, D. E. *Proc. Natl. Acad. Sci. USA* **1958**, 44, 98-104.
- (43) Lieberzeit, P. A.; Dickert, F. L. *Analytical and Bioanalytical Chemistry* **2008**, 391, 1629-1639.
- (44) Jelinek, R.; Kolusheva, S. *Chemical Reviews* **2004**, 104, 5987-6016.
- (45) Scheller, F.; Schubert, F.; Pfeiffer, D.; Hintsche, R.; Dransfeld, I.; Renneberg, R.; Wollenberger, U.; Riedel, K.; Pavlova, M.; Kuhn, M.; Muller, H. G.; Tan, P. M.; Hoffmann, W.; Moritz, W. *Analyst* **1989**, 114, 653-662.
- (46) Scheller, F. W.; Wollenberger, U.; Warsinke, A.; Lisdat, F. *Current Opinion in Biotechnology* **2001**, 12, 35-40.
- (47) Braguglia, C. M. *Chemical and Biochemical Engineering Quarterly* **1998**, 12, 183-190.
- (48) Li, W.; Li, S. J. *Oligomers Polymer Composites Molecular Imprinting* **2007**, 206, 191-210.
- (49) Eggins, B. R. *Chemical Sensors and Biosensors*; Wiley-VCH: West Sussex, 2002.
- (50) D'Souza, S. F. *Applied Biochemistry and Biotechnology* **2001**, 96, 225-238.
- (51) Jha, S. K.; Kanungo, M.; Nath, A.; D'Souza, S. F. *Biosensors & Bioelectronics* **2009**, 24, 2637-2642.
- (52) Leech, D. *Chemical Society Reviews* **1994**, 23, 205-213.
- (53) Eray, M.; Dogan, N. S.; Reiken, S. R.; Sutisna, H.; Vanwie, B. J.; Koch, A. R.; Moffett, D. F.; Silber, M.; Davis, W. C. *Biosystems* **1995**, 35, 183-188.
- (54) Wang, J.; Lin, M. S. *Analytical Chemistry* **1988**, 60, 1545-1548.
- (55) Schubert, F.; Scheller, F. W. *Methods in Enzymology* **1988**, 137, 152-160.
- (56) Scheller, F.; Kirstein, D.; Kirstein, L.; Schubert, F.; Wollenberger, U.; Olsson, B.; Gorton, L.; Johansson, G.; Alberry, W. J. *Philosophical Transactions of the Royal Society of London Series B-Biological Sciences* **1987**, 316, 85-94.
- (57) Wilson, R.; Turner, A. P. F. *Biosensors & Bioelectronics* **1992**, 7, 165-185.
- (58) Wilkins, E.; Atanasov, P. *Medical Engineering & Physics* **1996**, 18, 273-288.
- (59) Harwood, G. W.; Pouton, C. W. *Advanced Drug Delivery Reviews* **1996**, 18, 163-191.
- (60) Heller, A.; Feldman, B. *Accounts of Chemical Research* **2010**, 43, 963-973.
- (61) Pauling, L. *J. Am. Chem. Soc.* **1940**, 62, 2643-2657.
- (62) Abhyankar, A. V.; Bhargava, R.; Jana, A. M.; Sahni, A. K.; Rao, P. V. L. *Hybridoma* **2008**, 27, 191-198.
- (63) Iyer, Y. S.; Vasantha, K.; Manisha, P.; Jadhav, S.; Gupte, S. C.; Mohanty, D. *Indian Journal of Medical Research* **2006**, 123, 561-564.
- (64) Heise, C.; Bier, F. F. *Immobilisation of DNA on Chips Ii* **2005**, 261, 1-25.
- (65) Bier, F. E.; von Nickisch-Rosenegk, M.; Ehrentreich-Forster, E.; Reiss, E.; Henkel, J.; Strehlow, R.; Andresen, D. *Biosensing for the 21st Century* **2008**, 109, 433-453.
- (66) Zheng, J.; He, P. G.; Fang, Y. Z. *Progress in Chemistry* **2009**, 21, 732-738.
- (67) Shamah, S. M.; Healy, J. M.; Cload, S. T. *Accounts of Chemical Research* **2008**, 41, 130-138.
- (68) Nice, E.; Layton, J.; Fabri, L.; Hellman, U.; Engstrom, A.; Persson, B.; Burgess, A. W. *Journal of Chromatography* **1993**, 646, 159-168.
- (69) Dubs, M. C.; Altschuh, D.; Vanregenmortel, M. H. V. *Journal of Chromatography* **1992**, 597, 391-396.
- (70) Rutledge, R. D.; Huffman, B. J.; Cliffler, D. E.; Wright, D. W. *Journal of Materials Research* **2008**, 23, 3161-3168.
- (71) Willats, W. G. T. *Plant Molecular Biology* **2002**, 50, 837-854.
- (72) Staquicini, F. I.; Sidman, R. L.; Arap, W.; Pasqualini, R. *Advanced Drug Delivery Reviews* **2010**, 62, 1213-1216.
- (73) Israelachvili, J. *Intermolecular and Surface Forces*; Academic Press, 1991.
- (74) Agrawal, Y. K.; Kunji, S.; Menon, S. K. *Reviews in Analytical Chemistry* **1998**, 17, 69-139.
- (75) Otero-Espinar, F. J.; Torres-Labandeira, J. J.; Alvarez-Lorenzo, C.; Blanco-Mendez, J. *Journal of Drug Delivery Science and Technology* **2010**, 20, 289-301.
- (76) Bilensoy, E.; Hincal, A. A. *Expert Opinion on Drug Delivery* **2009**, 6, 1161-1173.
- (77) Ma, X.; Tian, H. *Chemical Society Reviews* **2010**, 39, 70-80.
- (78) Suffczynski, M. *Polish Journal of Chemistry* **1995**, 69, 157-184.
- (79) Menon, S. K.; Guha, T. B.; Agrawal, Y. K. *Reviews in Inorganic Chemistry* **2004**, 24, 97-133.
- (80) Lindhorst, T. *Essentials of Carbohydrate Chemistry and Biochemistry*; 3rd. rev. ed.; Wiley-VCH: Weinheim, 2007.
- (81) Bertozzi, C. R.; Kiessling, L. L. *Science* **2001**, 291, 2357-2364.
- (82) Shriver, Z.; Raguram, S.; Sasisekharan, R. *Nature Reviews Drug Discovery* **2004**, 3, 863-873.
- (83) Liu, Y.; Palma, A. S.; Feizi, T. *Biological Chemistry* **2009**, 390, 647-656.

- (84) Sharon, N.; Lis, H. *Scientific American* **1993**, 268, 82-89.
- (85) Chan, K.; Ng, T. B. *Protein and Peptide Letters* **2010**, 17, 1417-1425.
- (86) Chen, G. S. *Progress in Chemistry* **2010**, 22, 1753-1759.
- (87) Girardin, C. M.; Huot, C.; Gonthier, M.; Delvin, E. *Clinical Biochemistry* **2009**, 42, 136-142.
- (88) Yamamoto, T.; Seino, Y.; Fukumoto, H.; Koh, G.; Yano, H.; Inagaki, N.; Yamada, Y.; Inoue, K.; Manabe, T.; Imura, H. *Biochemical and Biophysical Research Communications* **1990**, 170, 223-230.
- (89) Taylor, C. J.; Baxter, P. S.; Hardcastle, J.; Hardcastle, P. T.; Goldhill, J. *Archives of Disease in Childhood* **1989**, 64, 759-759.
- (90) Busse, D.; Elsas, L. J.; Rosenber, L. *Journal of Clinical Investigation* **1970**, 49, A15-&.
- (91) Elsas, L. J.; Busse, D.; Rosenber, L. *Metabolism-Clinical and Experimental* **1971**, 20, 968-&.
- (92) Cohen, R. M.; Smith, E. P. *Current Opinion in Clinical Nutrition and Metabolic Care* **2008**, 11, 512-517.
- (93) Lemieux, R. U. *Chemical Society Reviews* **1989**, 18, 347-374.
- (94) Engström, H. A.; Johansson, R.; Koch-Schmidt, P.; Gregorius, K.; Ohlson, S.; Bergström, M. *Biomedical Chromatography* **2008**, 22, 272-277.
- (95) Gupta, G.; Suroliya, A.; Sampathkumar, S. G. *Omics-a Journal of Integrative Biology* **2010**, 14, 419-436.
- (96) Zak, I.; Lewandowska, E.; Gnyp, W. *Acta Biochimica Polonica* **2000**, 47, 393-412.
- (97) Bouwman, L. H.; Roep, B. O.; Roos, A. *Human Immunology* **2006**, 67, 247-256.
- (98) Kennedy, J. F.; Palva, P. M. G.; Corella, M. T. S.; Cavalcanti, M. S. M.; Coelho, L. C. B. B. *Carbohydrate Polymers* **1995**, 26, 219-230.
- (99) Singh, R. S.; Bhari, R.; Kaur, H. P. *Critical Reviews in Biotechnology* **2010**, 30, 99-126.
- (100) Sack, J. S.; Saper, M. A.; Quioco, F. A. *Journal of Molecular Biology* **1989**, 206, 171-191.
- (101) Sharon, N. *Biochemical Society Transactions* **2008**, 36, 1457-1460.
- (102) Sharon, N. *Trends in Biochemical Sciences* **1993**, 18, 221-226.
- (103) Weis, W. I.; Drickamer, K. *Annual Review of Biochemistry* **1996**, 65, 441-473.
- (104) Quioco, F. A. *Pure and Applied Chemistry* **1989**, 61, 1293-1306.
- (105) Quioco, F. A. *Current Topics in Microbiology and Immunology* **1988**, 139, 135-148.
- (106) Cygler, M.; Rose, D. R.; Bundle, D. R. *Science* **1991**, 253, 442-445.
- (107) Zdanov, A.; Li, Y.; Bundle, D. R.; Deng, S. J.; Mackenzie, C. R.; Narang, S. A.; Young, N. M.; Cygler, M. *Proceedings of the National Academy of Sciences of the United States of America* **1994**, 91, 6423-6427.
- (108) Macholan, L.; Skladal, P.; Bohackova, I.; Krejci, J. *Biosensors & Bioelectronics* **1992**, 7, 593-598.
- (109) Compain, P.; Chagnault, V.; Martin, O. R. *Tetrahedron-Asymmetry* **2009**, 20, 672-711.
- (110) Compain, P.; Martin, O. R. *Current Topics in Medicinal Chemistry* **2003**, 3, 541-560.
- (111) Witczak, Z.; Culhane, J. *Applied Microbiology and Biotechnology* **2005**, 69, 237-244.
- (112) Arjona, O. N.; Gomez, A. M.; Lopez, J. C. b.; Plumet, J. N. *Chemical Reviews* **2007**, 107, 1919-2036.
- (113) Giangiacomo, R. *Food Chemistry* **2006**, 96, 371-379.
- (114) Davis, A. P.; Wareham, R. S. *Angewandte Chemie International Edition* **1999**, 38, 2978-2996.
- (115) Blau, A.; University of Kaiserslautern: Kaiserslautern, 2007.
- (116) Schneider, H. J. *Angewandte Chemie-International Edition* **2009**, 48, 3924-3977.
- (117) Schneider, H. J.; Strongin, R. M. *Accounts of Chemical Research* **2009**, 42, 1489-1500.
- (118) Grimme, S. *Angewandte Chemie International Edition* **2008**, 47, 3430-3434.
- (119) Komiyama, M.; Takeuchi, T.; Mukawa, T.; Asanuma, H. *Molecular Imprinting*; Wiley-VCH: Weinheim, 2003.
- (120) Mazik, M. *Chemical Society Reviews* **2009**, 38, 935-956.
- (121) Mazik, M.; Cavga, H. s. *The Journal of Organic Chemistry* **2006**, 71, 2957-2963.
- (122) Zhang, H. Q.; Ye, L.; Mosbach, K. *Journal of Molecular Recognition* **2006**, 19, 248-259.
- (123) Mayes, A. G.; Whitcombe, M. J. *Advanced Drug Delivery Reviews* **2005**, 57, 1742-1778.
- (124) Athikomrattanakul, U.; Katterle, M.; Gajovic-Eichelmann, N.; Scheller, F. W. *Biosensors & Bioelectronics* **2009**, 25, 82-87.
- (125) Athikomrattanakul, U.; Promptmas, C.; Katterle, M. *Tetrahedron Letters* **2009**, 50, 359-362.
- (126) Bui, B. T. S.; Haupt, K. *Analytical and Bioanalytical Chemistry* **2010**, 398, 2481-2492.
- (127) Haupt, K. *Chemical Communications* **2003**, 171-178.
- (128) Schweitz, L.; Andersson, L. I.; Nilsson, S. *Journal of Chromatography A* **1998**, 817, 5-13.
- (129) Kirsch, N.; Alexander, C.; Davies, S.; Whitcombe, M. J. *Analytica Chimica Acta* **2004**, 504, 63-71.
- (130) Kirsch, N.; Alexander, C.; Lubke, M.; Whitcombe, M. J.; Vulfson, E. N. *Polymer* **2000**, 41, 5583-5590.

- (131) Diltemiz, S. E.; Denizli, A.; Ersoz, A.; Say, R. *Sensors and Actuators B-Chemical* **2008**, *133*, 484-488.
- (132) Matsui, J.; Nicholls, I. A.; Takeuchi, T.; Mosbach, K.; Karube, I. *Analytica Chimica Acta* **1996**, *335*, 71-77.
- (133) Mayes, A. G.; Andersson, L. I.; Mosbach, K. *Analytical Biochemistry* **1994**, *222*, 483-488.
- (134) Kirk, C.; Jensen, M.; Kjaer, C. N.; Smedskjaer, M. M.; Larsen, K. L.; Wimmer, R.; Yu, D. H. *Biosensors & Bioelectronics* **2009**, *25*, 623-628.
- (135) Striegler, S. *Analytica Chimica Acta* **2005**, *539*, 91-95.
- (136) Striegler, S.; Dittel, M. *Inorganic Chemistry* **2005**, *44*, 2728-2733.
- (137) Ishi-i, T.; Iguchi, R.; Shinkai, S. *Tetrahedron* **1999**, *55*, 3883-3892.
- (138) Ishi-i, T.; Nakashima, K.; Shinkai, S. *Chemical Communications* **1998**, 1047-1048.
- (139) Kanekiyo, Y.; Inoue, K.; Ono, Y.; Sano, M.; Shinkai, S.; Reinhoudt, D. N. *Journal of the Chemical Society-Perkin Transactions 2* **1999**, 2719-2722.
- (140) Friggeri, A.; Kobayashi, H.; Shinkai, S.; Reinhoudt, D. N. *Angewandte Chemie-International Edition* **2001**, *40*, 4729-+.
- (141) Ko, D. Y.; Lee, H. J.; Jeong, B. *Macromolecular Rapid Communications* **2006**, *27*, 1367-1372.
- (142) Byrne, M. E.; Hilt, J. Z.; Peppas, N. A. *Journal of Biomedical Materials Research Part A* **2008**, *84A*, 137-147.
- (143) Fang, C.; Yi, C.; Wang, Y.; Cao, Y.; Liu, X. *Biosensors and Bioelectronics* **2009**, *24*, 3164-3169.
- (144) Ates, Z.; Guven, O. *Radiation Physics and Chemistry* **2010**, *79*, 219-222.
- (145) Striegler, S. *Tetrahedron* **2001**, *57*, 2349-2354.
- (146) Malitesta, C.; Losito, I.; Zambonin, P. G. *Analytical Chemistry* **1999**, *71*, 1366-1370.
- (147) Yang, D. H.; Takahara, N.; Lee, S. W.; Kunitake, T. *Sensors and Actuators B-Chemical* **2008**, *130*, 379-385.
- (148) Oral, E.; Peppas, N. A. *Journal of Biomedical Materials Research Part A* **2004**, *68A*, 439-447.
- (149) Ersoz, A.; Denizli, A.; Ozcan, A.; Say, R. *Biosensors & Bioelectronics* **2005**, *20*, 2197-2202.
- (150) Yoshimi, Y.; Narimatsu, A.; Sakai, K. *Journal of Bioscience and Bioengineering* **2009**, *108*, S31-S31.
- (151) Sallacan, N.; Zayats, M.; Bourenko, T.; Kharitonov, A. B.; Willner, I. *Analytical Chemistry* **2002**, *74*, 702-712.
- (152) Chen, G. H.; Guan, Z. B.; Chen, C. T.; Fu, L. T.; Sundaresan, V.; Arnold, F. H. *Nature Biotechnology* **1997**, *15*, 354-357.
- (153) Parmpi, P.; Kofinas, P. *Biomaterials* **2004**, *25*, 1969-1973.
- (154) Tan, J.; Wang, H. F.; Yan, X. P. *Analytical Chemistry* **2009**, *81*, 5273-5280.
- (155) Hashidzume, A.; Zimmerman, S. C. *Tetrahedron Letters* **2009**, *50*, 2204-2207.
- (156) Wulff, G.; Schauhoff, S. *Journal of Organic Chemistry* **1991**, *56*, 395-400.
- (157) Rajkumar, R.; Katterle, M.; Warsinke, A.; Moehwald, H.; Scheller, F. W. *Biosensors & Bioelectronics* **2008**, *23*, 1195-1199.
- (158) Chuang, S. W.; Rick, J.; Chou, T. C. *Biosensors & Bioelectronics* **2009**, *24*, 3170-3173.
- (159) Fazal, F. M.; Hansen, D. E. *Bioorganic & Medicinal Chemistry Letters* **2007**, *17*, 235-238.
- (160) Hall, D. G. *Boronic acids: preparation and applications in organic synthesis and medicine*; 1. Edition ed.; Wiley-VCH: Weinheim, 2005.
- (161) Brown, H. C. *Organic Synthesis via Boranes*; Wiley-VCH: Weinheim, 1975.
- (162) Suzuki, A. *Journal of Organometallic Chemistry* **1999**, *576*, 147-168.
- (163) Franzen, R. *Canadian Journal of Chemistry-Revue Canadienne De Chimie* **2000**, *78*, 957-962.
- (164) Franzen, R.; Xu, Y. J. *Canadian Journal of Chemistry-Revue Canadienne De Chimie* **2005**, *83*, 266-272.
- (165) Ainley, A. D.; Challenger, F. *Journal of the Chemical Society (Resumed)* **1930**, 2171-2180.
- (166) Huber, M. L.; Pinhey, J. T. *Journal of the Chemical Society-Perkin Transactions 1* **1990**, 721-722.
- (167) Prakash, G. K. S.; Panja, C.; Mathew, T.; Surampudi, V.; Petasis, N. A.; Olah, G. A. *Organic Letters* **2004**, *6*, 2205-2207.
- (168) Snyder, H. R.; Kuck, J. A.; Johnson, J. R. *Journal of the American Chemical Society* **1938**, *60*, 105-111.
- (169) Brown, H. C.; Basavaiah, D. *The Journal of Organic Chemistry* **1982**, *47*, 3806-3808.
- (170) Al-Zoubi, R. M.; Marion, O.; Hall, D. G. *Angewandte Chemie-International Edition* **2008**, *47*, 2876-2879.
- (171) Zheng, H. C.; McDonald, R.; Hall, D. G. *Chemistry-a European Journal* **2010**, *16*, 5454-5460.
- (172) Trippier, P. C.; McGuigan, C. *Medchemcomm* **2010**, *1*, 183-198.
- (173) Matteson, D. S. *Medicinal Research Reviews* **2008**, *28*, 233-246.
- (174) Dick, L. R.; Fleming, P. E. *Drug Discovery Today* **2010**, *15*, 243-249.

- (175) Mader, H. S.; Wolfbeis, O. S. *Microchimica Acta* **2008**, *162*, 1-34.
- (176) Ho, O. C.; Soundararajan, R.; Lu, J. H.; Matteson, D. S.; Wang, Z. M.; Chen, X.; Wei, M. Y.; Willett, R. D. *Organometallics* **1995**, *14*, 2855-2860.
- (177) Matteson, D. S.; Man, H. W.; Ho, O. C. *Journal of the American Chemical Society* **1996**, *118*, 4560-4566.
- (178) Dahlhoff, W. V.; Koster, R. *Heterocycles* **1982**, *18*, 421-449.
- (179) Taba, K. M.; Dahlhoff, W. V. *Synthesis-Stuttgart* **1982**, 652-653.
- (180) Dederichs, W., University of Düsseldorf, 1983.
- (181) Luithle, J. E. A.; Pietruszka, J. *European Journal of Organic Chemistry* **2000**, 2557-2562.
- (182) Luithle, J. E. A.; Pietruszka, J. *Journal of Organic Chemistry* **1999**, *64*, 8287-8297.
- (183) Kuivila, H. G.; Keough, A. H.; Soboczenski, E. J. *The Journal of Organic Chemistry* **1954**, *19*, 780-783.
- (184) Böeseken, J. *Adv. Carb. Chem.* **1949**, *4*, 189-210.
- (185) Böeseken, J. *Berichte der deutschen chemischen Gesellschaft* **1913**, *46*, 2612-2628.
- (186) Lorand, J. P.; Edwards, J. O. *The Journal of Organic Chemistry* **1959**, *24*, 769-774.
- (187) Edwards, J. O.; Morrison, G. C.; Ross, V. F.; Schultz, J. W. *Journal of the American Chemical Society* **1955**, *77*, 266-268.
- (188) Draffin, S. P.; Duggan, P. J.; Fallon, G. D. *Acta Crystallographica Section E-Structure Reports Online* **2004**, *60*, O1520-O1522.
- (189) Freyhardt, C. C.; Wiebcke, M.; Felsche, J. *Acta Crystallographica Section C-Crystal Structure Communications* **2000**, *56*, 276-278.
- (190) Bhat, K. L.; Howard, N. J.; Rostami, H.; Lai, J. H.; Bock, C. W. *Journal of Molecular Structure-Theochem* **2005**, *723*, 147-157.
- (191) Grotstollen, W., University of Düsseldorf, 1981.
- (192) Wulff, G. *Pure and Applied Chemistry* **1982**, *54*, 2093-2102.
- (193) Yang, X. P.; Lee, M. C.; Sartain, F.; Pan, X. H.; Lowe, C. R. *Chemistry-a European Journal* **2006**, *12*, 8491-8497.
- (194) Pal, A.; Berube, M.; Hall, D. G. *Angewandte Chemie-International Edition* **2010**, *49*, 1492-1495.
- (195) Jay, J. I.; Lai, B. E.; Myszka, D. G.; Mahalingam, A.; Langheinrich, K.; Katz, D. F.; Kiser, P. F. *Molecular Pharmaceutics* **2010**, *7*, 116-129.
- (196) Adamczyk-Wozniak, A.; Cyranski, M. K.; Zubrowska, A.; Sporzynski, A. *Journal of Organometallic Chemistry* **2009**, *694*, 3533-3541.
- (197) Gunasekera, D. S.; Gerold, D. J.; Aalderks, N. S.; Chandra, J. S.; Maanu, C. A.; Kiprof, P.; Zhdankin, V. V.; Reddy, M. V. R. *Tetrahedron* **2007**, *63*, 9401-9405.
- (198) Lennarz, W. J.; Snyder, H. R. *Journal of the American Chemical Society* **1960**, *82*, 2172-2175.
- (199) Sporzynski, A.; Lewandowski, M.; Rogowska, P.; Cyranski, M. K. *Applied Organometallic Chemistry* **2005**, *19*, 1202-1203.
- (200) Dabrowski, M.; Kurach, P.; Lulinski, S.; Serwatowski, J. *Applied Organometallic Chemistry* **2007**, *21*, 234-238.
- (201) Zhdankin, V. V.; Persichini, P. J.; Zhang, L.; Fix, S.; Kiprof, P. *Tetrahedron Letters* **1999**, *40*, 6705-6708.
- (202) Yamamoto, Y.; Ishii, J.-i.; Nishiyama, H.; Itoh, K. *Journal of the American Chemical Society* **2005**, *127*, 9625-9631.
- (203) Yoon, J.; Czarnik, A. W. *Journal of the American Chemical Society* **1992**, *114*, 5874-5875.
- (204) James, T. D.; Sandanayake, K. R. A. S.; Iguchi, R.; Shinkai, S. *Journal of the American Chemical Society* **1995**, *117*, 8982-8987.
- (205) James, T. D.; Sandanayake, K. R. A. S.; Shinkai, S. *Nature* **1995**, *374*, 345-347.
- (206) Yang, W.; He, H.; Drucekhammer, D. G. *Angewandte Chemie-International Edition* **2001**, *40*, 1714-1718.
- (207) Devi, P. A.; Heagy, M. D. *Tetrahedron Letters* **1999**, *40*, 7893-7896.
- (208) Cao, H. S.; Diaz, D. I.; DiCesare, N.; Lakowicz, J. R.; Heagy, M. D. *Organic Letters* **2002**, *4*, 1503-1505.
- (209) James, T. D.; Sandanayake, K. R. A. S.; Shinkai, S. *Angewandte Chemie-International Edition in English* **1994**, *33*, 2207-2209.
- (210) Norrild, J. C.; Eggert, H. *Journal of the Chemical Society-Perkin Transactions 2* **1996**, 2583-2588.
- (211) Angyal, S. J. *Advances in Carbohydrate Chemistry and Biochemistry* **1984**, *42*, 15-68.
- (212) Angyal, S. J.; Derek, H. In *Advances in Carbohydrate Chemistry and Biochemistry*; Academic Press: 1991; Vol. Volume 49, p 19-35.
- (213) Norrild, J. C.; Eggert, H. *Journal of the American Chemical Society* **1995**, *117*, 1479-1484.

- (214) Bielecki, M.; Eggert, H.; Norrild, J. C. *Journal of the Chemical Society-Perkin Transactions 2* **1999**, 449-455.
- (215) Freeman, R.; Finder, T.; Bahshi, L.; Willner, I. *Nano Letters* **2009**, *9*, 2073-2076.
- (216) Chalagalla, S.; Sun, X. L. *Reactive & Functional Polymers* **2010**, *70*, 471-476.
- (217) Ivanov, A. E.; Solodukhina, N.; Wahlgren, M.; Nilsson, L.; Vikhrov, A. A.; Nikitin, M. P.; Orlov, A. V.; Nikitin, P. I.; Kuzimenkova, M. V.; Zubov, V. P. *Macromolecular Bioscience*, n/a-n/a.
- (218) Huang, X.; Li, S. Q.; Schultz, J. S.; Wang, Q.; Lin, Q. *Sensors and Actuators B-Chemical* **2009**, *140*, 603-609.
- (219) Huang, X.; Li, S. Q.; Schultz, J.; Wang, Q.; Lin, Q. *Journal of Microelectromechanical Systems* **2009**, *18*, 1246-1254.
- (220) Notley, S. M.; Chen, W.; Pelton, R. *Langmuir* **2009**, *25*, 6898-6904.
- (221) Tierney, S.; Volden, S.; Stokke, B. T. *Biosensors & Bioelectronics* **2009**, *24*, 2034-2039.
- (222) Yu, C.; Yam, V. W. W. *Chemical Communications* **2009**, 1347-1349.
- (223) Li, S. Q.; Davis, E. N.; Anderson, J.; Lin, Q.; Wang, Q. *Biomacromolecules* **2009**, *10*, 113-118.
- (224) Zenkl, G.; Klimant, I. *Microchimica Acta* **2009**, *166*, 123-131.
- (225) Preinerstorfer, B.; Lammerhofer, M.; Lindner, W. *Journal of Separation Science* **2009**, *32*, 1673-1685.
- (226) Shen, W. W.; Ma, C. N.; Wang, S. F.; Xiong, H. M.; Lu, H. J.; Yang, P. Y. *Chemistry-an Asian Journal* **2010**, *5*, 1185-1191.
- (227) Kitahara, K. I.; Noguchi, Y.; Itoh, S.; Chiba, N.; Tohyama, T.; Nagashima, K.; Hanada, T.; Yoshihama, I.; Arai, S. *Journal of Chromatography A* **2009**, *1216*, 7415-7421.
- (228) Qing, G. Y.; Wang, X.; Jiang, L.; Fuchs, H.; Sun, T. L. *Soft Matter* **2009**, *5*, 2759-2765.
- (229) Yakuphanoglu, F.; Senkal, B. F. *Polymer Engineering and Science* **2009**, *49*, 722-726.
- (230) Deore, B. A.; Freund, M. S. *Macromolecules* **2009**, *42*, 164-168.
- (231) Sharrett, Z.; Gamsey, S.; Hirayama, L.; Vilozny, B.; Suri, J. T.; Wessling, R. A.; Singaram, B. *Organic & Biomolecular Chemistry* **2009**, *7*, 1461-1470.
- (232) Shibata, H.; Heo, Y. J.; Okitsu, T.; Matsunaga, Y.; Kawanishi, T.; Takeuchi, S. *Proceedings of the National Academy of Sciences of the United States of America* **2010**, *107*, 17894-17898.
- (233) Shiino, D.; Matsuyama, K.; Koyama, Y.; Kataoka, K.; Sakurai, Y.; Okano, T. *Advanced Biomaterials in Biomedical Engineering and Drug Delivery Systems* **1996**, 369-370 381.
- (234) Shiino, D.; Kataoka, K.; Koyama, Y.; Yokoyama, M.; Okano, T.; Sakurai, Y. *Journal of Intelligent Material Systems and Structures* **1994**, *5*, 311-314.
- (235) Matsumoto, A.; Kurata, T.; Shiino, D.; Kataoka, K. *Macromolecules* **2004**, *37*, 1502-1510.
- (236) Samoei, G. K.; Wang, W. H.; Escobedo, J. O.; Xu, X. Y.; Schneider, H. J.; Cook, R. L.; Strongin, R. M. *Angewandte Chemie-International Edition* **2006**, *45*, 5319-5322.
- (237) Schneider, H. J.; Kato, K.; Strongin, R. M. *Sensors* **2007**, *7*, 1578-1611.
- (238) Potter, O. G.; Hilder, E. F. *Journal of Separation Science* **2008**, *31*, 1881-1906.
- (239) Connors, K. A. *Binding Constants*; Wiley Interscience: New York, 1987.
- (240) Motulsky, H. *The GraphPad Guide for Analyzing Radioligand Binding Data*; Graph Pad Prism: S San Diego, 1995.
- (241) Li, R.; Dai, B. C.; Zhao, Y. D.; Lu, K. *Spectroscopy and Spectral Analysis* **2009**, *29*, 240-243.
- (242) Liu, Y.; Han, B. H.; Zhang, H. Y. *Current Organic Chemistry* **2004**, *8*, 35-46.
- (243) Fielding, L. *Current Topics in Medicinal Chemistry* **2003**, *3*, 39-53.
- (244) Shin, Y. G.; van Breemen, R. B. *Biopharmaceutics & Drug Disposition* **2001**, *22*, 353-372.
- (245) Brodbelt, J. S. *International Journal of Mass Spectrometry* **2000**, *200*, 57-69.
- (246) Iqbal, N.; Mustafa, G.; Rehman, A.; Biedermann, A.; Najafi, B.; Lieberzeit, P. A.; Dickert, F. L. *Sensors* **2010**, *10*, 6361-6376.
- (247) Jenik, M.; Schirhagl, R.; Schirk, C.; Hayden, O.; Lieberzeit, P.; Blaas, D.; Paul, G.; Dickert, F. L. *Analytical Chemistry* **2009**, *81*, 5320-5326.
- (248) Jenik, M.; Seifner, A.; Krassnig, S.; Seidler, K.; Lieberzeit, P. A.; Dickert, F. L.; Jungbauer, C. B. *Biosensors & Bioelectronics* **2009**, *25*, 9-14.
- (249) Nagel, T.; Gajovic-Eicheimann, N.; Tobisch, S.; Schulte-Spechtel, U.; Bier, F. F. *Clinica Chimica Acta* **2008**, *394*, 110-113.
- (250) Bier, F. F.; Kleinjung, F.; Scheller, F. W. *Sensors and Actuators B-Chemical* **1997**, *38*, 78-82.
- (251) Springsteen, G.; Wang, B. H. *Chemical Communications* **2001**, 1608-1609.
- (252) Garcia-Calzon, J. A.; Diaz-Garcia, M. E. *Sensors and Actuators B-Chemical* **2007**, *123*, 1180-1194.

- (253) Umpleby, R. J.; Baxter, S. C.; Rampey, A. M.; Rushton, G. T.; Chen, Y. Z.; Shimizu, K. D. *Journal of Chromatography B-Analytical Technologies in the Biomedical and Life Sciences* **2004**, *804*, 141-149.
- (254) Rampey, A. M.; Umpleby, R. J.; Rushton, G. T.; Iseman, J. C.; Shah, R. N.; Shimizu, K. D. *Analytical Chemistry* **2004**, *76*, 1123-1133.
- (255) Chiad, K.; Stelzig, S. H.; Gropeanu, R.; Weil, T.; Klapper, M.; Mullen, K. *Macromolecules* **2009**, *42*, 7545-7552.
- (256) Behbehani, G. R.; Saboury, A. A.; Divsalar, A. *Acta Biochimica Et Biophysica Sinica* **2008**, *40*, 964-969.
- (257) Schmidtchen, F. P. In *Analytical Methods in Supramolecular Chemistry*; 1 ed.; Schalley, C. A., Ed.; Wiley-VCH: Weinheim, 2006.
- (258) Pierce, M. M.; Raman, C. S.; Nall, B. T. *Methods-a Companion to Methods in Enzymology* **1999**, *19*, 213-221.
- (259) Lewis, E. A.; Murphy, K. P. In *Methods in Molecular Biology*; Nienhaus, G. E., Ed.; Humana Press: Totowa, 2003; Vol. 305.
- (260) Kortüm, G. *Lehrbuch der Elektrochemie*; 3. ed.; Verlag Chemie GmbH: Weinheim, 1962.
- (261) Wiseman, T.; Williston, S.; Brandts, J. F.; Lin, L. N. *Analytical Biochemistry* **1989**, *179*, 131-137.
- (262) Dowlut, M., University of Alberta, 2006.
- (263) Babcock, L.; Pizer, R. *Inorganic Chemistry* **1980**, *19*, 56-61.
- (264) Friedman, S.; Pace, B.; Pizer, R. *Journal of the American Chemical Society* **1974**, *96*, 5381-5384.
- (265) Salehnia, M., University of Düsseldorf, 1985.
- (266) Tschampel, P.; Snyder, H. R. *Journal of Organic Chemistry* **1964**, *29*, 2168-2172.
- (267) Poll, H.-G., University of Düsseldorf, 1985.
- (268) Torun, O.; Dudak, F. C.; Bas, D.; Tamer, U.; Boyaci, I. H. *Sensors and Actuators B-Chemical* **2009**, *140*, 597-602.
- (269) Leavitt, S.; Freire, E. *Current Opinion in Structural Biology* **2001**, *11*, 560-566.
- (270) Dunitz, J. D. *Chemistry & Biology* **1995**, *2*, 709-712.
- (271) Starikov, E. B.; Norden, B. *Journal of Physical Chemistry B* **2007**, *111*, 14431-14435.
- (272) Cornish-Bowden, A. *Journal of Biosciences* **2002**, *27*, 121-126.
- (273) Horn, J. R.; Russell, D.; Lewis, E. A.; Murphy, K. P. *Biochemistry* **2001**, *40*, 1774-1778.
- (274) Ito, S.; Miyoshi, T. *Journal of Applied Phycology* **1993**, *5*, 15-21.
- (275) Taylor, M. J.; Hunt, C. J. *British Journal of Ophthalmology* **1981**, *65*, 815-819.
- (276) Webb, G. N.; Byrd, R. A. *Biotechnic & Histochemistry* **1994**, *69*, 181-185.
- (277) Palit, D. K.; Pal, H.; Mukherjee, T.; Mittal, J. P. *Journal of the Chemical Society-Faraday Transactions* **1990**, *86*, 3861-3869.
- (278) Faouzi, A. M.; Nasr, B.; Abdellatif, G. *Dyes and Pigments* **2007**, *73*, 86-89.
- (279) Mahanthesh, K. R.; Swamy, B. E. K.; Chandra, U.; Bodke, Y. D.; Pai, K. V. K.; Sherigara, B. S. *International Journal of Electrochemical Science* **2009**, *4*, 1237-1247.
- (280) Mouchrek, V. E.; Marques, A. L. B.; Zhang, J. J.; Chierice, G. O. *Electroanalysis* **1999**, *11*, 1130-1136.
- (281) Mouchrek, V. E.; Chierice, G. O.; Marques, A. L. B. *Quimica Nova* **1999**, *22*, 312-315.
- (282) Ardakani, M. M.; Karimi, M. A.; Mirdehghan, S. M.; Zare, M. M.; Mazidi, R. *Sensors and Actuators B-Chemical* **2008**, *132*, 52-59.
- (283) Deng, P. H.; Fei, J. J.; Zhang, J.; Li, J. N. *Electroanalysis* **2008**, *20*, 1215-1219.
- (284) Bonne, M. J.; Galbraith, E.; James, T. D.; Wasbrough, M. J.; Edler, K. J.; Jenkins, A. T. A.; Helton, M.; McKee, A.; Thielemans, W.; Psillakis, E.; Marken, F. *Journal of Materials Chemistry* **2010**, *20*, 588-594.
- (285) Soriaga, M. P.; Hubbard, A. T. *Journal of the American Chemical Society* **1982**, *104*, 2735-2742.
- (286) Paulke, B. R.; Hartig, W.; Bruckner, G. *Acta Polymerica* **1992**, *43*, 288-291.
- (287) Beres, L.; Sturteva, J. *Biochemistry* **1971**, *10*, 2120-&.
- (288) Bekiroglu, S.; Kenne, L.; Sandstrom, C. *Carbohydrate Research* **2004**, *339*, 2465-2468.
- (289) Kirchner, R.; Seidel, J.; Wolf, G.; Wulff, G. *Journal of Inclusion Phenomena and Macrocyclic Chemistry* **2002**, *43*, 279-283.
- (290) Cannizzo, C.; Amigoni-Gerbier, S.; Larpent, C. *Polymer* **2005**, *46*, 1269-1276.
- (291) Somani, B. L.; Khanade, J.; Sinha, R. *Analytical Biochemistry* **1987**, *167*, 327-330.
- (292) Gypser, A.; Michel, D.; Nirschl, D. S.; Sharpless, K. B. *Journal of Organic Chemistry* **1998**, *63*, 7322-7327.
- (293) Draffin, S. P.; Duggan, P. J.; Fallon, G. D.; Tyndall, E. M. *Acta Crystallographica Section E-Structure Reports Online* **2005**, *61*, O1733-O1735.
- (294) Hovelmann, C. H.; Muniz, K. *Chemistry-a European Journal* **2005**, *11*, 3951-3958.

- (295) Kabsch, W. *Acta Crystallographica Section A* **1978**, *34*, 827-828.
- (296) Kabsch, W. *Acta Crystallographica Section A* **1976**, *32*, 922-923.
- (297) McLachlan, A. D. *European Journal of Biochemistry* **1979**, *100*, 181-187.
- (298) Rose, J.; Eisenmenger, F. *Journal of Molecular Evolution* **1991**, *32*, 340-354.
- (299) Holm, L.; Sander, C. *Trends in Biochemical Sciences* **1995**, *20*, 478-480.
- (300) Orengo, C. A.; Michie, A. D.; Jones, S.; Jones, D. T.; Swindells, M. B.; Thornton, J. M. *Structure* **1997**, *5*, 1093-1108.

APPENDIX

Table A1. Literature survey on molecularly imprinted polymers for glucose, fructose and fructosyl valine as templates

Template	Functional monomer	Polymer type	Polymer format	Rebinding	Remarks	Literature
	N-acryl-L-phenylalanine	NIPAM, Methylene bisacrylamide	Core-shell nanoparticles	PBS	Thermoresponsive core-shell NP, Differentiation to fructose, Comparison to non-particle system	141
	Acryl amide	Poly(acrylamide)-co-PEGDMA	Polymer film	Deionised water	Rebinding was carried out with glucose analogue with fluorescent tag, Use of these films as drug carrier	142
	Maleic anhydride	Styrene, photosensitive coumarin as crosslinker	Polymer film	Deionised water, electrolytes $K_3[Fe(CN)_6]$ and KNO_3	Electrochemical rebinding characterisation	143
Glucose	2-Hydroxyethylmethacrylate	Polypropylene, glycol dimethacrylate, diethylene glycol diacrylate, triethyleneglycol dimethacrylate	Films	Not specified	Radiation induced MIPs, HPLC measurements showed higher retention for glucose compared to fructose and galactose	144
	[(4-(N-Vinylbenzyl)diethylenetriamine)copper(II)] diformate	Pentaerythritol tetraacrylate	Bulk	Alkaline, but also physiological		145
	(o-phenylene diamine)	(o-phenylene diamine)	Electropolymerisation	Acetate buffer	QCM-read out	146
	Titanium <i>n</i> -butoxide	Titanium <i>n</i> -butoxide	Surface sol-gel process	Deionised water	QCM	147
Star-shaped polyethylene glycol	EGDMA	Star-shaped polymers	Deionised water		Starshaped PEG crosslinked with EGDMA, recognition to glucose prior to fructose, polymer is pH sensitive	148
Cu-methacrylamidohistidine	EGDMA	Film	carbonate buffered solution pH=10		QCM	149
Vinylphenylboronic	Methylene	Grafted electrode			Cyclic voltammetry of	150

	acid	bisacrylamide	ferrocyanide	
3a/3b	Acrylamidophenylboronic acid	Acrylamide	0.05 M HEPES, pH 7.4	ISFET sensor 151
Methyl-β-D-glucopyranoside	Polymerisable Cu ²⁺ -triazacylcononane	N,N'-methylenebisacrylamide	Above pH 10	When glucose binds to the polymer, protons are released in proportion to glucose concentration, measurements in porcine serum 152
D-glucose 6-phosphate monobarium salt	Poly(allylamine)hydrochloride	Poly(allylamine)hydrochloride crosslinked with epichlorohydrin	In deionised water and BES-buffer pH=7	Rebinding of glucose, lower binding of fructose 153
	3-aminophenylboronic acid	Silica	Phosphate buffer, pH 7.4	Indicator displacement assay with ARS 154
	3,5-Dibromophenylboronic acid	Polyglycerol	In 1:1:1 DCM, MeOH, THF	One-binding site dendrimer, Binding evaluation with MALDI-TOF, Fructose selectivity, if TEMED is added, mannose exhibit higher binding constant 155
3a	4-Vinylphenylboronic acid	TRIM, EGDMA	In 10% MeOH, carbonate buffer, pH 11.4	TRIM polymers show better binding behaviour than EGDMA, Characterisation with Batch binding studies and thermistor 39
	4-Vinylphenylboronic acid	EGDMA	MeOH 2% Water,	Enantiomeric characterisation of binding sites, HPLC measurement for discrimination values 156
Fructosyl valine	4-Vinylphenylboronic acid	TRIM	In 10% MeOH, carbonate buffer, pH 11.4	Thermistor measurements showed 40-times higher heat signal of the imprint compared to a control 157
	3-Aminophenylboronic acid	Electrodeposited film	0.1 M phosphate buffer, pH 7.0	Electrochemical characterisation of binding with open circuit potential 158

Table A2. Survey of recent literature: Polymeric networks bearing arylboronic acids for different applications

Boronic acid derivative	Polymeric system	Morphology/Format	Application/Remark	Literature
1c	Immobilisation on CdSe/ZnS quantum dots		Binding of boronic acid to NADH, after reduction, NAD ⁺ quenches the QD	215
	Acrylamide	Coupled to magnet beads	Glycoprotein and carbohydrate functionalisation	216
	Acrylamide	Surface brushes	Carbohydrate-mediated adhesion and cultivation of cells	217
	Acrylamide	Polymer gel within a chamber	Continuous glucose monitoring (CGM)	218
1d	Acrylamide	Gel in chamber	MEMS affinity sensor for glucose	219
	Polyvinylamine	Surface film	Adhesion between cellulose surface under aqueous condition is enhanced	220
	Acrylamide/DMAPAA	Gel	Glucose sensing; Fabry-Perot cavity	221
	Acrylamide	Polyanion formation	After binding to saccharides ionisation of the boron and positively charged trimethylpentylammoniumbromide binds	222
1d/Allylaminocarbonyl Phenylboronic acid	Acrylamide	Grafted Copolymer	Sensing fluid for CGM	223
	NIPAM	Nanoparticles	Swelling of nanoparticles and FRET	224
1e	Polyepoxymethacrylate	Beads	Trapping of transferring, radical immobilisation to thiols (made from epoxy)	225
	SNO ₂ @Poly(HEMA-co-styrene-co-VPBA)	Core-shell particles	Glycoprotein capturing and subsequent MALDI-TOF	226
1e/f	DVB	Resin	Elution behaviour of mono- and disaccharides	227
	3-(acryloylthioureido)phenylboronic acid	Polymer film	Switch of hydrophilicity on exposure to sugar solutions	228
3-Thiophene boronic acid	Polythiophene	Film	Organic semiconductor based on electrical and optical properties	229
	Poly(aniline boronic acid)	Dispersion / film	Addition of fluorides leads to self-doped polymer film	230
Boronic acid quencher	HEMA, PEGDMA, SPM	Gel	Dye and quencher system (polymer gel)	231

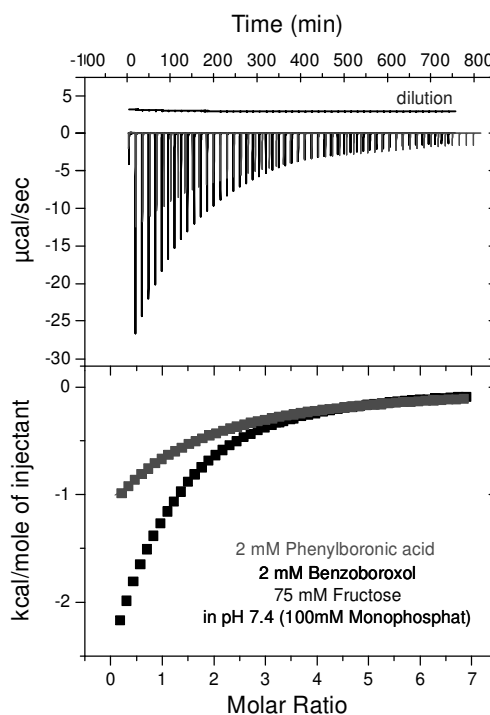


Figure A1. Raw ITC-data of phenylboronic acid (gray) or benzoboroxole (black) interaction fructose

Determination of binding constants using the ARS-displacement assay

The binding constants of the NP-system with fructose or glucose were determined as described by Berubé and Hall (JOC, 2008) with displacement of ARS. Shortly, a plot $[Sugar]/P$ vs. Q was drawn. Q is defined as $Q = [RI]/[I] = (ARI - A) / (A - AI)$, in which R is the concentration of receptor, A the measured absorbance, ARI the absorbance of the receptor-indicator complex and AI the absorbance of the ARS alone. The other parameter P is defined as $P = [R] - 1 / (Q * K_{ARS}) - I_0 / (Q+1)$ with $I_0 = c(ARS)$ and K_{ARS} as the binding constant between the receptor and ARS: in this case the ARS-boroxole binding constant obtained by Hall et al. ($1200 M^{-1}$) was used. The binding constant K_a of the saccharide-boroxole interaction can then be derived from the slope of the plot $[Sugar]/P$ in which $[Sugar]/P = K_{ARS}/K_a Q + 1$, where $[Sugar]$ is sugar concentration.

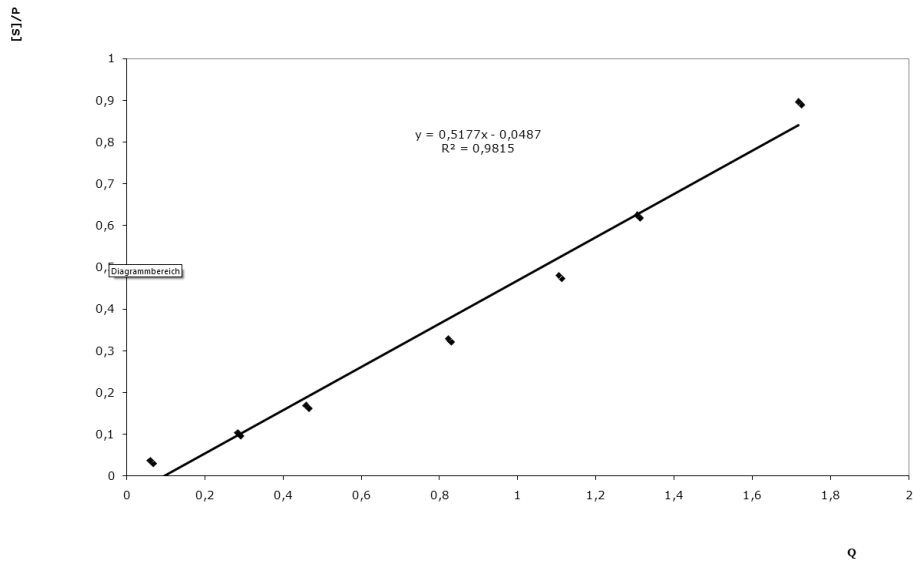


Figure A2. Determination of binding constant between the benzoboroxole-NP and fructose by means of the ARS-assay (S/P vs. Q).

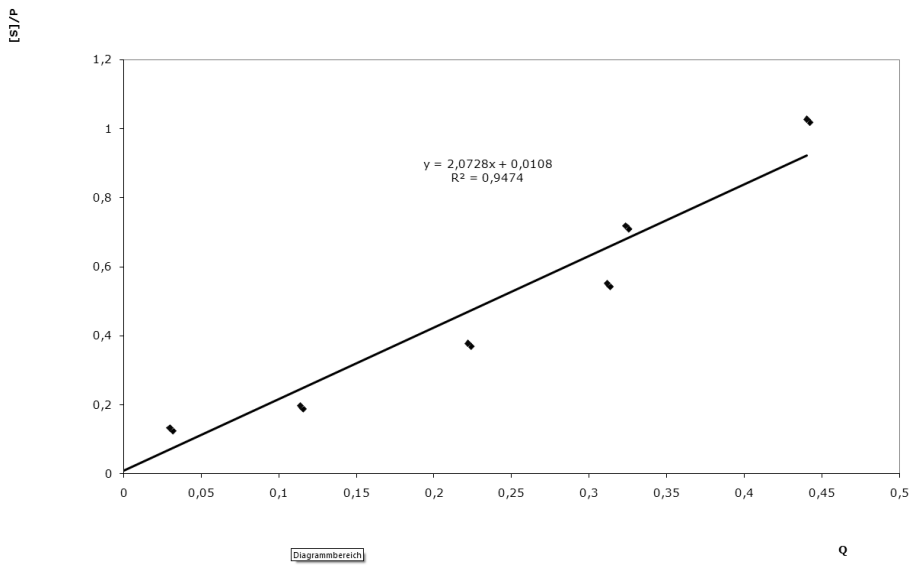


Figure A3. Determination of binding constant between the benzoboroxole-NP and glucose by means of the ARS-assay (S/P vs. Q).

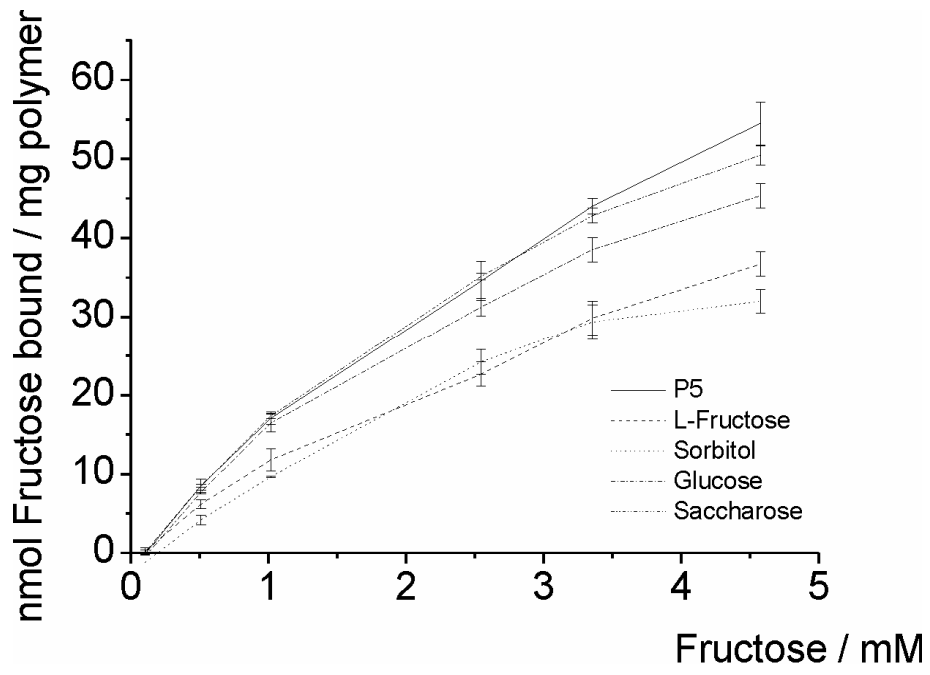


Figure A4. Binding isotherms for competitive binding

Table A3. X-ray crystallographic and refinement data for *rac-4e* and *rac-4f*.

	<i>rac-4e</i>	<i>rac-4f</i>
formula	C ₁₇ H ₁₆ B ₂ O ₄	C ₁₈ H ₁₈ B ₂ O ₄
<i>M</i> _r [g·mol ⁻¹]	305.92	319.94
crystal size [mm]	1.0 x 0.2 x 0.15	0.5 x 0.35 x 0.2
crystal system	orthorhombic	monoclinic
space group	<i>Pna</i> 2 ₁	<i>P</i> 2 ₁ / <i>a</i>
<i>a</i> [Å]	18.472(4)	13.2725(15)
<i>b</i> [Å]	6.1029(10)	9.4769(10)
<i>c</i> [Å]	13.121(2)	14.0435(14)
α [°]	90	90
β [°]	90	110.977(8)
γ [°]	90	90
<i>V</i> [Å ³]	1479.2(5)	1649.3(3)
ρ_{calc} [g·cm ⁻³]	1.374	1.288
<i>Z</i>	4	4
μ [mm]	0.094	0.088
<i>F</i> (000)	640	672
θ range	2.21 – 26.95	2.71 – 24.73
index ranges	-22 ≤ <i>h</i> ≤ 23 -7 ≤ <i>k</i> ≤ 7 -16 ≤ <i>l</i> ≤ 10	-15 ≤ <i>h</i> ≤ 15 -11 ≤ <i>k</i> ≤ 11 -15 ≤ <i>l</i> ≤ 16
reflns collected	5366	9750
independent reflns	2474	2733
<i>R</i> _{int}	0.0713	0.1158
parameters	257	272
<i>S</i> on <i>F</i> ²	0.969	0.949
<i>R</i> ₁ [<i>F</i> >2 σ (<i>F</i>)] ^[a]	0.0423	0.0384
<i>wR</i> ₂ (all data) ^[b]	0.1006	0.0831

$$[a] \quad R_1 = \frac{\sum ||F_o| - |F_c||}{\sum |F_o|}$$

$$[b] \quad wR_2 = \frac{[\sum(F_o^2 - F_c^2)]}{\sum w(F_o^2)^{1/2}}$$

Eidesstattliche Erklärung

Hiermit versichere ich an Eides statt, dass ich diese Arbeit selbstständig verfasst habe. Ich habe keine anderen Quellen und Hilfsmittel, als diese in der Arbeit angegeben, verwendet.

Potsdam, den

Soeren Schumacher